dti

ADVANCED PEM STACK DEVELOPMENT

Final report

CONTRACT NUMBER: F/02/00273/00/00

URN NUMBER: 06/1805

dti

The DTI drives our ambition of 'prosperity for all' by working to create the best environment for business success in the UK.
We help people and companies become more productive by promoting enterprise, innovation and creativity.

We champion UK business at home and abroad. We invest heavily in world-class science and technology. We protect the rights of working people and consumers. And we stand up for fair and open markets in the UK, Europe and the world.

ADVANCED PEM STACK DEVELOPMENT

CONTRACT NUMBER: F/02/00273/REP

URN NUMBER: 06/1805

Contractor

Intelligent Energy Ltd

Prepared by

Simon Foster

David Myers

Peter Gray (Johnson Matthey Fuel Cells Ltd)

The work described in this report was carried out under contract as part of the DTI Technology Programme: Emerging Energy Technologies, which is managed by Future Energy Solutions. The views and judgements expressed in this report are those of the contractor and do not necessarily reflect those of the DTI or Future Energy Solutions.

First published 2006

EXECUTIVE SUMMARY

This report describes work carried out at Intelligent Energy (IE) to design and build a 50kW PEM fuel cell stack based upon etched plate technology, whilst simultaneously designing and developing a pressed plate technology capable of meeting the long term cost targets deemed necessary for full-scale commercialisation of PEM fuel cell technology. Also reported are the results of a joint collaboration with Johnson Matthey under which the design of a membrane electrode assembly specifically matched to IE's unique stack architecture was addressed.

PEM fuel cells are widely predicted to impact upon the automotive, micro-CHP and portable power generation sectors, but must successfully address their present high capital cost in order to do so. Intelligent Energy's unique evaporatively-cooled architecture provides the basis for a number of cost reduction strategies by simplifying the componentry required for efficient fluid delivery, distribution and cooling. This technology, which does not require separate cooling plates, has been demonstrated in single stacks up to 12.5kW and in a twin stack configuration delivering 20kW nett from a 23kW gross system. However, the existing technology, which utilises thin (0.6mm) stainless steel plates manufactured by photochemical etching, has not been demonstrated at automotive power levels (>50kW) and cost analyses have shown that etched plate technology is unable to achieve the stack cost targets proposed by USDoE for automotive applications.

The work carried out under this programme was specifically aimed at tackling these two issues of scale-up and cost reduction, by developing the etched plate technology and demonstrating a 50kW single stack unit whilst in parallel developing a pressed plate manifestation of the architecture, manufactured using high volume techniques (pressing, injection moulding etc.) thereby, clearly demonstrating that the resultant technology is capable of meeting the power output requirements and cost objectives.

The ultimate objective of delivering a 50kW stack required a singular critical development in the etched technology, scale-up of the cell active area from 200cm^2 to 600cm^2. However, the risk associated with assembly of such a unit required a critical assessment of the design and manufacturing methodology of every individual component. An initial assessment highlighted areas where the scale-up would present the greatest risk, allowing the effort to be focused on these components. In developing the etched plate technology, the manufacturing methods of each component and the stack assembly methods were individually reviewed. Improving the manufacturing yield of components required the redesign of some components.

A 336-cell, 600cm^2 stack using etched plate technology, was successfully designed, assembled and tested. It was demonstrated delivering 70kW, exceeding the programme target by 40% and as a result of quality control and design improvements performed at an efficiency level above that previously demonstrated in smaller scale units.

In a parallel work stream, the development of a pressed plate implementation of the architecture was carried out. After an initial concept design phase, the manufacture of fundamental elements such as the plate and a fluid distribution component were

addressed; specific tool features were developed in order to achieve satisfactory forming of the plate and design compromises were needed in order to simplify the manufacture of the fluid distribution component.

Single cell testing of the pressed plate technology showed that performance similar to that of the etched plate could be achieved, but stack testing highlighted performance imbalances believed to be due to the difficulty of matching diffuser dimensions to the working dimensions of the other components. Scaling up of the pressed component to triple width was successfully achieved and short stacks demonstrated performance similar to that of the single width pressed plate.

Analysis of the pressed technology performance data showed that despite the slightly poorer performance (attributable in the main to the use of a lower conductivity steel alloy), the resultant gravimetric power density exceeded that of the etched plate architecture, whilst the pressed bipolar plate cost was projected at less than 10% of the cost of etched bipolar plates in volumes of 3 million per annum. The costing highlighted that some components, notably the MEA and diffusers and fluid distribution components, require further development in order to bring their costs in-line with those of the bipolar plate achieved under this programme.

In a parallel collaborative task, Johnson Matthey Fuel Cells (JMFC) addressed the development of their MEA technology for use in IE fuel cells. In Phase 1 of this project, the primary objective was to develop a MEA for operation on pure hydrogen that demonstrated progress in IE single cell hardware towards enhanced and stable performance, with a goal of at least 0.65V at 400mA cm^{-2} measured off gold tabs, between the gas diffusion layer (GDL) and stainless steel flow field plates, in Phase 1 single cell hardware. The secondary objective was to develop a MEA for operation on reformate that would achieve at least 95% of the hydrogen target (0.618V at 400mA cm^{-2}).

In Phase 2 of this project more aggressive targets were set. The primary objective was to develop a MEA for operation on pure hydrogen that demonstrated progress in IE single cell hardware towards enhanced and stable performance, with a goal of at least 0.65V at 500mA cm^{-2} measured directly off the stainless steel flow field plates. The secondary objective was to develop a MEA for operation on reformate (50ppm CO) that demonstrated progress in IE single cell hardware towards an enhanced and stable performance, with a goal of at least 95% of the pure hydrogen performance at 500mA cm^{-2} (618mV), with a maximum anode air bleed of 2.0%. These represent significant performance improvements over that previously achieved in this hardware.

The MEA development work performed in Phase 1 employed developmental JM GDL materials in Phase 1, and a commercial GDL material (currently used by IE) in Phase 2, and specific commercially available membranes selected for good water diffusional characteristics. The focus of the MEA design for hydrogen operation was on the development of improved catalyst layers with optimized performance and stability in combination with the selected GDL and membrane materials. For reformate operation, the focus of the MEA design was on the development of improved reformate tolerant anode catalyst layers with optimized performance and stability. The catalyst-coated membrane (CCM) approach to MEA construction was

employed throughout to minimize any influence of the substrate on the catalyst layer structure properties.

In Phase 2, a new etched-plate heated single cell was developed by IE for use in this activity, with the intention of simulating more closely the operating conditions within IE stack hardware. This was an improved design, based on learning in the first phase of the project. In the commissioning phase significant work was performed to optimize the protocol for measuring the voltage off the cell stainless steel plates. Voltage measuring points off the plates were determined that best represented the voltages that would be measured in a full stack configuration. These were used for the subsequent MEA testing, and the performance data obtained in this activity is expected to translate more closely to full stack data.

In the final phase of the project, MEA designs for hydrogen operation demonstrated excellent performances, in excess of the targets by 10mV, but with high degradation rates due to water build up in the cathode layer. Further gains in performance were obtained by improving the structural interactions to increase the effective activity of the cathode catalyst, but the key was to maintain this important characteristic, whilst also altering the catalyst layer to enhance transport properties within the catalyst layer and improve stability. The final optimized MEA structure demonstrated both excellent performance of around 670mV at 0.5A cm^{-2}, some 20mV in excess of the new performance target, and maintained this performance level for well over the 100 hours that the MEAs were evaluated over in this activity.

Also in Phase 2, under reformate operation, the best new MEA types comfortably exceeded the performance target of 618mV @ 500mA cm^{-2} at the start of testing, and consistently achieved ca. 650mV. These results were also achieved at the target air bleed level of 2%, significantly lower than that used previously. The MEAs could be run for longer than 500 hours at the 2% air bleed level without any dramatic MEA performance failure due to significant reactant gas crossover arising from membrane weakening and pin holing. There was however, a decrease in performance over the 500 hours of testing, of ca.150mV, that diagnostics indicated were due equally to losses at the anode and cathode. The anode losses were thought to be due partly to anode flooding but also to the low level of air bleed being not quite sufficient to avoid a slow build up of CO and long term poisoning of the anode. Cathode losses were consistent with a build up of water in the cathode GDL and catalyst layers, but there was also evidence that a loss of oxygen reduction activity could also have contributed to the losses.

In conclusion, the MEA design approaches followed in this activity have enabled significant advances in hydrogen operation performance and stability over that previously attained in IE hardware, and the advanced performance targets set for this project have been successfully met. These are practical MEA designs and are immediately amenable to manufacturing in volumes without significant further process developments. JMFC and IE will pursue possible opportunities for further exploitation beyond the scope of this project. The stack development targets of this programme have also been successfully achieved. IE has shown that its stack technology is scaleable to automotive size units and successfully addressed the necessary technical issues in doing so. Fundamental aspects of the pressed plate technology (injection moulding of the plastic fluid distribution component,

overmoulding of a rubber seal onto this component and pressing of a thin metal bipolar plate by conventional pressing means) have been shown to be practical for high volume manufacturing techniques, but in order to meet programme deadlines they were not always used in the demonstrated stack technology.

CONTENTS

1 INTRODUCTION

Intelligent Energy (IE) is the UK's leading developer of PEM fuel cell stack and system technology. Its unique, evaporatively cooled PEM stack architecture has class-leading capabilities; stacks are able to deliver >2kW/L and have been employed in micro-CHP, automotive and aerospace applications. This technology offers many advantages over conventional liquid cooled architecture, including reduced component count, simplicity and greater uniformity of heat and fluid management, whilst also permitting the rationalisation of external plant hardware in fully integrated systems. However, two major obstacles have yet to be addressed, scale and cost.

Prior to this project the technology had not been demonstrated in a full automotive scale system. Individual stacks have been limited to a maximum of 12.5kW by fluid management, manufacturing and cost issues, hence high power systems had been constructed using a multi-stack architecture, which places unnecessary constraints on the system design in order to evenly distribute fuel, oxidant and coolant between multiple stacks and also requires tight quality control to "balance" stacks. The design and demonstration of a single automotive scale unit is a critical task in the development programme and in proving IE stack technology.

IE's stacks are presently assembled using thin (0.6mm) bipolar plates manufactured by a photochemical etching technique. This method offers high levels of precision, design flexibility due to low tooling costs and relatively quick manufacture but will not, in the long term allow the manufacture of bipolar plates at the costs necessary to bring about full scale commercialisation of PEM fuel cells.

The overall aims of this programme were to further develop the existing etched plate based architecture and demonstrate it in a single ~50kW scale unit, whilst in parallel developing a pressed plate manifestation which would demonstrate a gravimetric power density double that of the etched plate (i.e. 1kW/kg) maintaining the same volumetric power density (2kW/L) and also showing a clear route to volume production and the associated cost benefits; the programme thus progressed in two streams.

The *"etched route"* focused on the development and scale-up of IE's small-scale proven technology, the principal focus was the design and associated engineering of an enlarged format bipolar plate, but these processes also required a detailed analysis of component manufacturing capabilities to ensure that the design could be produced and that the completed stack could be assembled and would function to specification when complete.

The *"pressed route"* faced a greater challenge, since at the outset of the programme none of the conceptual componentry had a manufacturing history – unlike IE's etched plates whose production technology was already well understood, IE had little experience in the design and manufacture of pressed plates or the associated functional parts. This route, therefore, needed to explore the capabilities of metal pressing and plastic moulding whilst simultaneously developing a design concept which was within their means.

A major advantage of this programme construct was that the pressed route would "lag" behind the etched route and thus, the lessons learnt during etched plate scale-up would benefit the pressed plate development and scale-up programme.

In a parallel work package, Johnson Matthey Fuel Cells were supplied with a specifically designed and built single cell assembly enabling them to test and develop their MEA-diffuser technology under IE's unique fuel cell operating conditions. The aim of this work was to achieve and exceed the performance of IE's incumbent (third party) MEA-diffuser technology (80A at 0.65V) by directly addressing the performance limiting factors and optimising the MEA and diffuser characteristics accordingly. It was originally intended that initial work would focus on the implementation of the JMFC MEA and diffuser materials under hydrogen and CO-contaminated reformate conditions thereafter the technology would be applied to the pressed plate technology and modified as required; however, the pressed plate development process was slower than expected due to tooling lead-times and as a result the second half of the JMFC programme was realigned such that instead of developing a first phase MEA for pressed plate technology , they developed a second phase MEA for etched plate technology with more aggressive performance targets (100A at >0.65V).

2 ETCHED PLATE DESIGN AND SCALE-UP

2.1 Design Intent

The primary aim of the etched plate development work stream was to scale-up the technology to allow the assembly and demonstration of a 50kW unit. It was clear that such a task would be impractical using IE's incumbent 200cm^2 active area, where the current would be limited to a maximum of 140A (based upon state-of-the-art performance levels), and as such the stack would require over 500 cells. Increasing the active area (by designing in a "multiple width" manner) was deemed to be a more flexible solution; this enabled the stack to deliver more current at a given voltage whilst an additional benefit of this approach was that it broadened the portfolio of stack sizes which IE could offer. However, even with an active area increase, a 50kW unit was expected to contain more cells than had previously been assembled in a single unit by IE (previous max size was 80cells), thus successfully building a 50kW unit would require a detailed experimental programme to allow fluid port sizes to be correctly sized.

Further objectives within the scale-up brief were to address the design of all components such that their functionality (and hence stack performance) was as close to optimum as possible whilst also gearing the designs towards medium scale-manufacturability (since the pressed plate development was the true, full scale manufacturing target), making the most efficient use of raw materials and, where possible reducing the costs of manufacture by minimising the number of processing steps. Simplistically, this was achieved on a component-by-component basis, but in reality compromises to some components were required in order to facilitate the optimisation of other, more expensive items. Perhaps the most important aspect was to analyse the design-related factors which had a negative impact upon manufactured stack quality and performance; this necessitated an analysis of typical and most frequent assembly faults and the design of solutions to prevent them.

2.2 Component Manufacturing and Quality Constraints

A rapid design process was initiated during which the sizes of "multi-width" components were calculated and the manufacturers interrogated as to the capabilities and limitations of their manufacturing techniques. Ultimately, two factors determined the size of the scaled-up design (i) maximum MEA size capability of IE's incumbent supplier, (ii) bipolar plate handleability. However, during the development process, issues were highlighted with all components.

2.2.1 Membrane-Electrode Assembly

At the outset of this programme, discussions with IE's MEA supplier identified a number of possible problems with regard to enlarged MEAs. The most important was manufacturability and it transpired that IE's MEA design was particularly difficult to manufacture because of the porting arrangements which required a large number of complex shaped cutting tools which were neither cheap nor quick to manufacture. Although a principal aim of the work was to optimise the ports, IE design centre did not believe that the fluid management functions required from the porting arrangement could be satisfied using a reduced porting arrangement, hence a technology strategy decision was taken to design the MEA with no fluid ports, this allowed the MEA manufacture to be simplified and therefore reduce the MEA cost,

but also offered a potential benefit in terms of inventory, since the major development required in scaling up the number of cells in the stack is port sizing – by removing the porting requirement from the MEA it meant that MEAs could be ordered in advance without risking them being made unsuitable by port size changes (this is a particular advantage when in development mode since the MEAs are typically on a 14week lead time).

2.2.2 Bipolar Plate

IE's metallic bipolar plates are manufactured by a photochemical etching procedure – this method allows intrinsically good tolerances to be achieved for position of features but requires precise control to achieve depth tolerances (where features are partially etched as opposed to through-etched). IE has worked intensely with the manufacturer to develop and implement a bipolar plate quality control system which uses bespoke quality control equipment to measure the pressure drop of each plate.

The manufacturing procedure for 200cm^2 plates involves the etching of three plates side-by-side on a raw material sheet, see figure 1, hence, the manufacture of a "triple width" plate was a design which gave a high level of confidence. Manufacturing test runs were carried out to assess the consistency of etching across a triple width format, see figure 2, yielding unexpected results – whilst the depth and width of tracks was found to be well within tolerance, handling of the plate was awkward as the flowfield design tended to remove strength from one axis of the plate presenting potential assembly difficulties; this property effectively limited the upper size of the enlarged format since larger plates were deemed likely to be too large to handle safely and possibly even liable to stress failure during the manufacturing process because of their own mass.

Work also looked at methods to reduce the frequency of plate inspection required. Figure 3 shows the results of "mapping" the bipolar plate quality control parameter across a number of production sheets; the consistency indicates that measurement of only one plate can provide sufficient information regarding the quality of all plates on the sheet.

Bipolar Plate Sensitivity

Prior to this test programme, stack assembly was carried out using bipolar plates sorted according to the QC parameter as measured on the air face. This process was extremely laborious placing emphasis on stock control, plate identification and required a great deal of effort during the assembly in order to allocate the appropriate quantity of plates, arrange them in order and then identify and withdraw them from stock. The performance of two stacks was therefore compared, the first utilised the existing strategy whilst the second was built using stacks from one of two "bins". The bins were created by dividing the bipolar plates into "high" and "low" groups (the groups being respectively the upper and lower halves of the manufacturing tolerance band).

Figure 4 shows the cell voltage distribution of these two stacks operating at 80A. Clearly, there is a slight difference between the mean cell voltages of the stacks (and thus the overall stack voltages), but this could be due to many factors, including stack conditioning time, atmospheric pressure, ambient temperature etc. More important is the difference in standard deviation of the cell voltages; the stack with

sorted bipolar plates has a standard deviation of 8.3mV, the stack with “binned” i.e. non-sorted plates has a standard deviation of 9.1mV, this difference is effectively insignificant and meant that a large portion of the stack pre-assembly procedure could be simplified by dividing the bipolar plate stock into high and low groups.

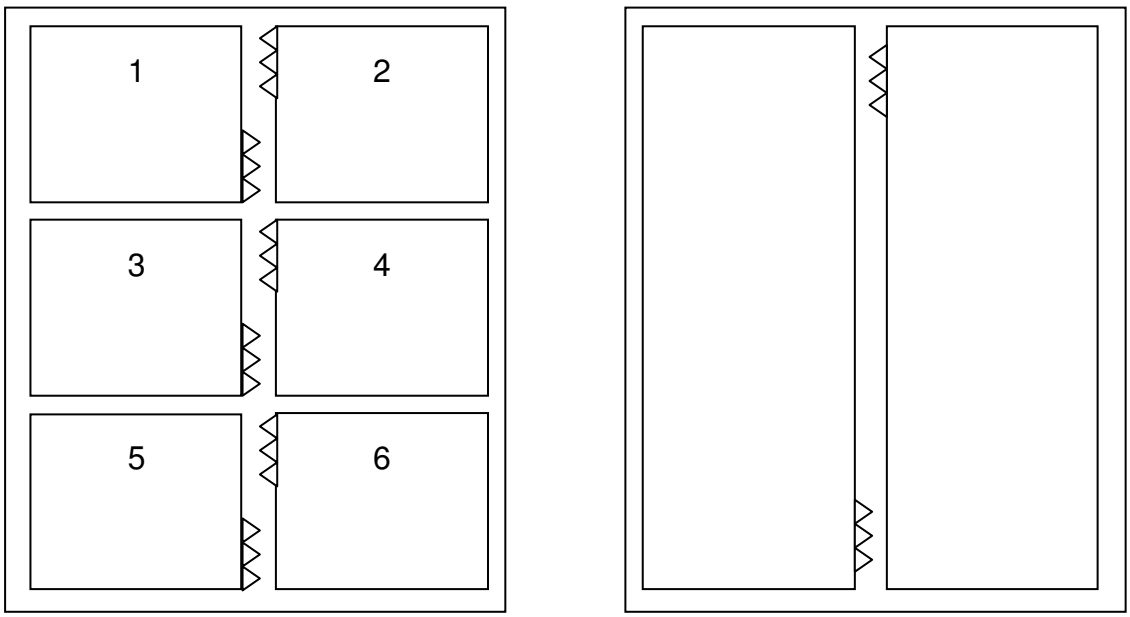

Figure 1. Arrangement of plates in the sheet for etching.

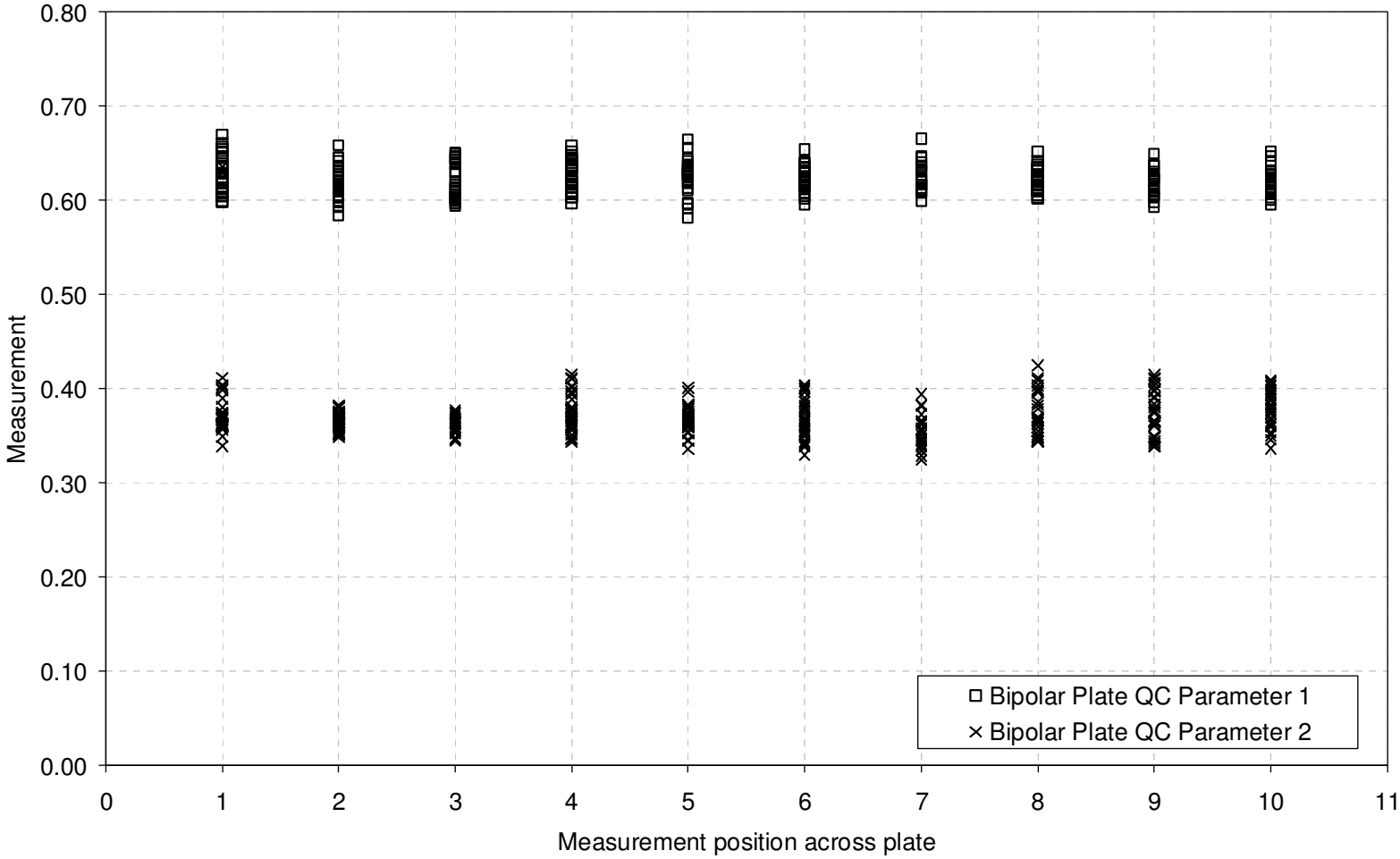

Figure 2. Variation of QC parameters across a triple width plate.

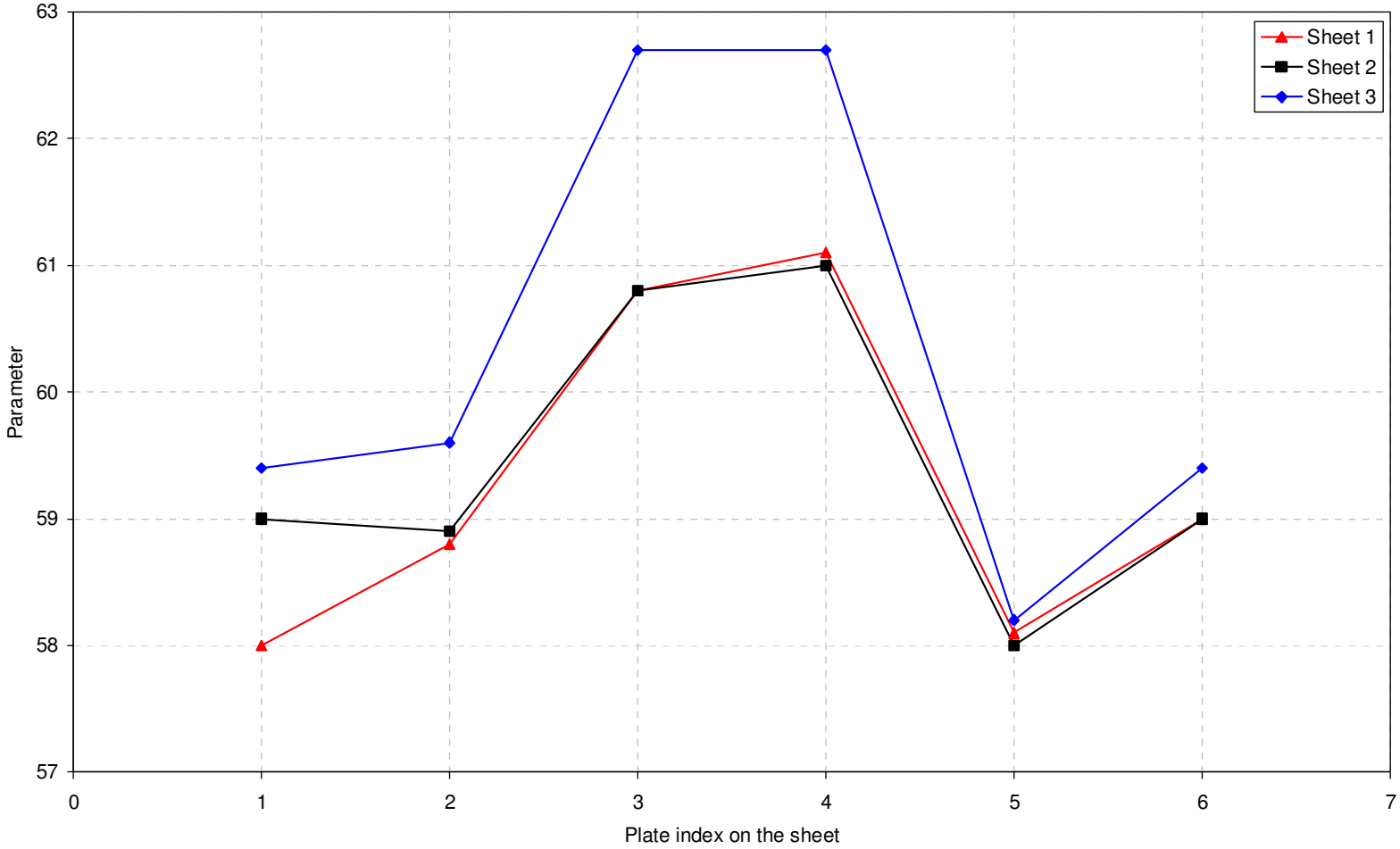

Figure 3. QC parameter vs. plate index position.

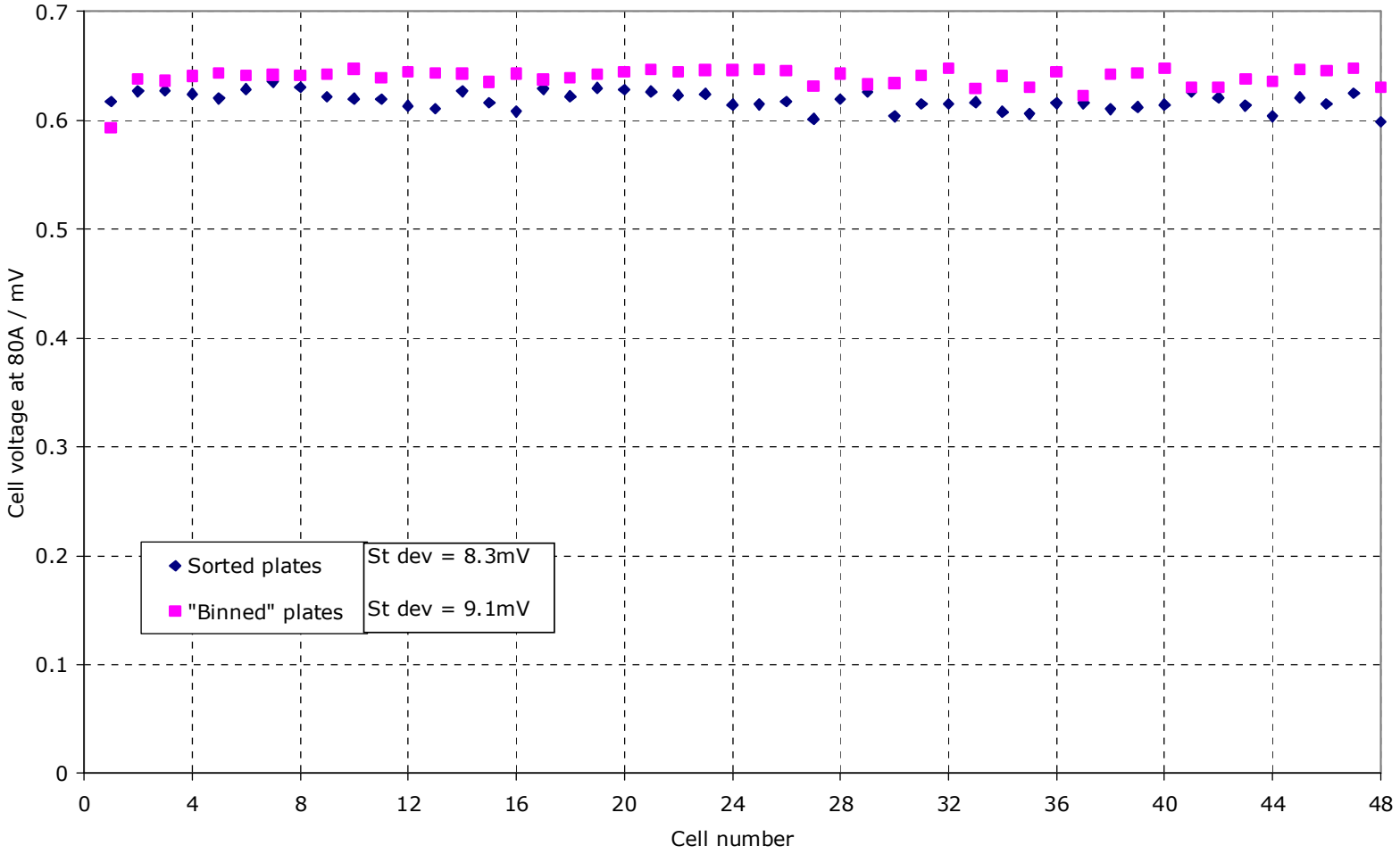

Figure 4. Cell balance at 80A for stacks with different bipolar plate selection strategies.

2.2.3 Diffusion Media

Dimensional issues were not found to present any difficulties for the production of the gas diffusion medium; the material is manufactured in a roll form and then cut to size using standard knife cutting tools on a press, and initial worries regarding handling were easily addressed by the introduction of pre-assembly jigs. However, quality control of this material had not previously been examined in detail and discussions with the manufacturer showed that there was only limited quality control carried out during its production.

As part of the quality assessment programme a series of tests were defined to measure basic parameters of the as-received material, the data generated was then compared with stack performance data acquired from stacks built using the test pieces. Diffuser measurements were;

1. Thickness
2. In-plane pressure drop
3. Mass

Test 1 – Thickness

Measuring the thickness of soft materials of this type (essentially a compressible fibrous material) presents a major technical issue – the act of executing the measurement invariably changes the rest dimension of the material and thus, in order for measurements to be reliable and reproducible they must be carried using a constant force gauge. Such instruments are freely available and a study of component thickness dimensions was carried using an appropriate instrument. It was observed that although highly reproducible measurements were produced on a single measurement point, the variability across each component was considerable, and as such generating an accurate reflection of the dimension of each component would be difficult. An alternative apparatus was designed, this comprised a 10kg mass with a digital dial test indicator (DTI) in-built; the measurement was then performed by laying the test component on a smooth granite engineering table and placing the 10kg mass on top of the component, the DTI then measured the distance from the underside of the mass to the table. The measurement so generated represented the average thickness of the component at a mean compressive force of 0.5N cm^{-2}.

Measurements generated by this method were checked for reproducibility by measuring the same component 10 times; this generated a data set with a standard deviation of 1.4 m.

Test 2 – In-Plane Pressure Drop (dP)

The characteristics of Intelligent Energy's stack technology mean that the in-plane pressure drop of the diffuser component is an important parameter. A measurement rig was designed and constructed such that this parameter could be characterised for each individual diffuser. The equipment uses a press to compress the diffuser to a test dimension (governed by a machined cavity within a test plate), whilst under compression a mass flow controller feeds air through the diffuser and a pressure transducer measures the back-pressure generated by the diffuser; this test

partially simulates the movement of gas within the stack. Figure 5 shows typical test results of both thickness and dP.

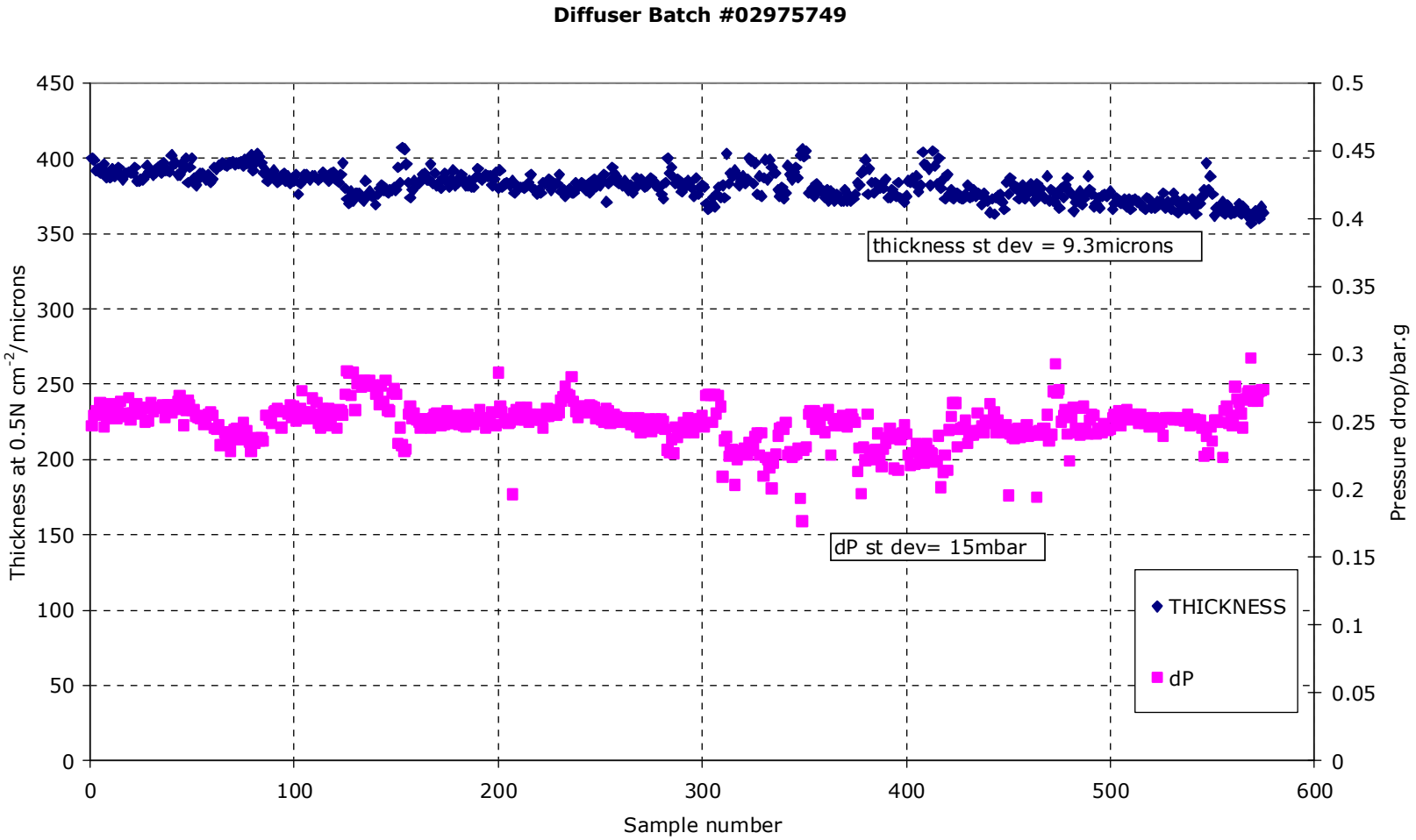

Figure 5. Typical diffuser test results.

Looking at the data from a purely material point-of-view, it was clear that variability was present within the samples, but that batch-to-batch variability was more significant (see table 1), this suggested that stack assembly may have to use material on a single batch basis. What was unclear from the data was the criticality of the thickness and dP properties to fuel cell performance.

	LOT	Quantity	Mean thickness/ m	St dev/ m	Mean dP	St dev/bar.g
1	02793039	442	408	8.3	0.288	0.020
2	02925607	225	436	6.2	0.194	0.021
3	02892097	375	431	5.6	0.261	0.011
4	02975747	464	372	11.6	0.270	0.023
5	02747325	150	424	3.7	0.294	0.019

Table 1. Test data for various diffuser batches.

Test 3 – Diffuser Mass

This was a simple measurement of the mass of the component measured on a six-place balance. Typical results are shown in figure 6 - the distribution is quite tight although there are noticeable outliers, the significance of these is difficult to determine because of the fragile nature of the material.

Diffuser Parameter Sensitivity

After designing and using the tests to accrue data characterising the diffusion media it was necessary to build and test stacks, analysing the data to elucidate any significant correlations between poorly performing cells and the data corresponding to the diffusers contained therein.

Simple attempts to correlate mass (figure 7), dP (figure 8) and thickness (figure 9) did not yield strong relationships and hence none of these parameters influence a cell's stable operating voltage. It was observed that air flow sensitivity was a critical stack performance parameter and that some cells were highly sensitive to air flow which resulted in the whole stack requiring higher than desired air flow (this is an important factor in integrated systems because of the associated impact upon compressor technology, sizing and parasitics). Thus, more complex correlations were examined and of these, one of the most interesting is shown in figure 10. In this chart, the difference between the anode and cathode diffuser thickness measurements is compared with the sensitivity of the cell to a decremental change in air flow; under such a change cells would normally be expected to fall in voltage, the chart indicates that such sensitivity to air flow is smallest when the cathode diffuser is thinner than the anode diffuser.

Similar tests showed sensitivity to diffuser dP, but found no correlations with diffuser mass; further stacks built using diffuser arrangement strategies showed that the dP parameter is more important than thickness in determining cell flow sensitivity. Despite this, testing also showed that whilst diffuser dP could be used as the primary diffuser QA parameter, certain diffuser thickness rules had to be observed and outliers or distribution end parts (see figure 11 and figure 12) needed to be discarded.

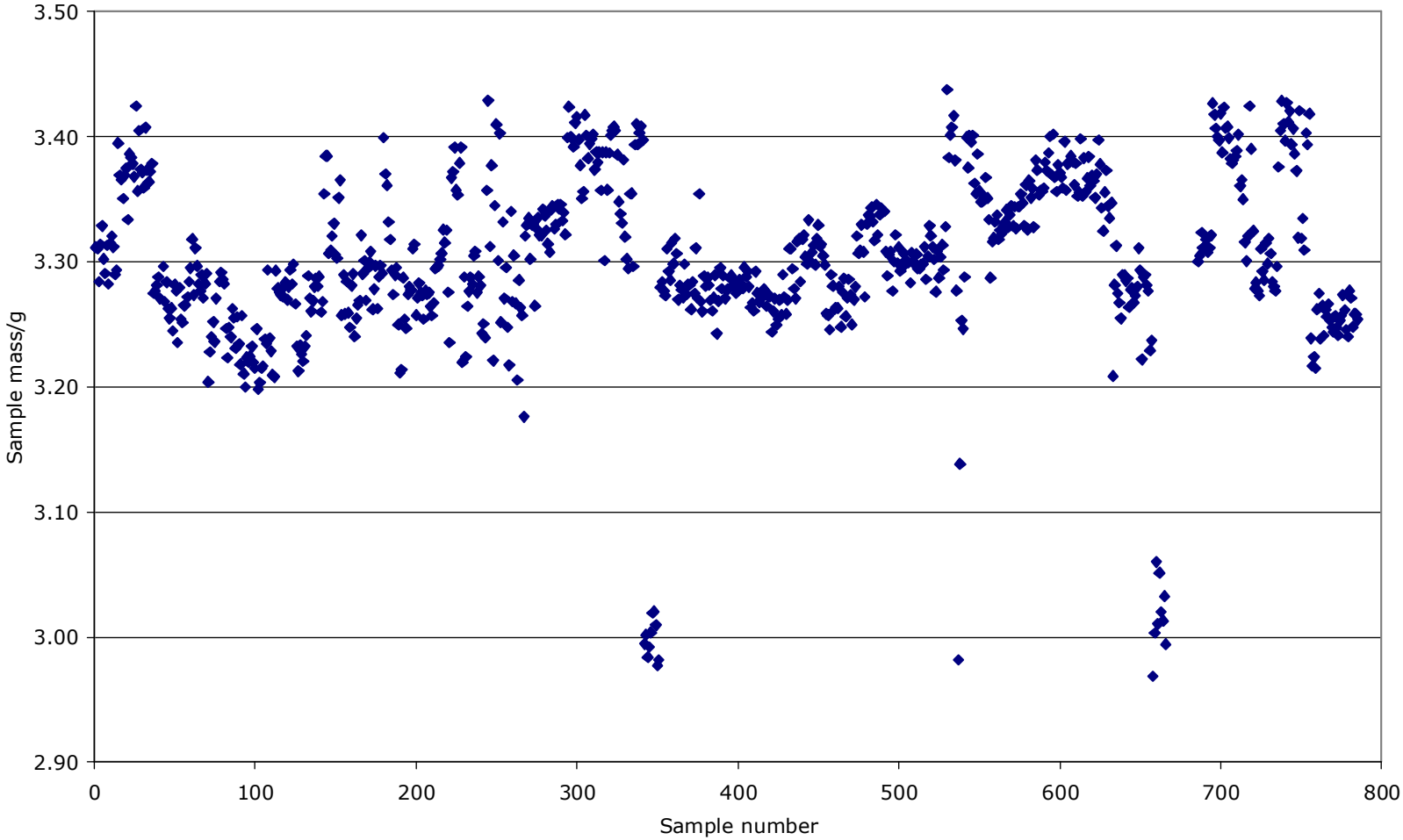

Figure 6. Diffuser mass results.

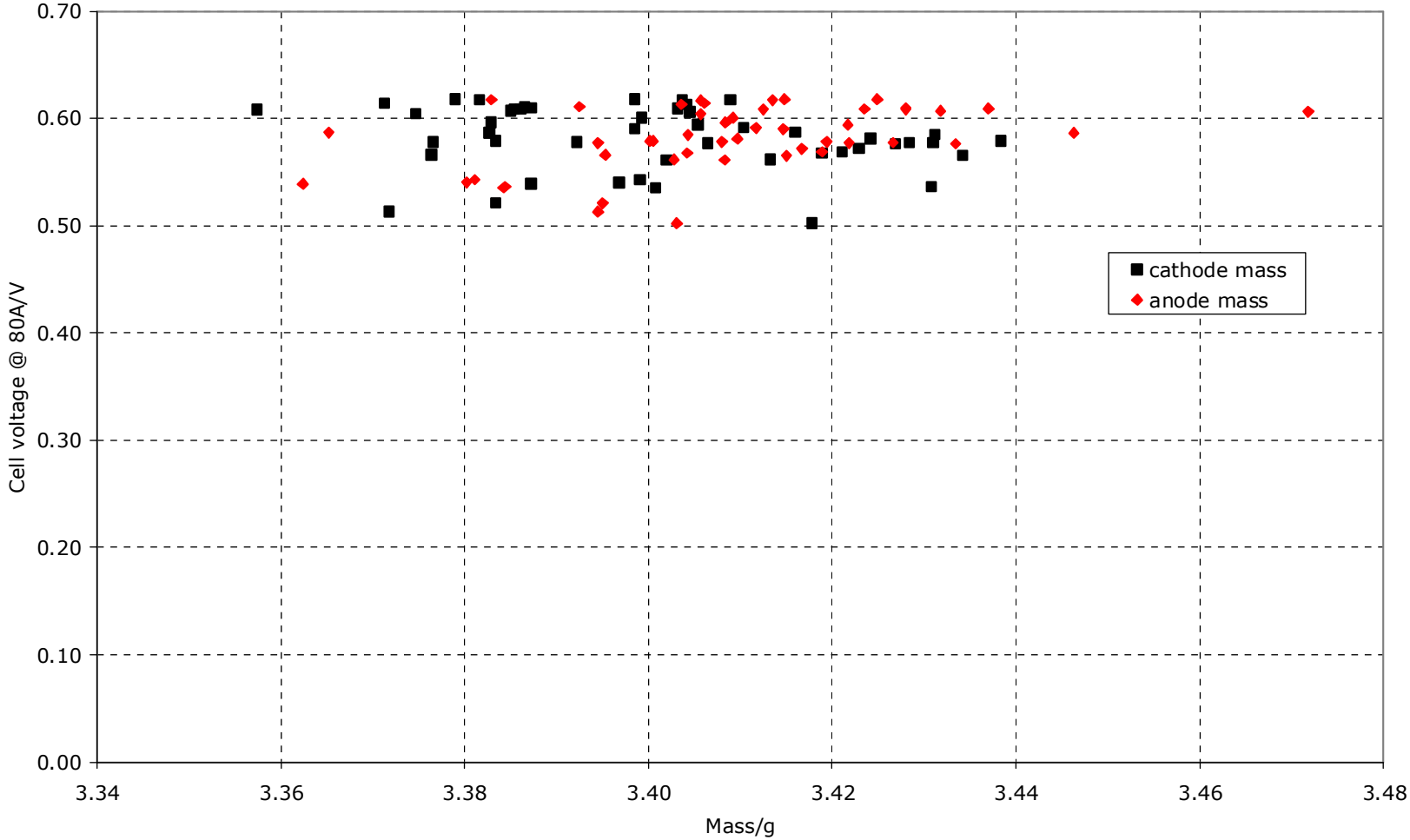

Figure 7. Cell voltage vs. diffuser mass.

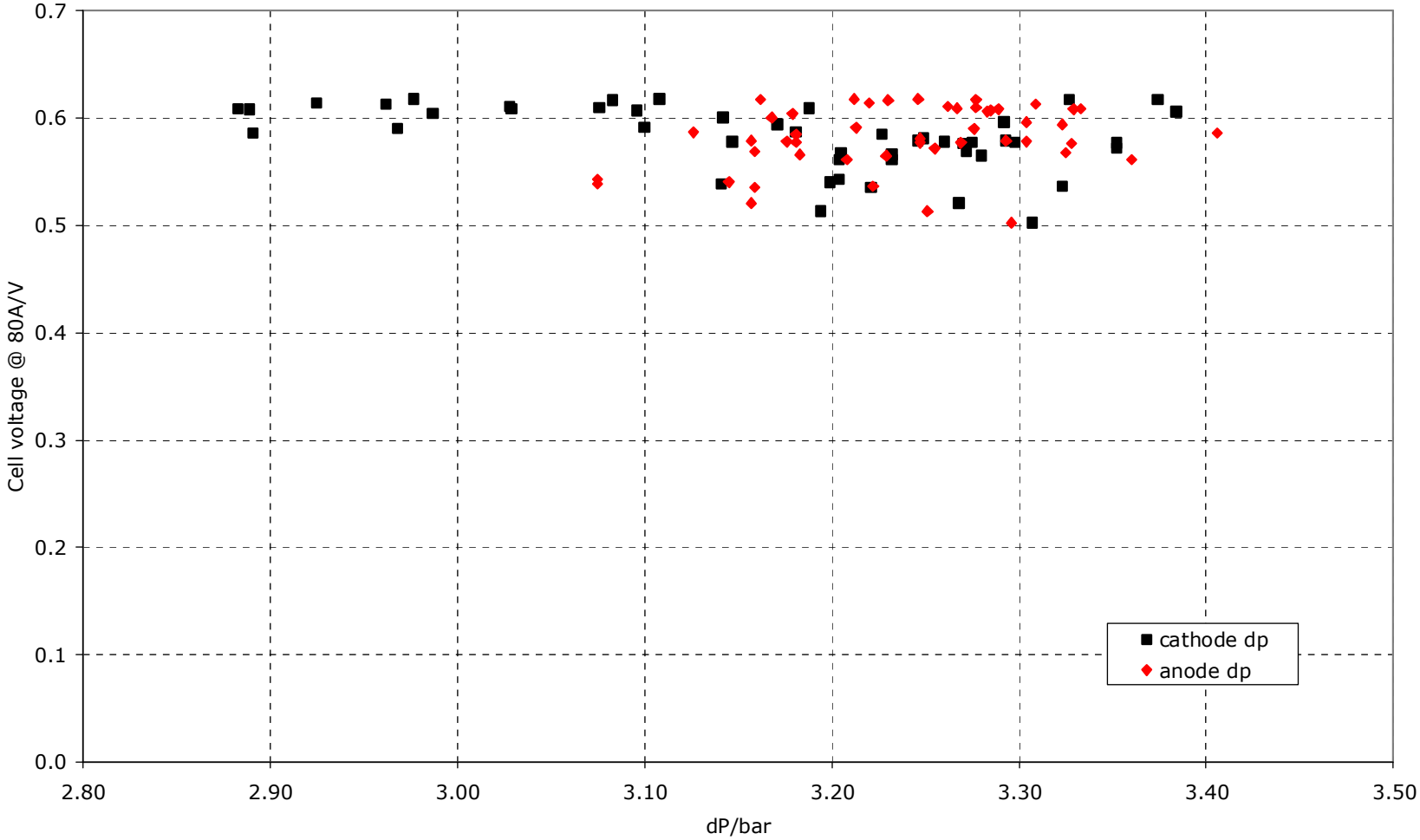

Figure 8. Cell voltage vs. diffuser dP.

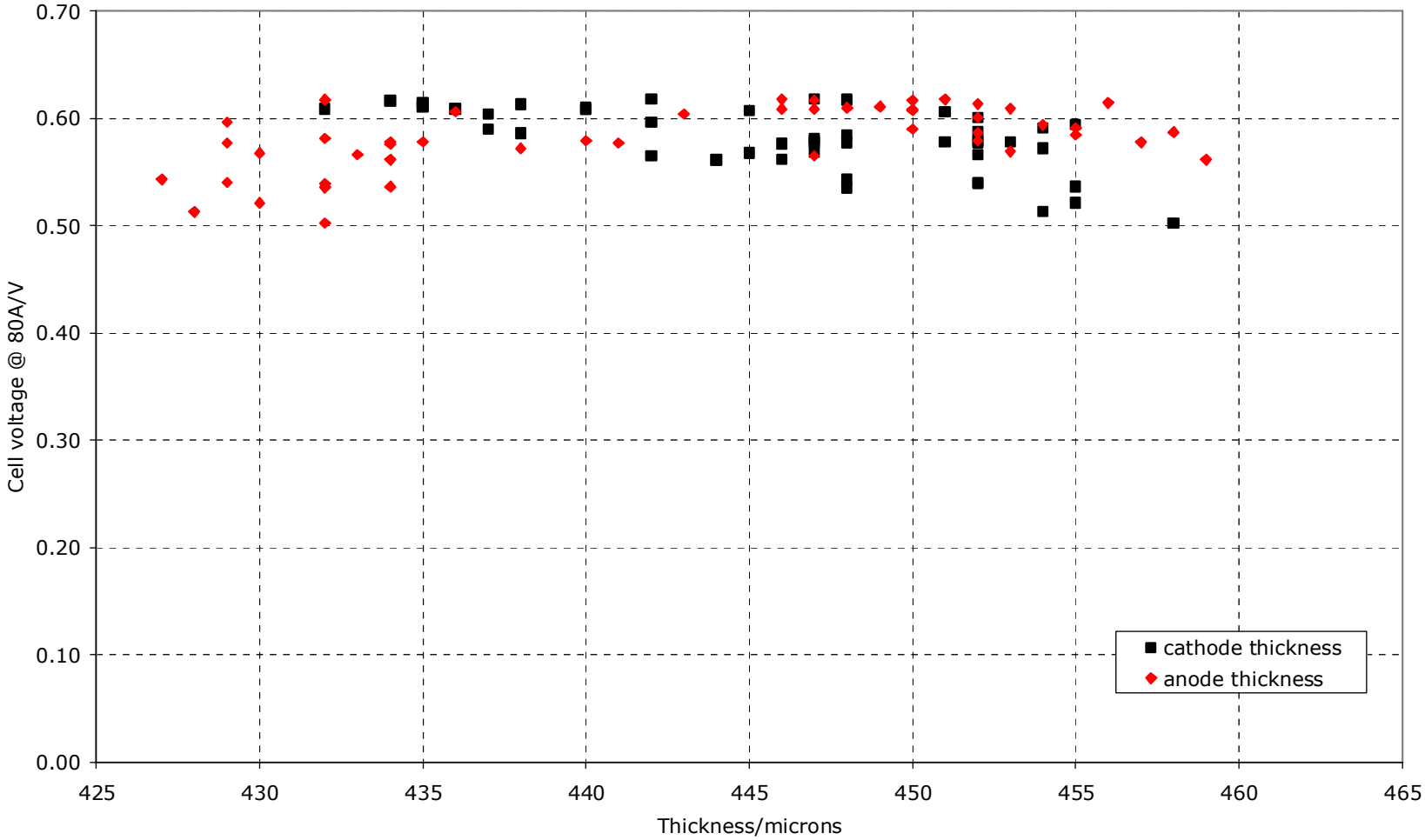

Figure 9. Cell voltage vs. diffuser thickness.

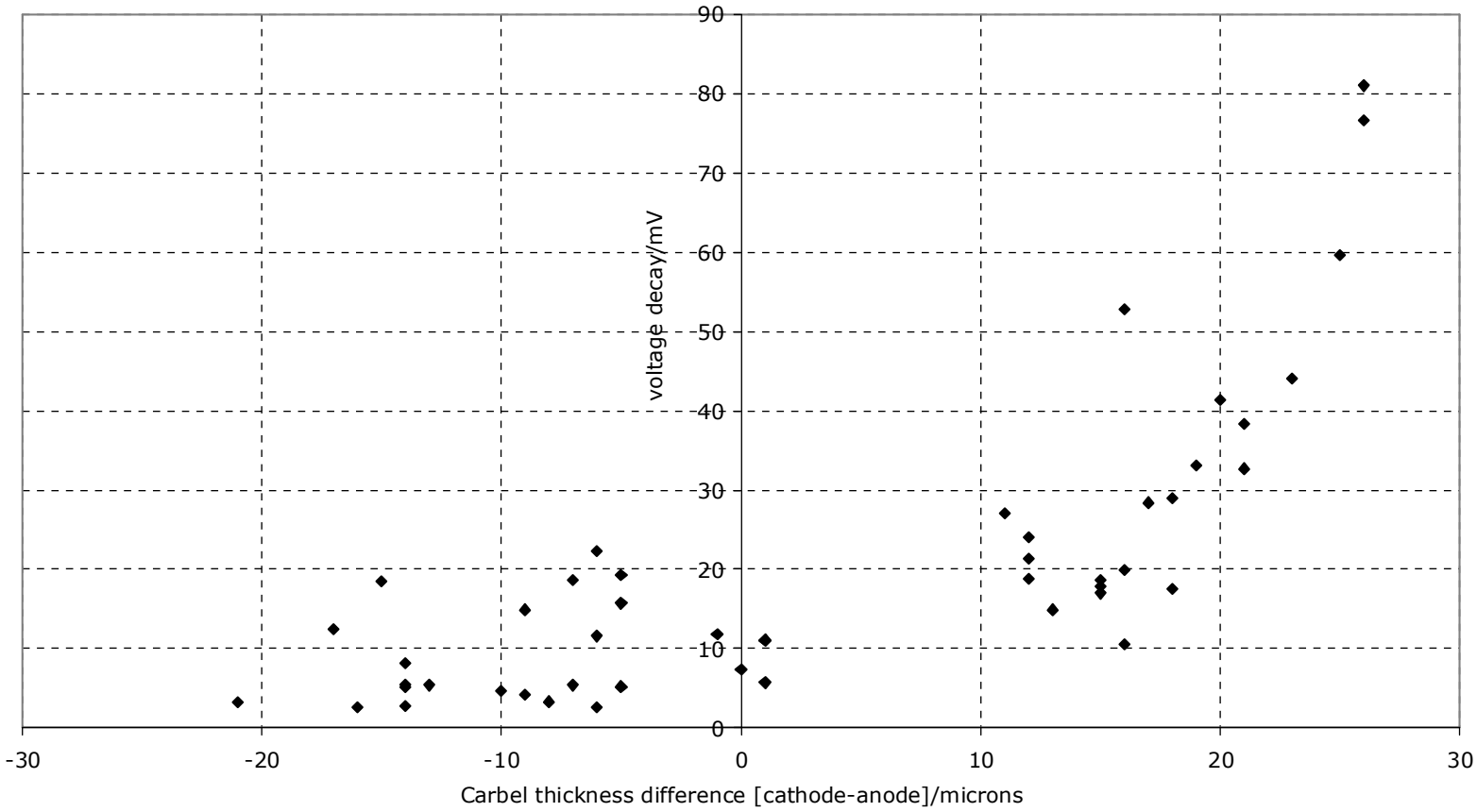

Figure 10. Relationship between air stoichiometry sensitivity and anode-cathode diffuser thickness difference.

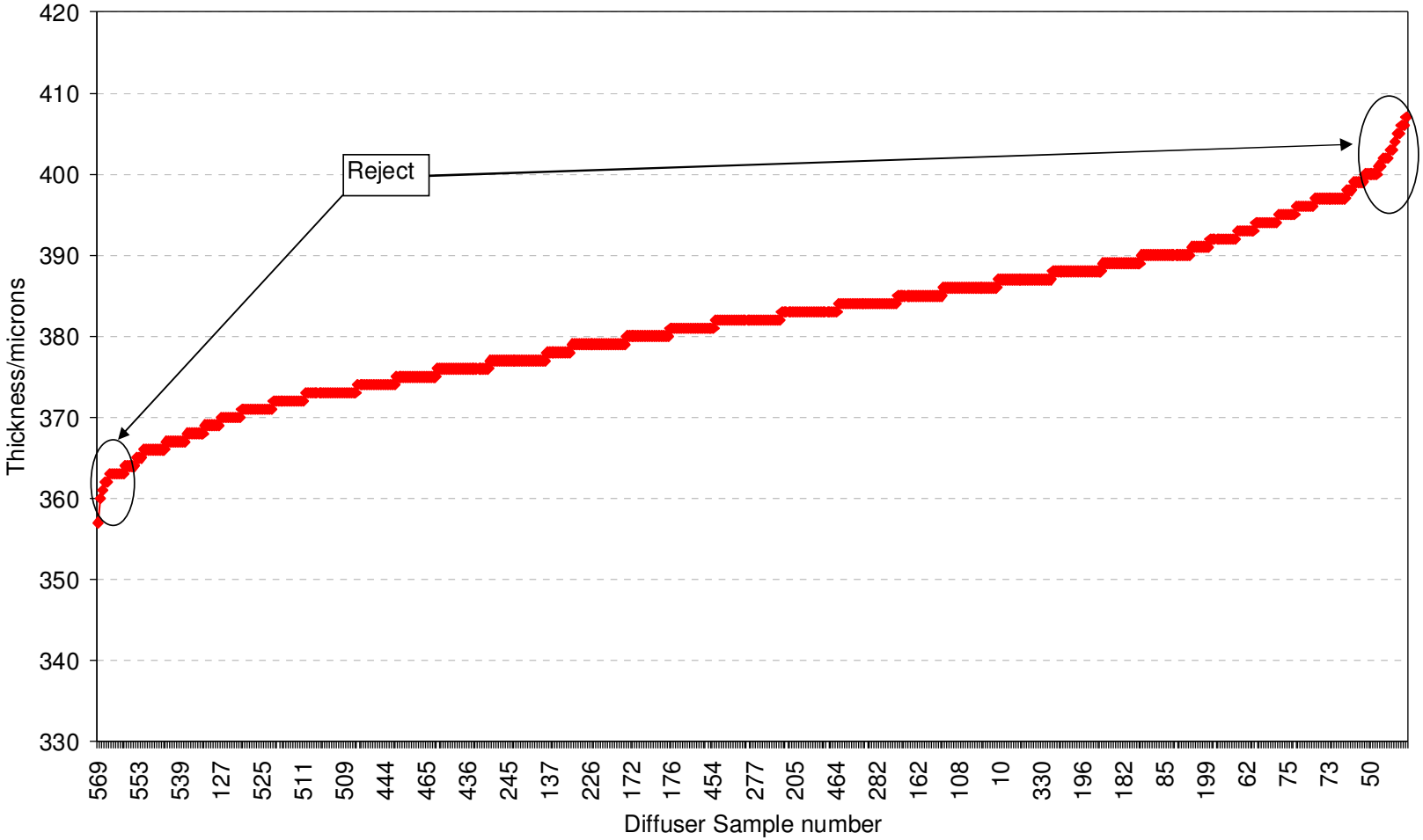

Figure 11. Ordered thickness profile of a diffuser batch showing parts rejected for assembly.

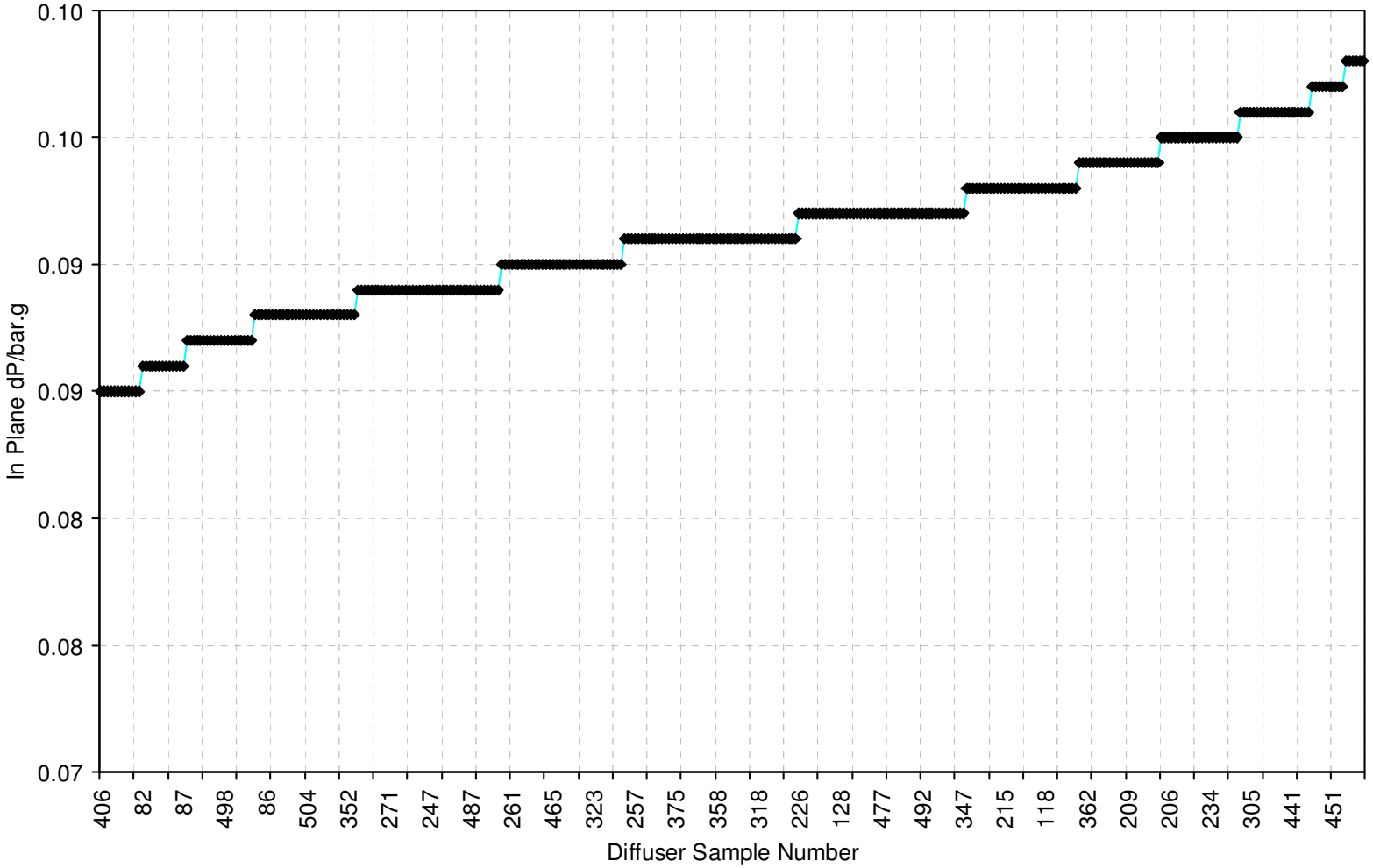

Figure 12. Ordered dP profile of a diffuser batch showing parts rejected for assembly.

The diffuser quality control procedures highlighted a critical problem – manufacturing batch size and the reject/discard rates discussed above, limited the number of cells and hence stack size that could be built to 200-220, selection of series' of diffusers with appropriately matched properties could not be achieved for bigger stacks (even though different batches had been successfully used for anode and cathode phases). Such a limitation would necessitate using a larger format stack, the upper limit of which had already been set at 600cm^2 (triple width) by bipolar plate handling and manufacture, as discussed.

A programme to identify alternative diffuser materials was carried out which, after considerable ex-situ testing to identify materials with suitable properties in terms of load vs. compression, resistance and porosity, identified a non-woven material (the incumbent diffusion medium was based upon a woven cloth). Whilst having suitable mechanical and electrical properties, this material was also up to 50% cheaper in volume. A quality control investigation was performed in a similar vein to that previously described in conjunction with in-situ characterisation (in working stacks and single cells). The data, shown in table 2, indicates that the statistical spread of parameters is similar to that of the woven diffuser, although the dP figure has a fractionally larger standard deviation.

	LOT	Quantity	Mean thickness/ m	St dev/ m	Mean dP	St dev/bar.g
1	1/04/17	100	413	9.1	0.277	0.030
2	1/04/11	259	363	7.5	0.374	0.043
3	1.04/15	394	378	10.4	0.354	0.032

Table 2. Quality control data for batches of the alternative diffuser.

Stack builds using this diffuser material showed a greatly reduced sensitivity to all diffuser parameters, in fact, the stacks performed well within specification, without a diffuser build strategy being required, no poor cells were identified and the weakest cells showed no diffuser related correlations.

2.2.4 Gaskets

The gaskets used by IE at the programme outset were manufactured by die-cutting of raw material produced in a roll format. Size/format issues were therefore not relevant once it had been established that the cutting tools and cutting process could be carried out satisfactorily; however, other issues were important:

1. the standard material (a silicone reinforced with a glass fabric) presents handling difficulties during assembly as it has little physical stiffness; this problem was shown to be important when triple width test pieces were cut.
2. the standard material has shown degradation during stack durability trials.
3. the standard material is not compatible with Intelligent Energy's development MEA concept (discussed previously)

To address these issues a programme of gasket development work was carried out.

Effort focused on the use of polyester film material which is compatible with the environment (high temperature, high humidity), has an acceptable degree of rigidity and is also physically strong, freely available and low cost. Initial testing showed that a basic polyester material was unusable as a gasket material as the interface

between metal and polyester did not seal to the degree required (see figure 13, this is principally due to the hardness of the polyester which has little "compliance" and hence cannot compensate for surface imperfections in the metal plate. Two streams of work were then initiated, the first looking at application of a compliant layer to the gasket material (polyester) and the second looking at applying it to the bipolar plate.

Initial work on the polyester-supported gasket focused on the use of a polyester film with an adhesive coating - these materials have some desirable properties including good sealing and the adhesive strength may become a benefit as mass-production becomes more of a reality, however it was found that at this stage the adhesives effectively make stack disassembly (for diagnostics, repair, post mortem etc) impossible, a seal which can be made and broken repeatedly is required.

Thus, the compliant seal material targeted was silicone rubber – it is likely that this is not a long term solution, degradation has already been identified as a problem but this material is available in a wide variety of specifications and curing methods, so it was decided that it would be the most appropriate starting point and that as the technology became better understood the transition to more suitable materials could be made.

Screen-printing was identified as a good manufacturing process to begin working with. This technique requires low cost tooling for initial trials (the cost of the screen and some locating jigs), but is capable of depositing thin layers of material in a precise manner. The design of the screen determines where material is printed so, in combination with a locating fixture, port hole features in the bipolar plate, for example can be printed around and the risk of depositing material in the flow field tracks may be eliminated.

Printing on Polyester

Initial work to assess the silicone application process indicated that the surface condition of the polyester was critical – polyester film is available in a variety of pre-treated forms, the pre-treatment being designed to promote "ink-adhesion" or reduce static charge accumulation for example. It was observed that in some cases the pre-treated surface had no affinity for the silicone ink and hence there was no transfer through the screen during the printing process – several grades have now been identified which are compatible. A further issue arose when the silicone was cured; the curing mechanism for the silicone that had been selected was thermal, at a temperature of 130°C, it transpired that some of the first polyester materials used as gasket substrates were manufactured in their finished thickness by stretching a thicker material at elevated temperature – thus, during curing of the silicone the polyester shrank producing a gasket which was too small.

Benefits of applying the seal to the polyester;

- the seal can be applied to the entire polyester sheet and then cut using standard cutting tools, this means that new screens will not be required if the port design is changed.
- The low mass of the component means that damage due to sliding of components across each other is less likely to result in damage.
- Defective gaskets can be identified during assembly and disposed of.

- The gasket can be manufactured in parallel to other stack components reducing lead times.

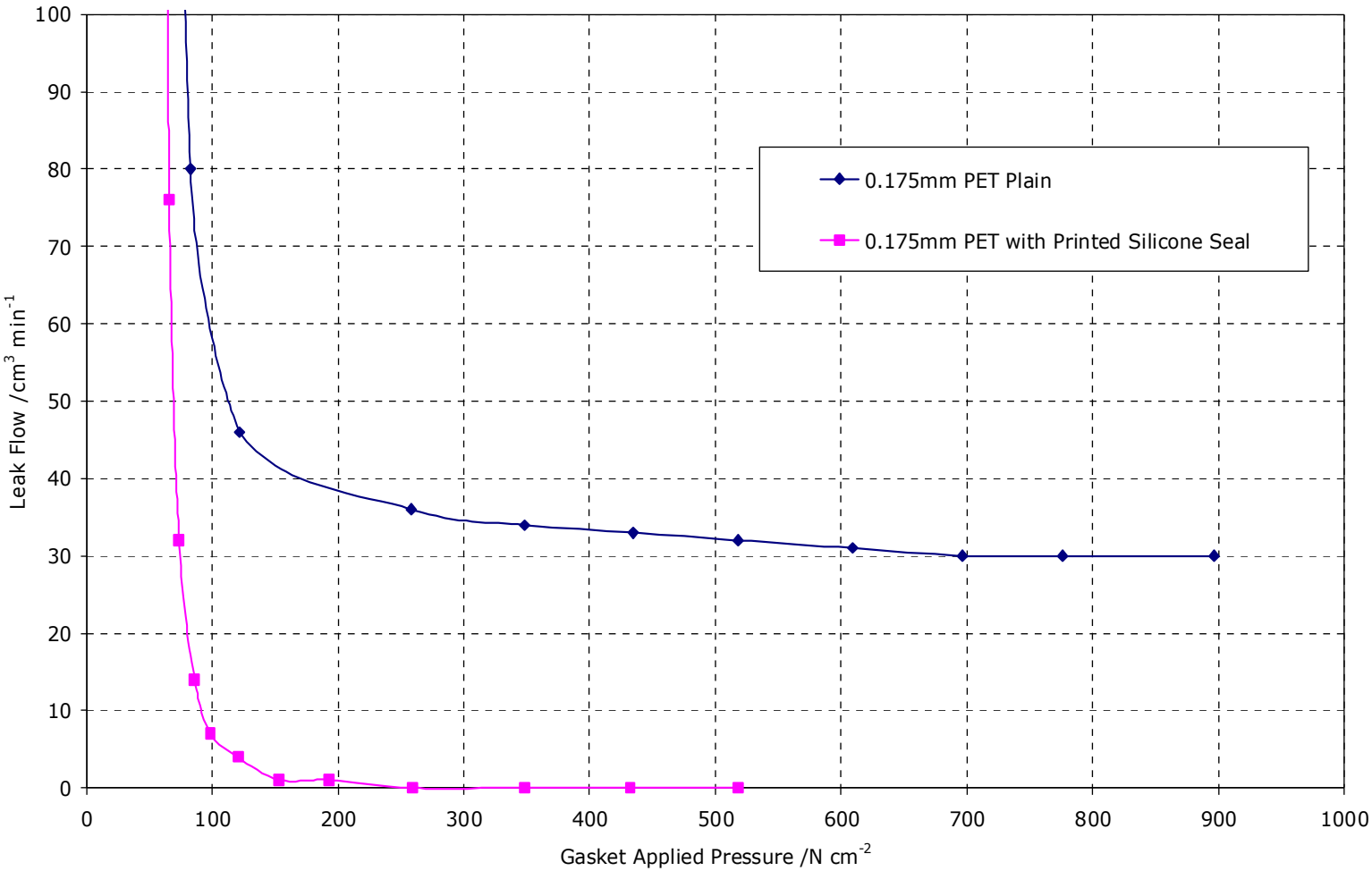

Figure 13. Pressure vs sealing for new silicone-printed polyester gaskets.

Disadvantages of applying the seal to the polyester;

- The cutting process could result in defective parts since the design is non-reversible (this is to prevent the other components from being incorrectly assembled).
- The seal material does not bond as well to the polyester as it does to the metal bipolar plate.

Printing on the Plate

Printing onto the bipolar plate produced different manufacturing challenges; the screen was of a different design to that for polyester printing because the plate print had to be clear of the flow field tracks to prevent silicone transferring and blocking flow features, in addition, an important aspect was the need to align the plate beneath the screen and ensure that the plate could not be printed on the wrong face.

Benefits of applying the seal to the bipolar plate;

- Better adhesion of the silicone to the metal.
- No orientation issues – the silicone can only be applied to the correct surface.

Disadvantages of applying the seal to the bipolar plate;

- The weight of the plate introduces storage problems; stacked plates could slide across each other and damage the print. This would require storage fixtures and/or interleaving with a separator paper.
- Damaged prints would require cleaning and reprinting, as plates could not, in the near term, be simply disposed of (because of cost) as the polyesters could.
- Lead times would be extended – bipolar plates could not be printed until they had been manufactured (plate manufacture is likely to be a more lengthy process than polyester supply).

Short Stack Testing

Two initial stack builds were carried out, both incorporated 0.175mm polyester gaskets and the new MEA concept, however one stack used printed polyester (stack #418) whilst the other used printed bipolar plates (stack #417). The principal purpose of the test was to evaluate the assemble-ability/disassemble-ability and leak–tightness of the different gasket prints.

Each stack was tested for approximately five days in the laboratory; polarisation curves are shown in figure 14. Clearly, and as expected there is little performance difference.

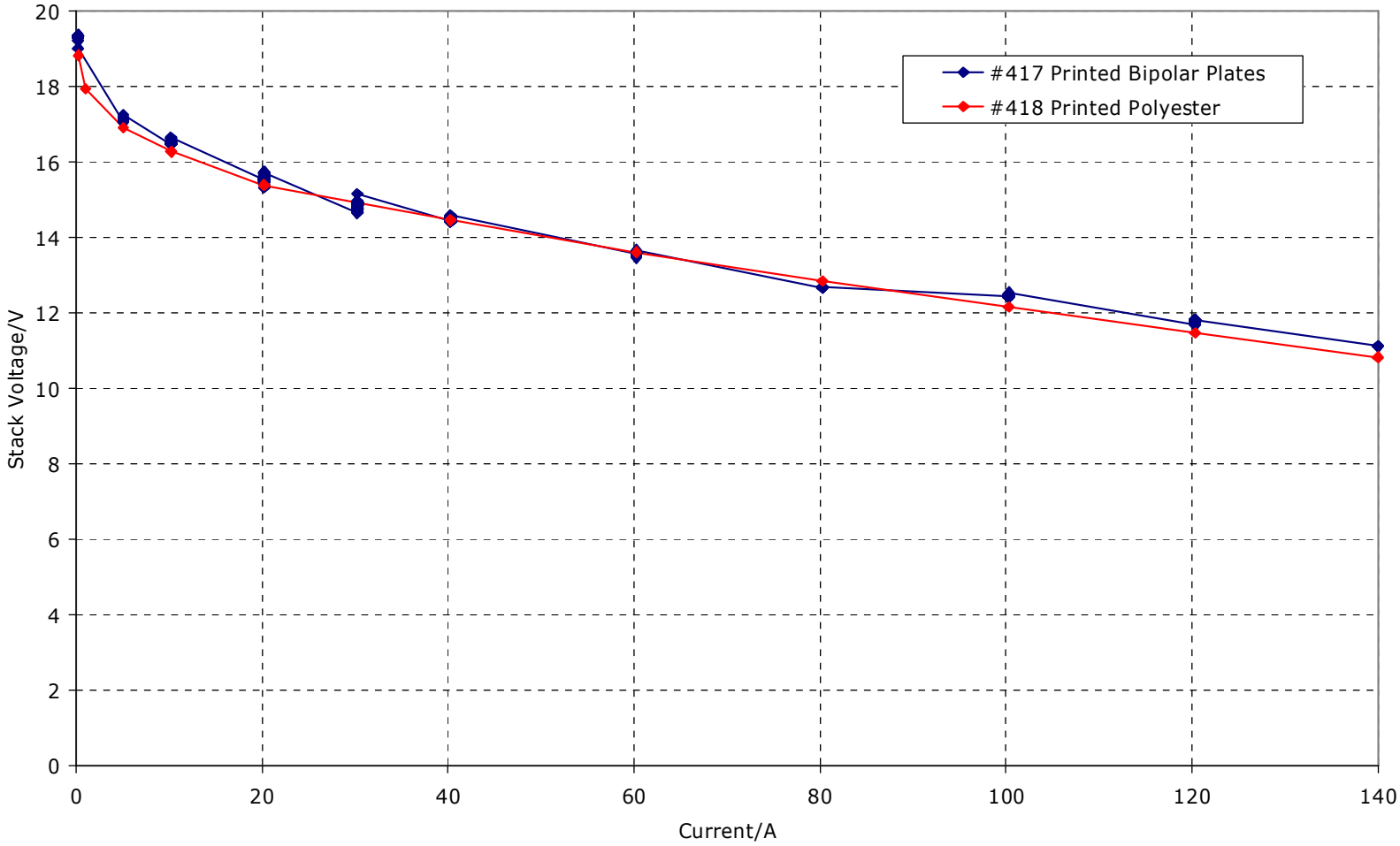

Figure 14. Performance of stacks with first iteration of printed gaskets.

2.2.5 End-Plates

Finite element analysis was used, in conjunction with measurement of load vs. displacement of end-plates in assembled stacks, to examine the benefits of alternative end-plate designs. The objectives of end-plate redesign were to identify a suitable multi-width design capable of maintaining stack compression along the longer cross-sectional axis whilst also developing the technology to address issues such as mass and electrical isolation.

Figure 15 to figure 18 show FE models examining the impact of changing the location of tiebars with respect to the plate perimeter. There is a considerable reduction in stress and displacement as the cantilevering effect upon the stud is reduced as it is brought in-board, this would allow the thickness and hence mass of the end-plate to be reduced but introduces gasket tooling issues. The design finally agreed, shown partially in figure 19, kept the studs outboard but reduced the spacing, thus keeping displacement down but retaining a degree of design flexibility.

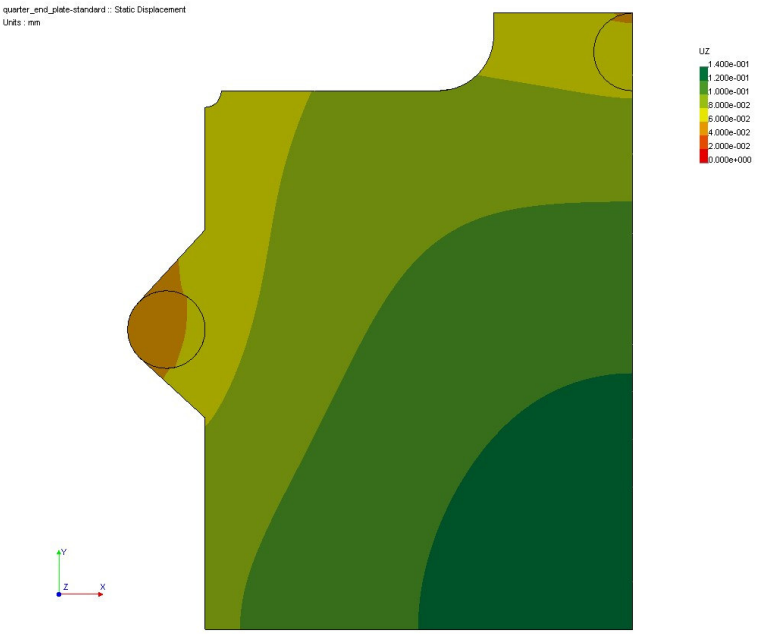

Figure 15. Plate deformation – standard design, fully outboard studs.

Figure 16. Plate deformation - Standard design, partially inboard studs (B).

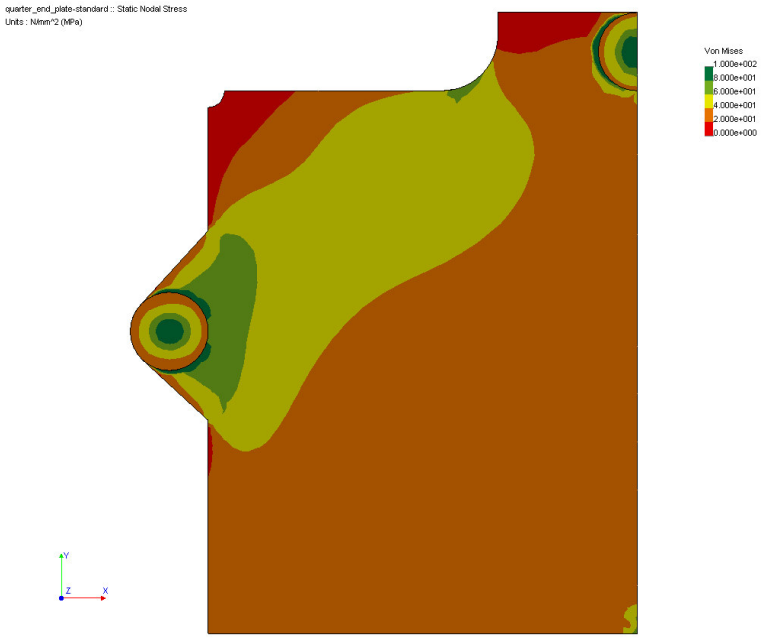

Figure 17. Stress distribution – standard design, fully outboard studs.

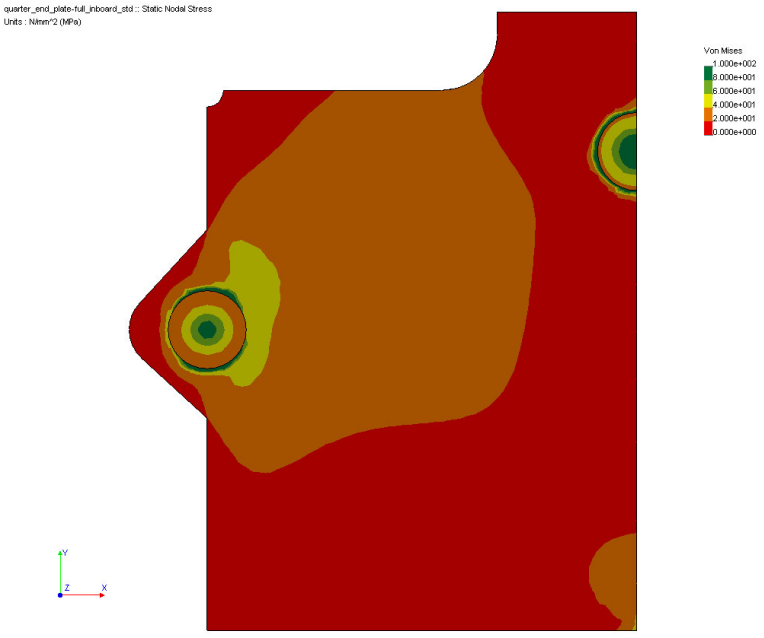

Figure 18. Stress distribution – standard design, partially inboard studs (B).

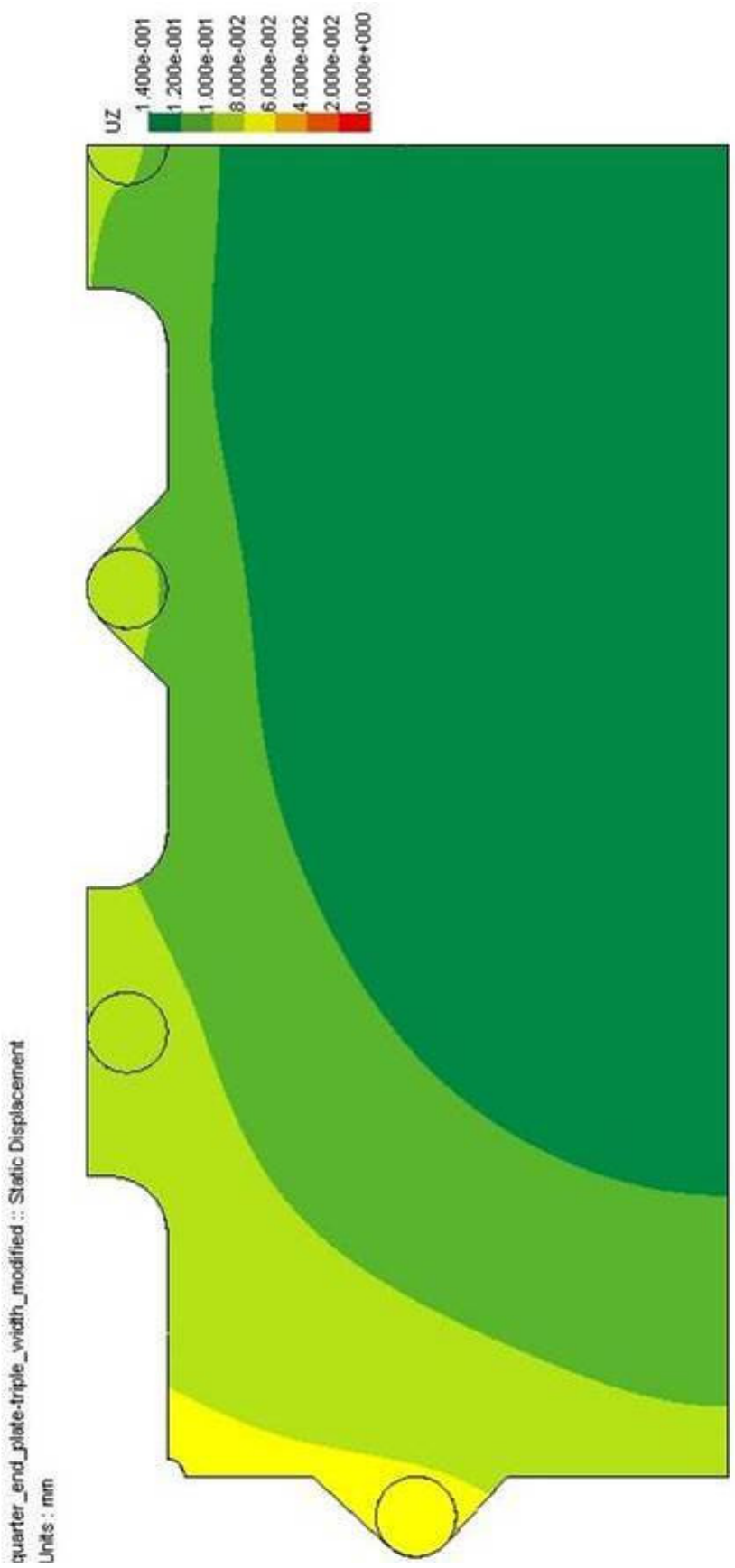

Figure 19. Plate deformation – triple width modified design.

2.3 Scale-up Process

In a parallel path to the multiple-width component development, the issue of scale-up in terms of number of cells was addressed.

2.3.1 Manifold Sizing

The principal issue when building long stacks is ensuring the manifolds are sufficiently large to ensure plenum flow of all fluids to the individual cells. Typically, for plenum flow in a manifold,

$$A >> 2Na$$

Where A is the manifold cross sectional area, N is the number of orifices fed by the manifold and a is the area of each orifice. Computational fluid dynamics may also be used to assist in manifold sizing but in practice the modelling is complicated by several factors:

1. fuel cells generally rely on two manifolds for each fluid (feed and exhaust), thus plenum flow in the manifolds may be possible where they are undersized if the imbalance in the feed manifold is cancelled out by the imbalance in the exhaust manifold
2. the volumetric flowrates of fluid changes from inlet to outlet because of (a) consumption of fuel/oxidant by the electrochemical reaction, (b) temperature changes to the fluid because of the generation of waste heat and (c) the absolute pressure of the fluid changes considerably from inlet to outlet manifold.
3. the exhaust manifold will almost certainly include a degree of two-phase flow due to the presence of entrained liquid water in the exhaust streams.

For these reasons it was decided that the most reliable method of determining the suitability of the manifolds was to build progressively larger stacks and measure the manifold pressure profiles under operational conditions. In order to achieve this, a manifold box and sensor probe were designed and manufactured; the probe could be positioned at the far end of a manifold (inlet or outlet) and slowly withdrawn, thus when coupled to a pressure transducer the gas pressure could be measured throughout the manifold.

Typical data is shown in figure 20. In this chart, the inlet manifold shows little variation for the three stacks illustrated however, in the outlet manifold there is a dramatic profile to the pressure measured for stack SN072 (a 168 cell unit), the measured pressure falling from 140mbar.g to 65mbar.g in the exit manifold box. This profile effectively demonstrates that the manifold was undersized for the required flowrates and explained the poor performance of the stack which would not operate at air flow stoichiometries below 3.5 due to overheating of the cells at the positive end which corresponds to the left hand end of the chart – here the cells have the lowest difference between inlet and outlet manifold pressure and therefore the lowest air flowrate. A modification to the stack design allowed the measurements SN072m to be taken, showing a considerable improvement in manifold pressure drop profile and this did indeed result in improved stack performance.

Similar tests were carried out on various sizes of single width units, enabling manifolds for all fluids to be correctly sized.

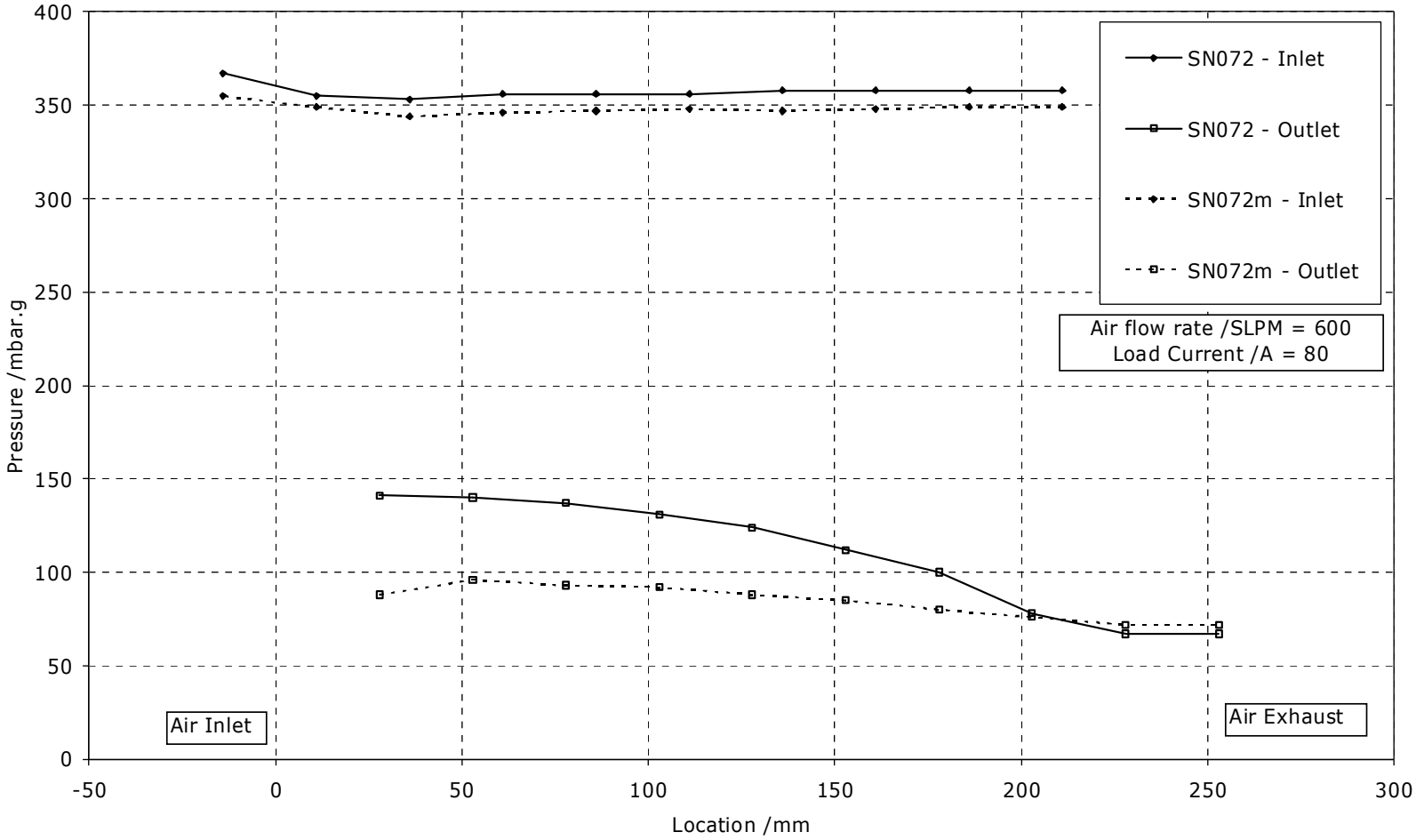

Figure 20. Manifold pressure probe data.

2.3.2 Triple Width Short Stack Tests

During the design cycle it was necessary to prove-out the triple width design, this process included manufacturing trials to assess the feasibility of producing the components, assembly trials to ensure "buildability" of the triple width technology and performance trials to elucidate any performance related problems. These trials were carried out by building short stacks of 20 or 48 cells in length (thereby removing concerns over manifold sizing). A 20-cell short stack is shown on the test station in figure 21 and normalised polarisation data is shown in figure 22 compared with typical 200cm^2 stack data; clearly at this stage the performance of the triple width technology was substantially below that was achieved in the single width. Component trials identified a coolant delivery and distribution problem which was rectified after ex-situ testing. A number of other problems arose with regard to gasket manufacture (one design variant included 2mm diameter manifolds, these proved difficult to manufacture due to poor ejection of waste material from the cutting tools and extremely difficult to align during stack assembly).

Data from a 48-cell stack incorporating the revised final design is shown in figure 23. This data indicates that the performance of the triple width (600cm^2) design was identical to that of the 200cm^2 design once electrode area had been accounted for, figure 24.

2.4 50kW Stack Build and Test

Results from short triple width stacks to identify cell width problems and single width long stacks to identify stack length (manifold sizing) issues were all successfully addressed prior to a design review and initiation of the 50kW stack component procurement and assembly process.

2.4.1 QA/QC Hardware

The equipment necessary to test the integrity of components was designed and built early during the triple width development process. Hardware was used to test bipolar plates and MEAs for pinholes, but as has already been discussed, the need to move to an alternative diffuser and the short stack results obtained using it, allowed the diffuser QC testing to be removed from the stack assembly procedure.

Bipolar plate QC parameter inspection was carried out, but on a reduced inspection basis as previously described.

2.4.2 Stack Assembly

A stack build assembly was designed which allowed the stack to be compressed using a hydraulic ram; coupled with a load cell and hydraulic pressure gauge, this provided valuable data about the compressive loads required to achieve stack sealing and working dimensions, this equipment was used to assemble triple width short stacks and reinforced the end-plate design work discussed previously. Figure 25 shows the 336-cell stack in the build assembly prior to compression beginning.

2.4.3 Test Rig

Figure 26 shows the completed 336-cell unit on a purpose built test station which included cell voltage monitoring, air mass flow controller, coolant conditioning and

delivery and a grid-connected inverting load unit (effectively delivering the generated power to the local electricity network).

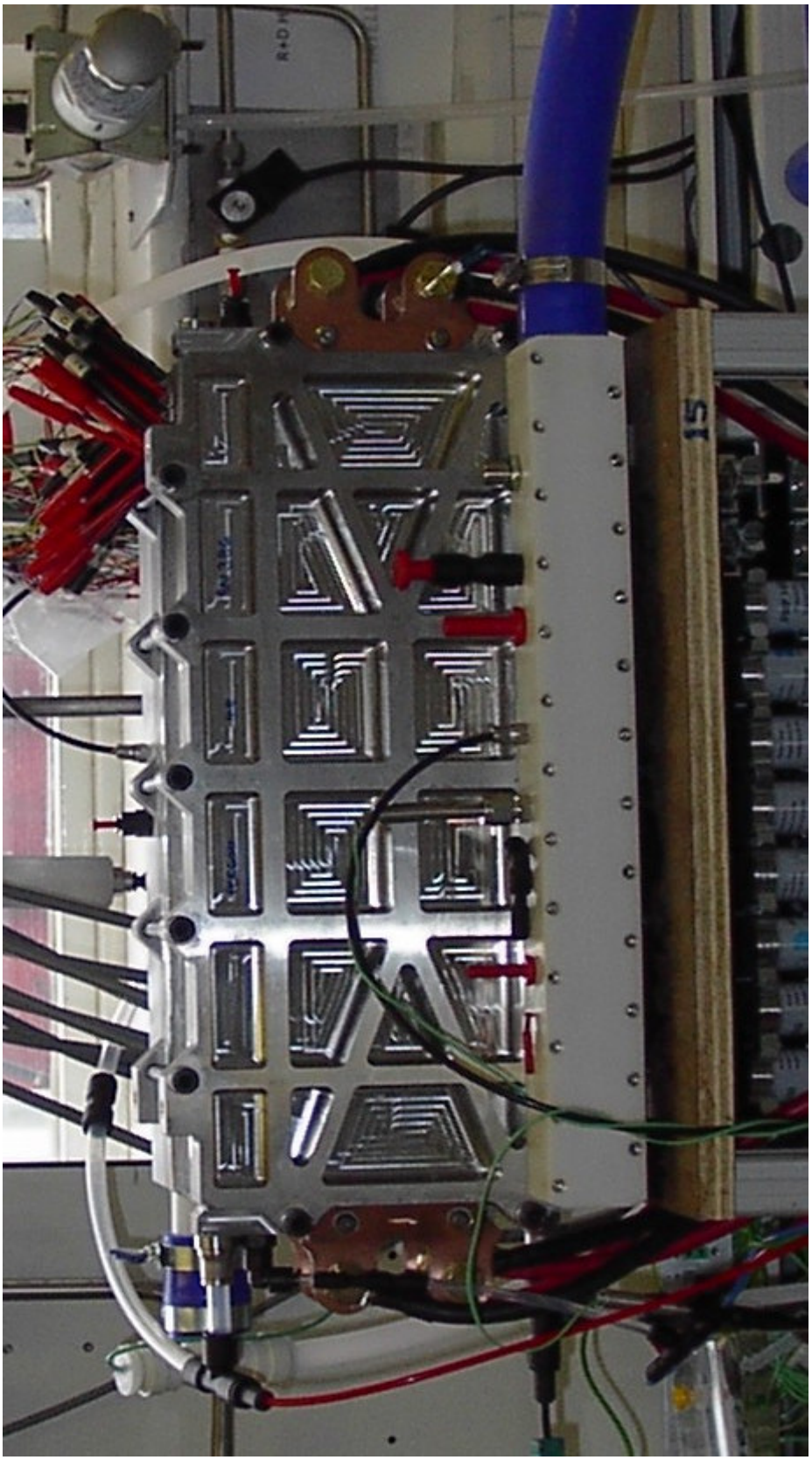

Figure 21. Triple width 20-cell short stack.

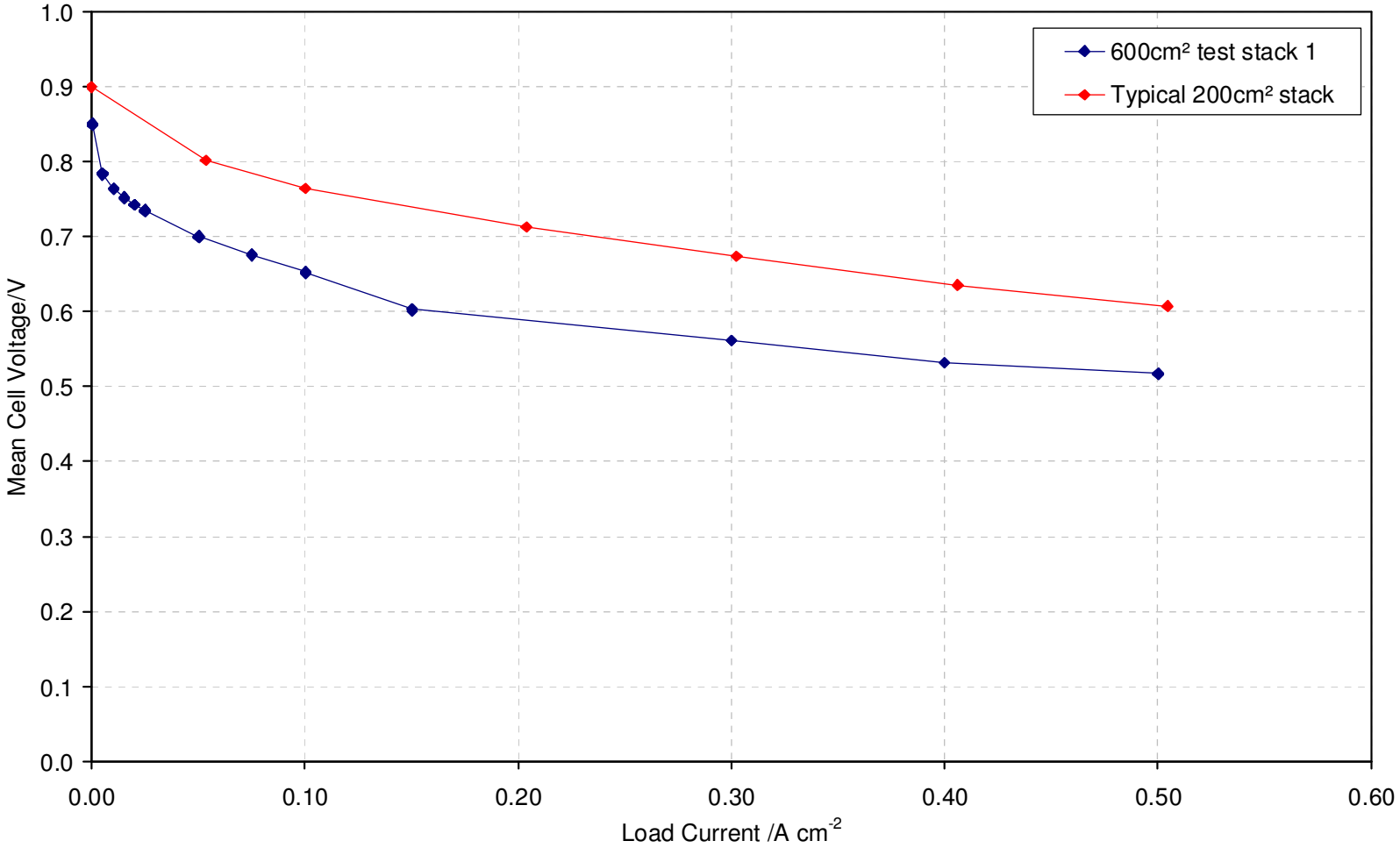

Figure 22. Polarisation from the first 600cm^2 test stack compared with typical 200cm^2 stack test data.

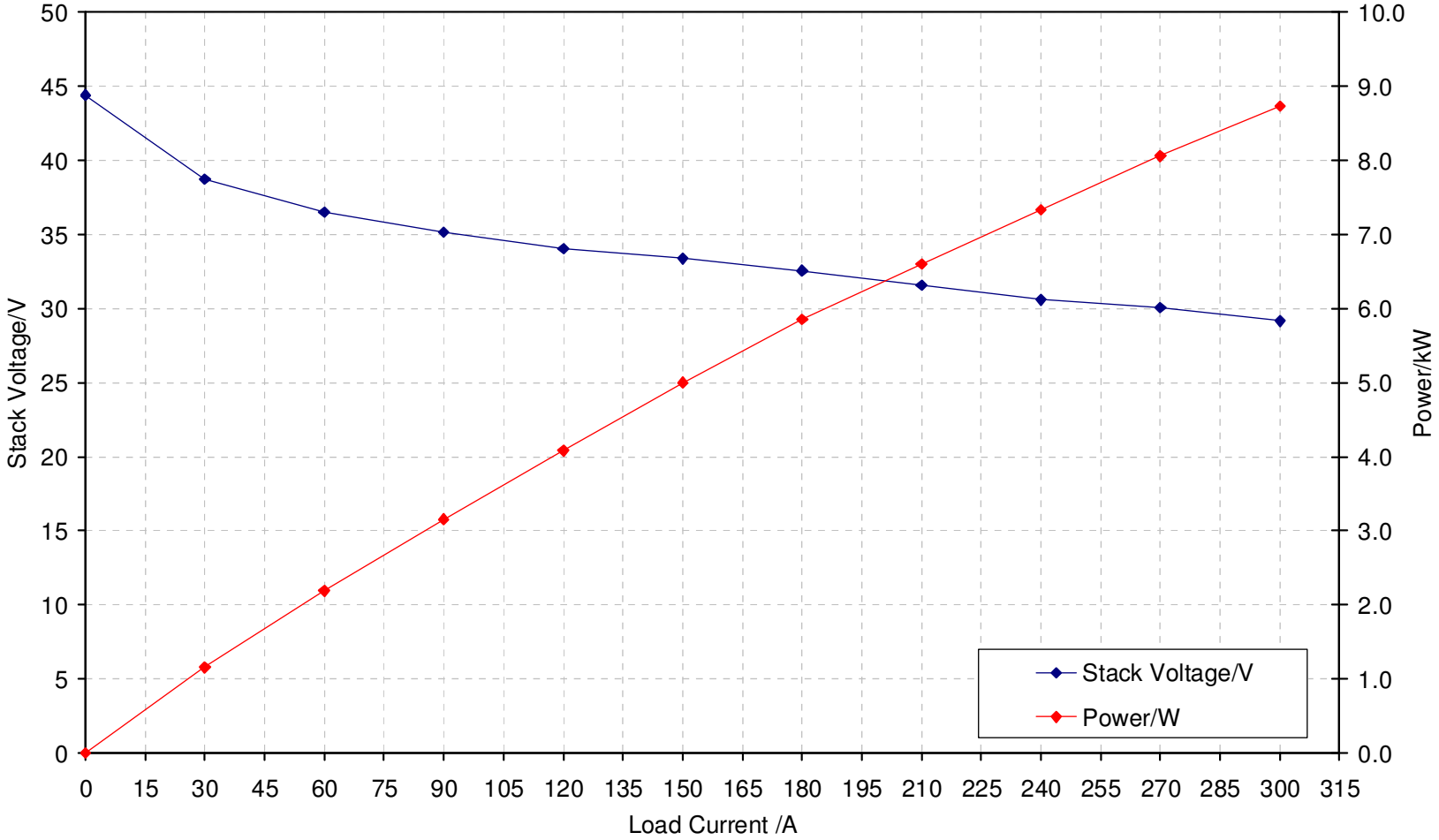

Figure 23. Polarisation data from a 48-cell triple-width stack.

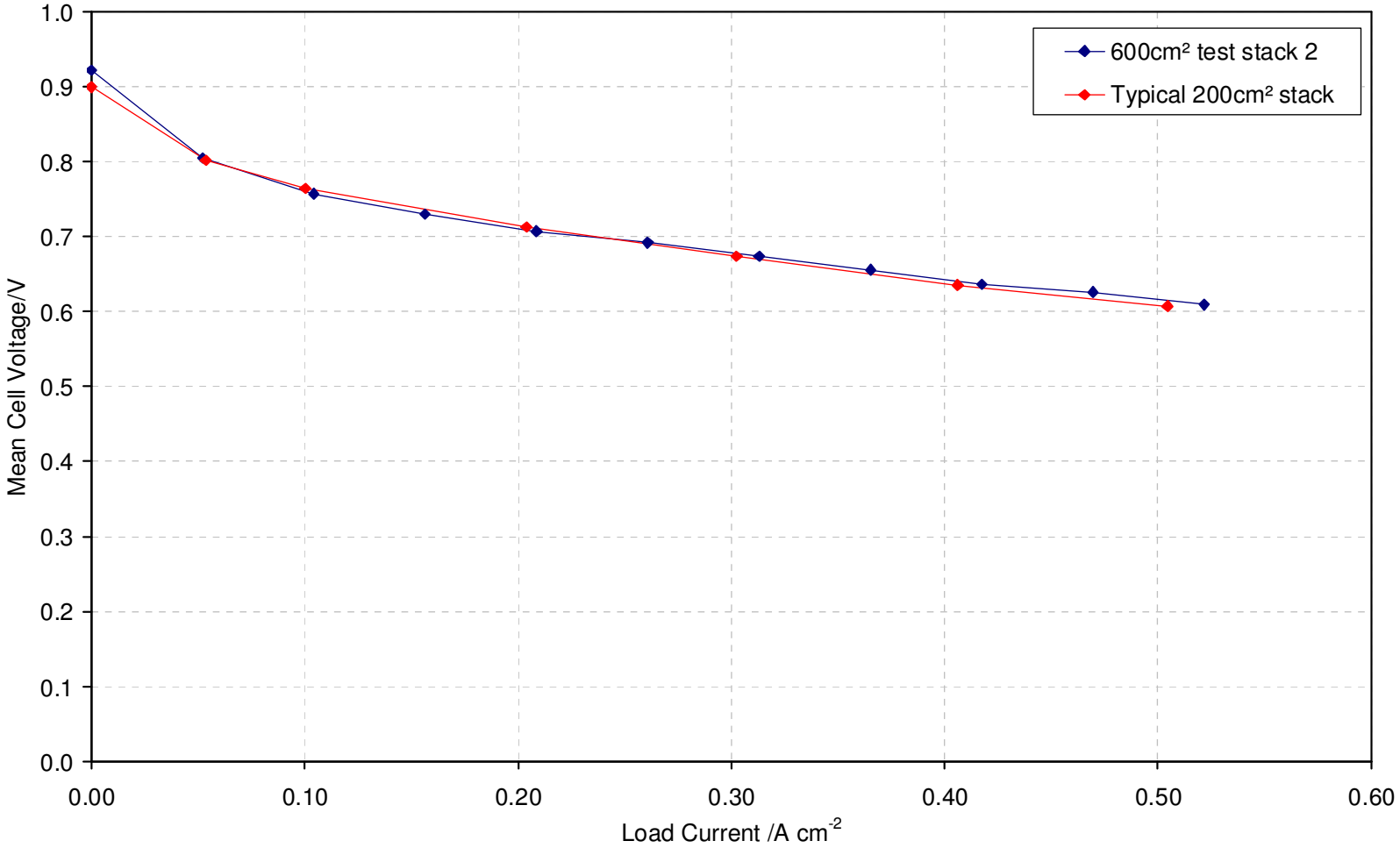

Figure 24. Comparison of 600cm^2 test stack with typical 200cm^2 data.

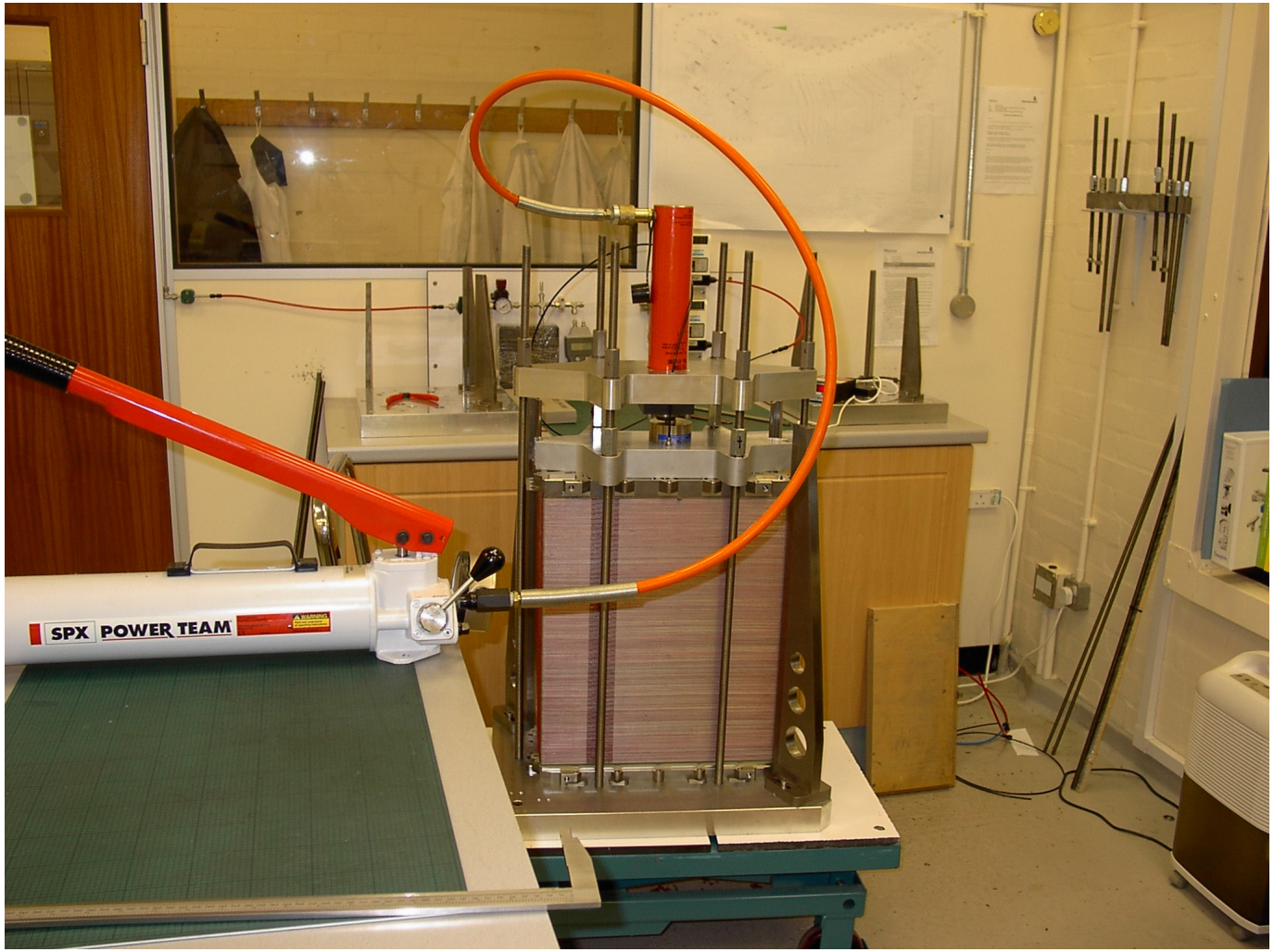

Figure 25. 336-cell stack in the build assembly prior to compression.

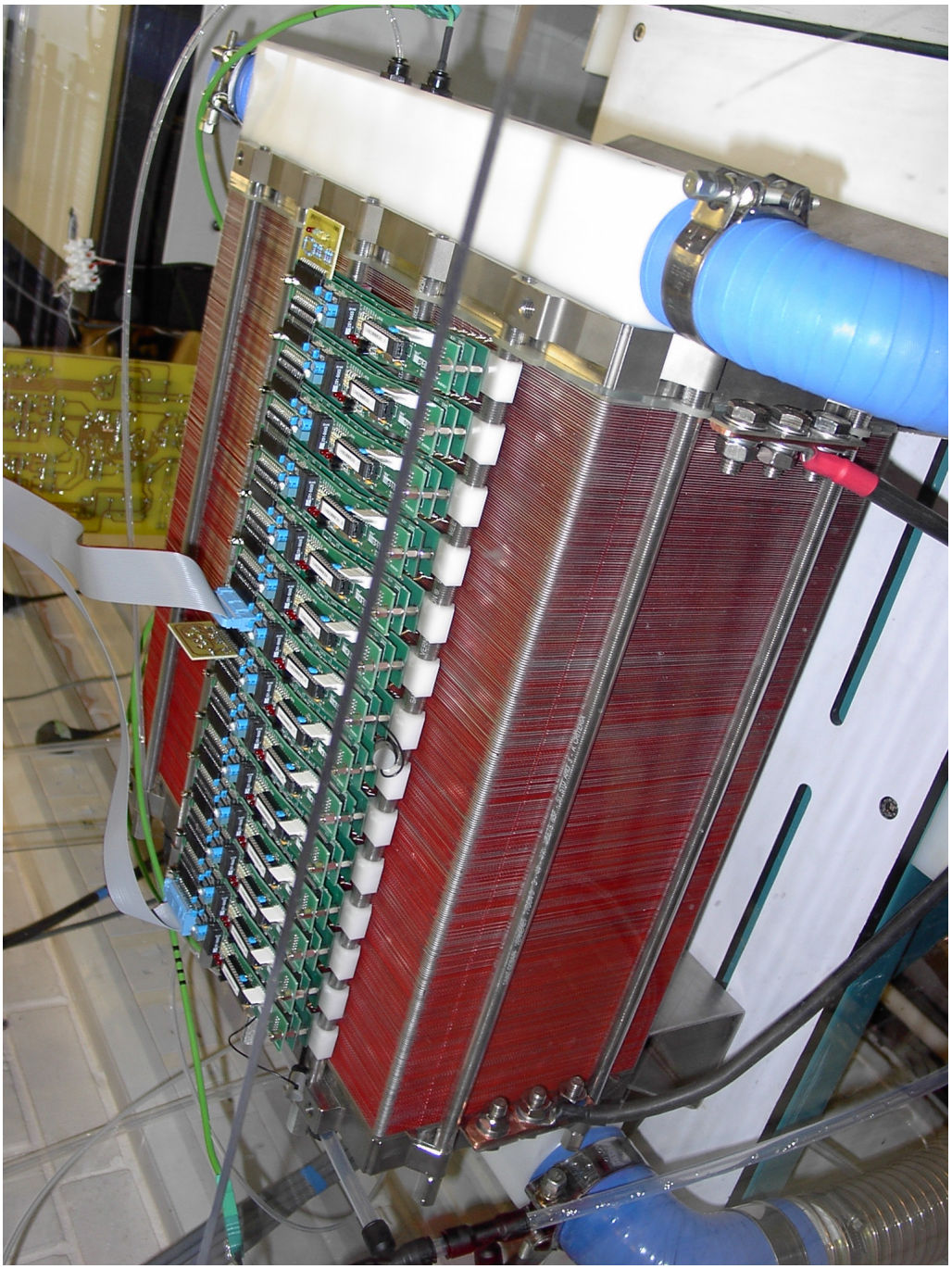

Figure 26. 336 cell stack on test station.

2.4.4 Test Results

The stack was worked through a conditioning programme designed to quickly bring the membranes up to a state of full hydration. Typical polarisation curves recorded during the conditioning process are shown in figure 27 and a final polarisation and power curve is shown in figure 28. When fully conditioned the stack achieved 70kW electric power and demonstrated polarisation behaviour better than that seen in typical single width stacks (see figure 29); these improvements can be attributed to improved fluid distribution due to both bipolar plate design and better diffuser performance.

Air manifold pressure probe results are shown in figure 30, the data shows a slight non-flat profile in inlet and exhaust manifolds but this did not appear to manifest as performance limiting and may simply be experimental error – the measured variation is only 6mbar on the inlet and 4mbar on the exhaust.

2.5 Etched Plate Scale-Up – Discussion

The targets for the etched plate aspect of this programme were to scale-up the active area by ~250%, address manufacturing issues for all components and deliver a 50kW manifestation of the so developed technology. All of these targets have been successfully achieved.

- The active area has been scaled up to three times its initial level; this size was the result of manufacturing and component handling analyses.
- Manufacturing methods have been examined and optimisations carried out where possible to improve the efficiency of manufacture; the production methodologies of all components were examined and optimisations carried out to maximise the yield of useful components from raw materials, quality control procedures were developed and tested to identify critical component properties allowing the stack construction procedure to be more finely controlled and resulting in the assembly of stacks with more consistent operating parameters.
- The technology has been proven in a single stack unit delivering 70kW, the largest ever constructed in the UK. In order to achieve this, fundamental testing to measure the suitability of existing manifold sizes and facilitate the design of manifolds appropriate to the delivery of the fluid flows required was carried out.

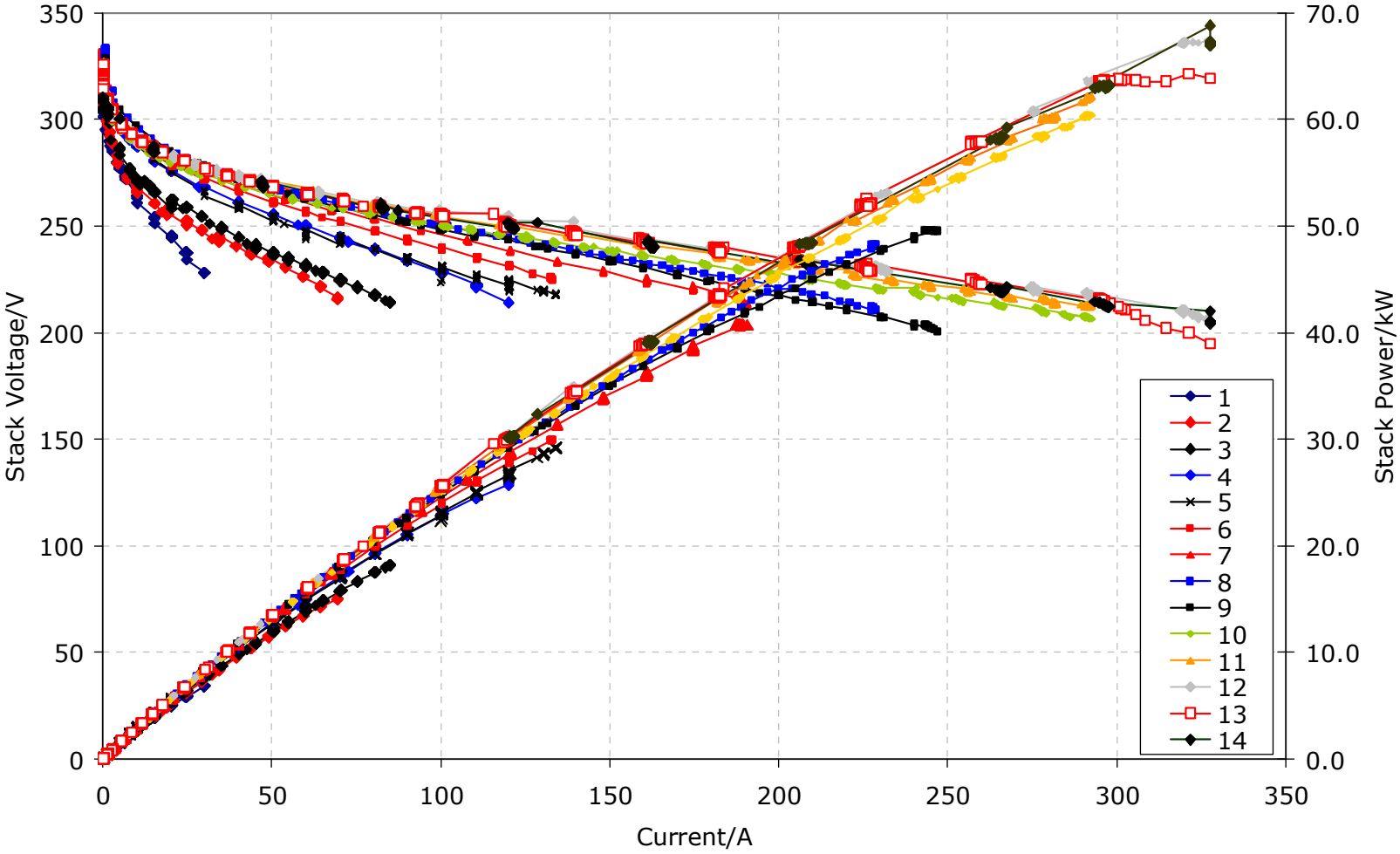

Figure 27. 336-cell stack – polarisation curves during conditioning.

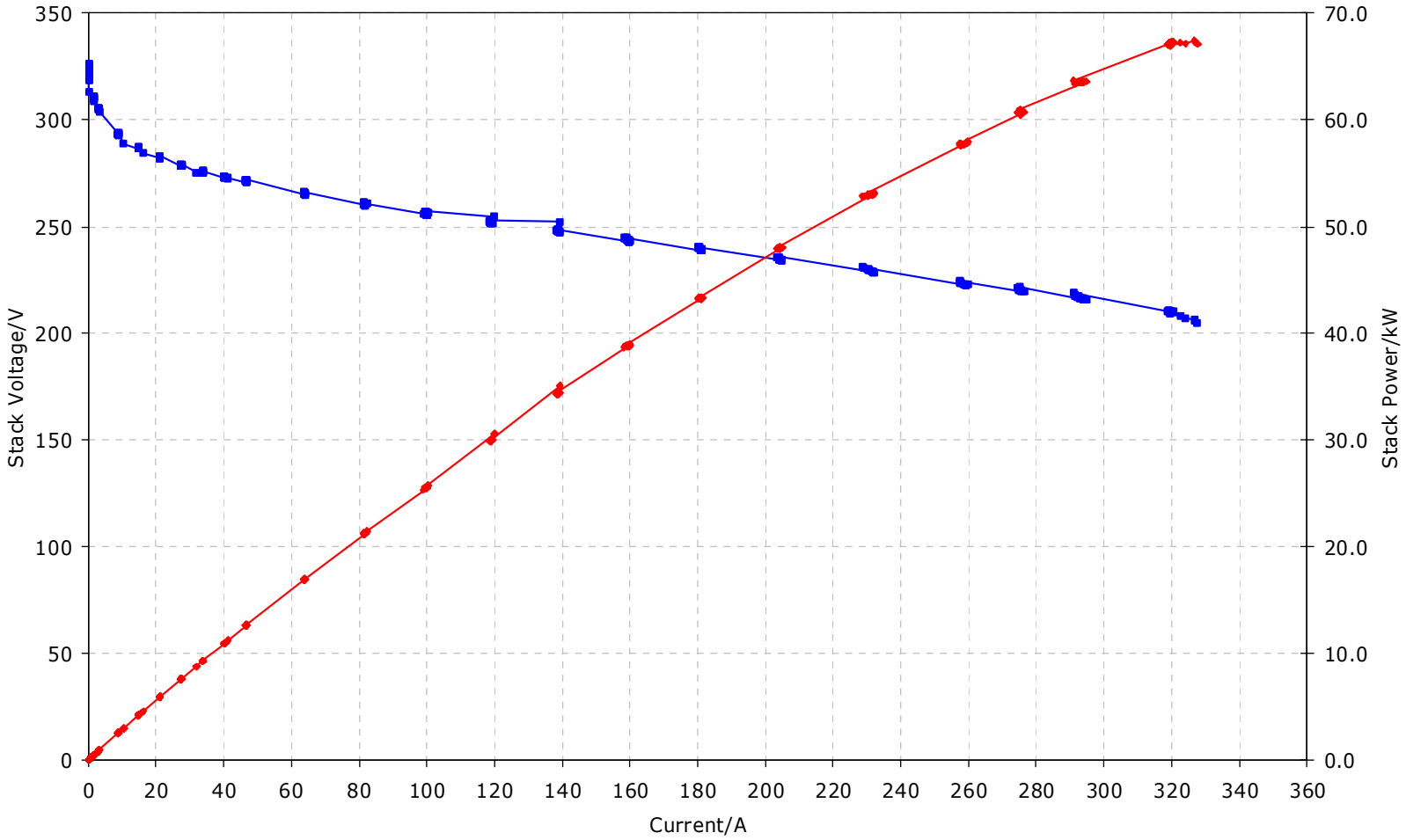

Figure 28. Fully conditioned polarisation curve from the 336-cell stack.

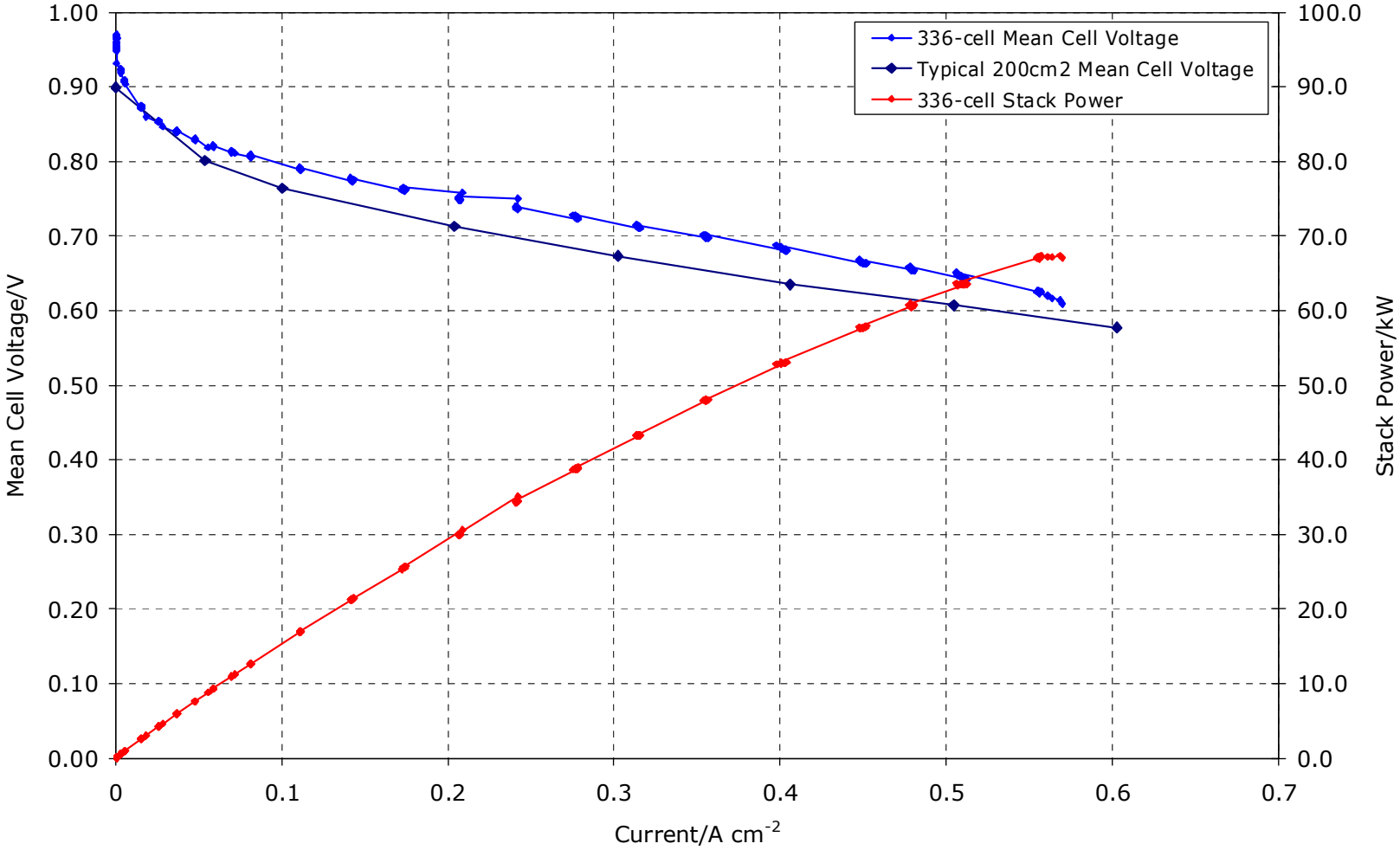

Figure 29. Fully conditioned polarisation curve from the 336-cell stack – normalised data.

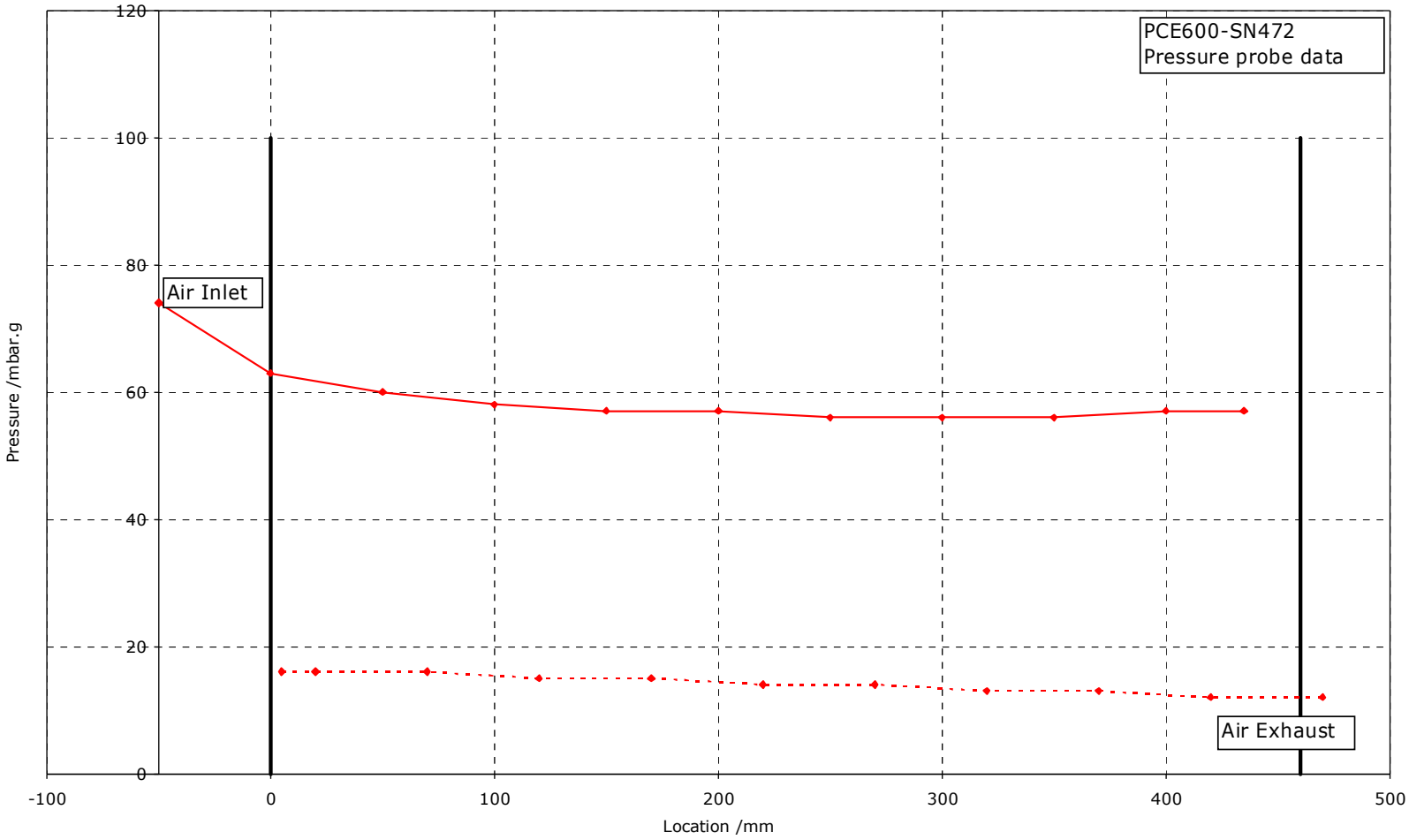

Figure 30. Manifold pressure probe profiles.

3 PRESSED PLATE DEVELOPMENT

3.1 Introduction

There are two key drivers behind the development of pressed plate technology to supersede the etched bipolar plates used to date; weight and cost. Pressed plates could have a quarter of the mass of their etched equivalent, and the cost of stamping plates is expected to be at least one order of magnitude lower than the cost of etching. The key performance targets for the pressed plate development were therefore

- Gravimetric power density, double that of the etched technology.
- Volumetric power density, equal to that of the etched technology.

This section details the design challenges faced during the development of the first working pressed plate stacks built and operated by Intelligent Energy, and how they have been overcome. It also reports test results from the pressed plate stacks assembled and tested as part of this programme.

3.2 Design Intent

The primary objective in drawing up pressed plate concepts was to find a way to replicate the features of the etched plate, using a much thinner metal plate and more rapid manufacturing techniques. Two primary concepts were conceived:

1. Corrugated Metal Concept.
2. Formed Metal Concept.

In the "***Corrugated Metal***" concept (see figure 31) a metal sheet is repeatedly folded to form a simple corrugated component, the folds of which form the flow channels on opposite sides of the plate. Manifolds and features capable of transferring fluids between these and the flow fields are formed from a plastic component which may be either moulded onto the metal part (insertion moulding) or could be pre-fabricated and then bonded (either with an adhesive or thermally bonded) onto the metal component.

In the "***Formed Metal***" concept (see figure 32) a series of deflections are introduced into the centre portion of a flat metal sheet, whilst maintaining a flat periphery. The flat region around the edge of the plate is then used as a foundation for a plastic component (probably quite similar to that discussed above), which again, may be thermally or adhesively bonded.

In principle it was felt that of the two concepts, the corrugated plate was the easiest in terms of manufacture of the metal component; metal corrugation is a well-established industrial process and metal folding machines are commercially available. There were some concerns as whether or not the pitch and definition of flow field tracks presently used by Intelligent Energy could be replicated using a folding process, but in general it was accepted that formation of a suitable corrugated metal component did not present a serious technical challenge. The major difficulty here is in the creation of the interface between metal and plastic components. Discussions with plastic injection-mould tool manufacturers revealed

concerns with regards to the manufacture of a metal component to the necessary tolerances required to “shut-out” the plastic during the moulding process (“shut-out” refers to closure of the periphery of the mould which prevents the plastic from flashing out of the tool); in this case failure of the tool to shut-out would result in plastic material flashing across the surface of the metal component, which would then require cleaning or (given the components cost involved) more accurately the component would be scrapped.

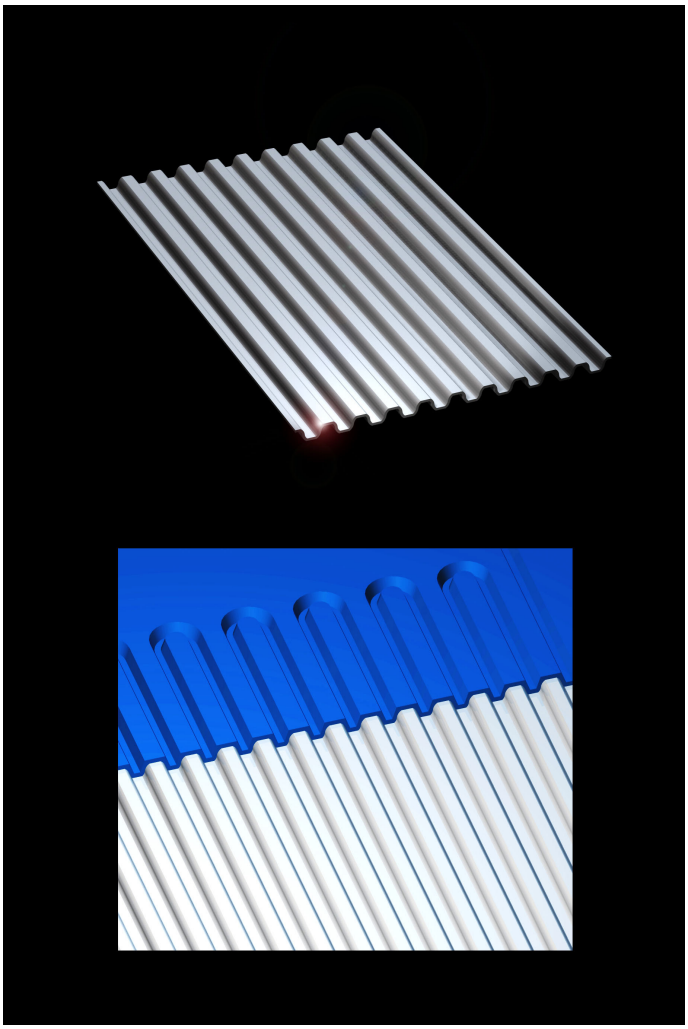

Figure 31. Corrugated metal concept.

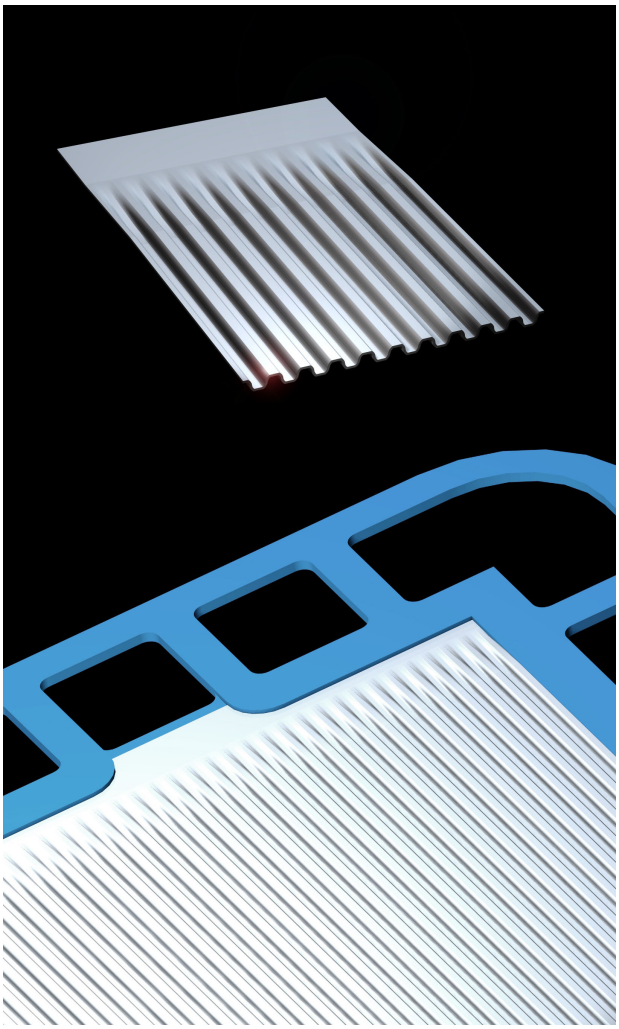

Figure 32. Formed metal concept.

The "Formed Metal" concept approach presented different areas of difficulty. The conceptual metal component had a flat "picture frame" around its edge which would overcome the moulding shut-out difficulties described above – insertion moulding onto a flat surface presents fewer technical issues; however, manufacture of the metal component would be less straightforward. Pressing (or embossing) of metal requires some degree of stretching or "flowing" of the metal; this leads to stresses and the possibility of splitting the material.

Other Issues

In both cases described, there are further issues involving the interfacing of the metal and plastic components. This interface must be physically stable and gas tight over a broad thermal operating range (ideally -40°C to at least 100°C); this presents a challenge in terms of plastic selection and manufacture, particularly with regard to thermal expansion of the different materials.

The pressed plate development programme therefore principally focused on manufacture of a component to the "formed metal" concept design. Two routes to the manufacture of the metal component required by that design were investigated:

1. Single operation/progressive pressing. This method is widely implemented in industry, though the manufacture of components to such a degree of complexity (in terms of feature density and deflection) is rare – as such a certain amount of development was required. The greatest benefits in terms of cost-reduction and material throughput would be achieved if the component could be formed in a single operation; however, it was possible that secondary operations would be necessary. In the worst case, a progressive tool might be required - effectively a series of individual tools which form the component in a stepwise manner – incurring a higher tooling cost and slower throughput.
2. Hydroforming. Hydroforming utilises a hardened steel tool onto which the virgin material is pushed using high pressure water (of the order of 60 000bar). The principal advantage of this technique is uniformity of deformation; in conventional pressing, the tooling initially only contacts the target material in selected areas, thus the stress and stretch imposed upon the material are unevenly distributed, this may lead to fracturing (splitting) or induced stress within the finished component which would manifest as a tendency towards "non-flatness". Conversely, hydroforming applies, by its nature, a uniform pressure across the surface of the material allowing free-flow around the features of the tool. Components manufactured in this manner are less susceptible to induced stress and splitting, but cycle times can be slow, typically 30seconds per component as opposed to <5seconds if conventional methods are applied.

3.3 Initial Pressing Trials

The suitability of conventional pressing technology was investigated using a prototype tool comprising male and female components. The tool was designed to produce metal parts which have flow-field tracks similar in pitch and depth to those in the etched plate stacks – although compromises were made to facilitate easier

tool manufacture. Initial tests sought to define the force required to close the tool and whether or not the speed of closure was critical to the integrity of the finished part. Other work looked at the sensitivity of the quality (crispness of form, tendency to split) of the finished part to the grain direction of the virgin material.

Whilst reasonable success was experienced with a conventional pressing route, problems were demonstrated with regard to the degree of folding and stretching of the metal, see figure 33 . The main manifestation of this was a "kink" feature developed at each corner of the ribbed flow field, which was believed to be caused by a build-up of gathered material where the metal was not stretching, implying that in the central region of the flow field rib formation was due to stretching of the metal whilst at the edge of the flow field gathering is the principal route to flow field formation. This phenomenon also manifests itself as differences in material thickness across the width of the component – where the material is stretched the component is shallower and hence the track depth is less. This was largely eliminated by the introduction of a tooling modification.

3.4 Ex-situ Testing

A series of experiments were carried out to investigate the strength, conductivity and structural integrity of the conventionally pressed trial parts. Figure 34 shows the pressure required to deflect the pressed component. This is particularly interesting in determining the tendency of the pressed part to want to "flatten" out again when built into a stack; such a tendency would cause the bipolar plate to widen, disrupting gaskets and causing the stack to fail. The test carried out involved mounting a test piece in an extensometer with a DTI (dial test indicator) capable of measuring the deflection of the part under compressive force, hence the force applied was steadily increased and the movement of the dial (representing the crushing/flattening of the part) was recorded. The data presented clearly shows that a pressure (geometric) in excess of 14,000kPa (140bar) is necessary to crush the part by 0.1mm, a highly encouraging result since this pressure is approximately an order of magnitude greater than the pressure applied to the flow field area in a standard stack and hence it indicates that crushing of the component in an assembled stack is not likely to be significant.

Figure 35 shows the force-resistance relationship of a system comprising two pressed parts and two pieces of a woven diffuser material; results show this system configured in two different ways, "land over land" and "land over drop", representing the two different manners in which flow field plates may be assembled together. The chart also shows the same relationship for the same diffuser compressed between etched metal parts. It is clear that irrespective of how the pressed plate system is assembled; the electrical resistance is greater than that of the etched system at any given compressive load. In addition, the lowest resistance configuration is "land over land" which presents a problem as this configuration requires two types of plate (one effectively being a half-pitch shift of the other). For the purposes of this work, to keep costs down and to limit lead-times as much as possible it was decided that the land over drop design would be pursued.

Figure 36 compares the woven material with the new non-woven material which had been successfully trialled in the etched plate technology and shows that although there is no improvement, the non-woven material offers no increase in resistance

over the woven material and thus it could be implemented as the choice diffusion medium.

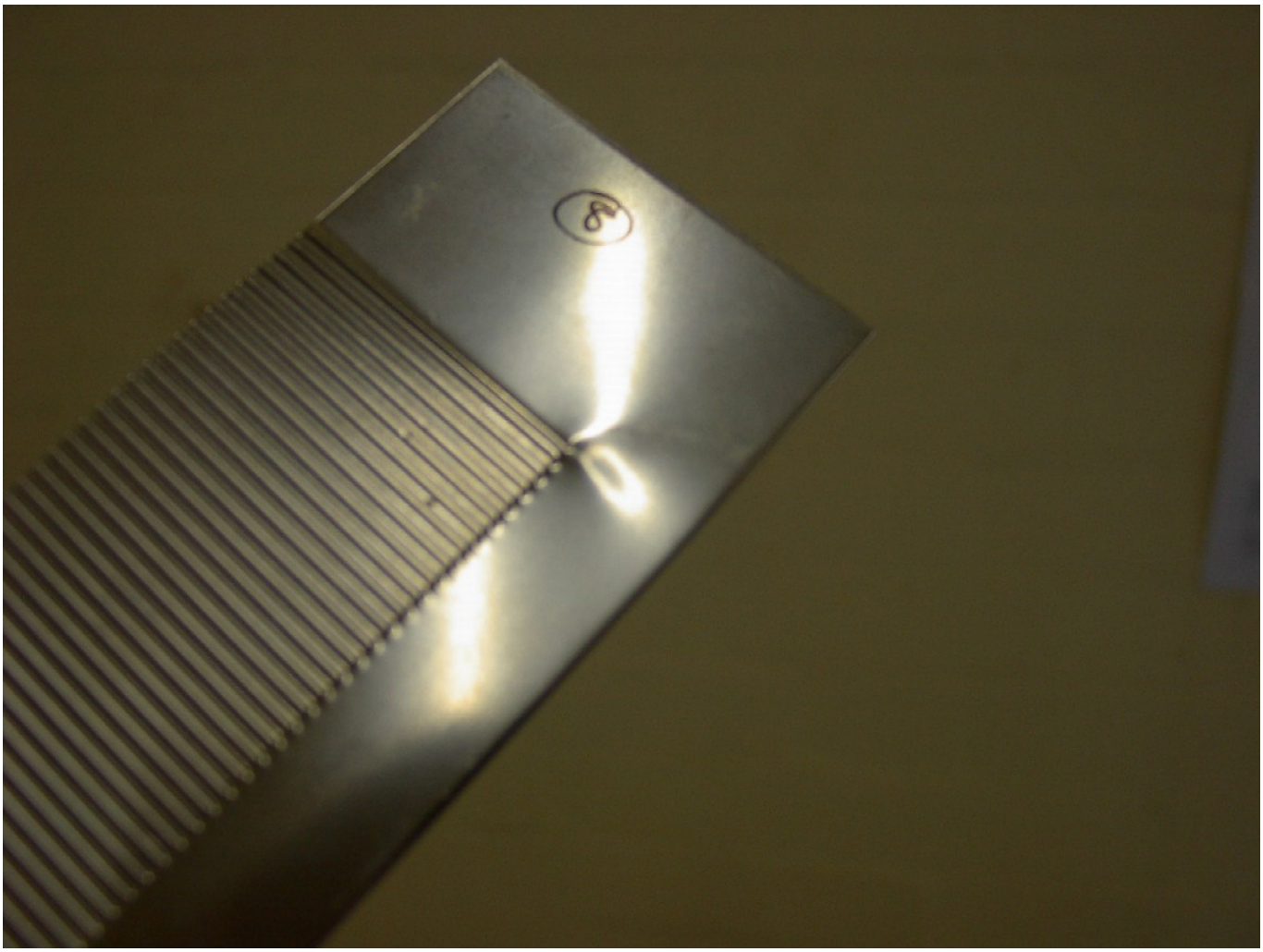

Figure 33. Prototype pressing showing “kink” feature.

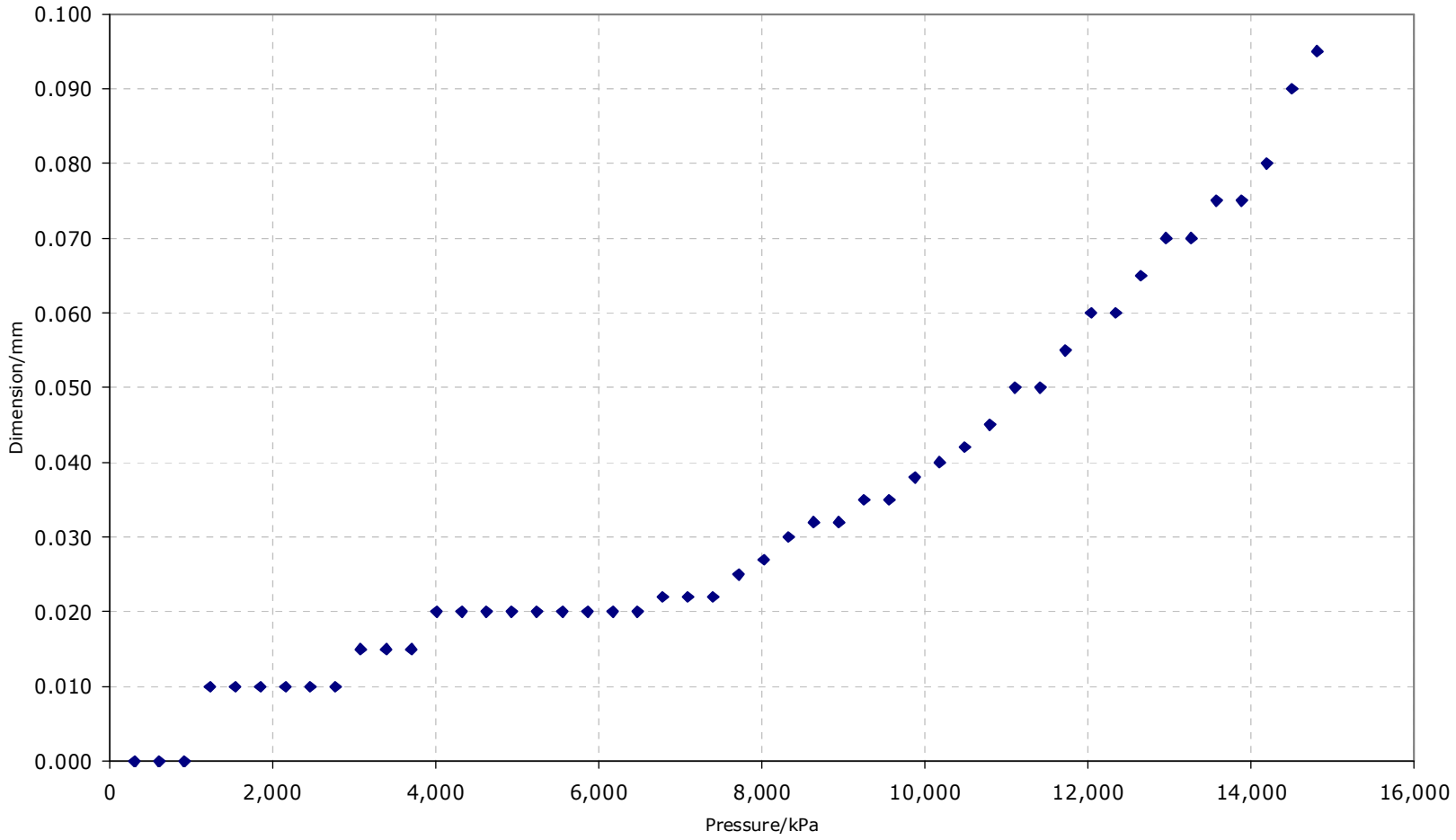

Figure 34. Force-dimension measurement of a pressed component.

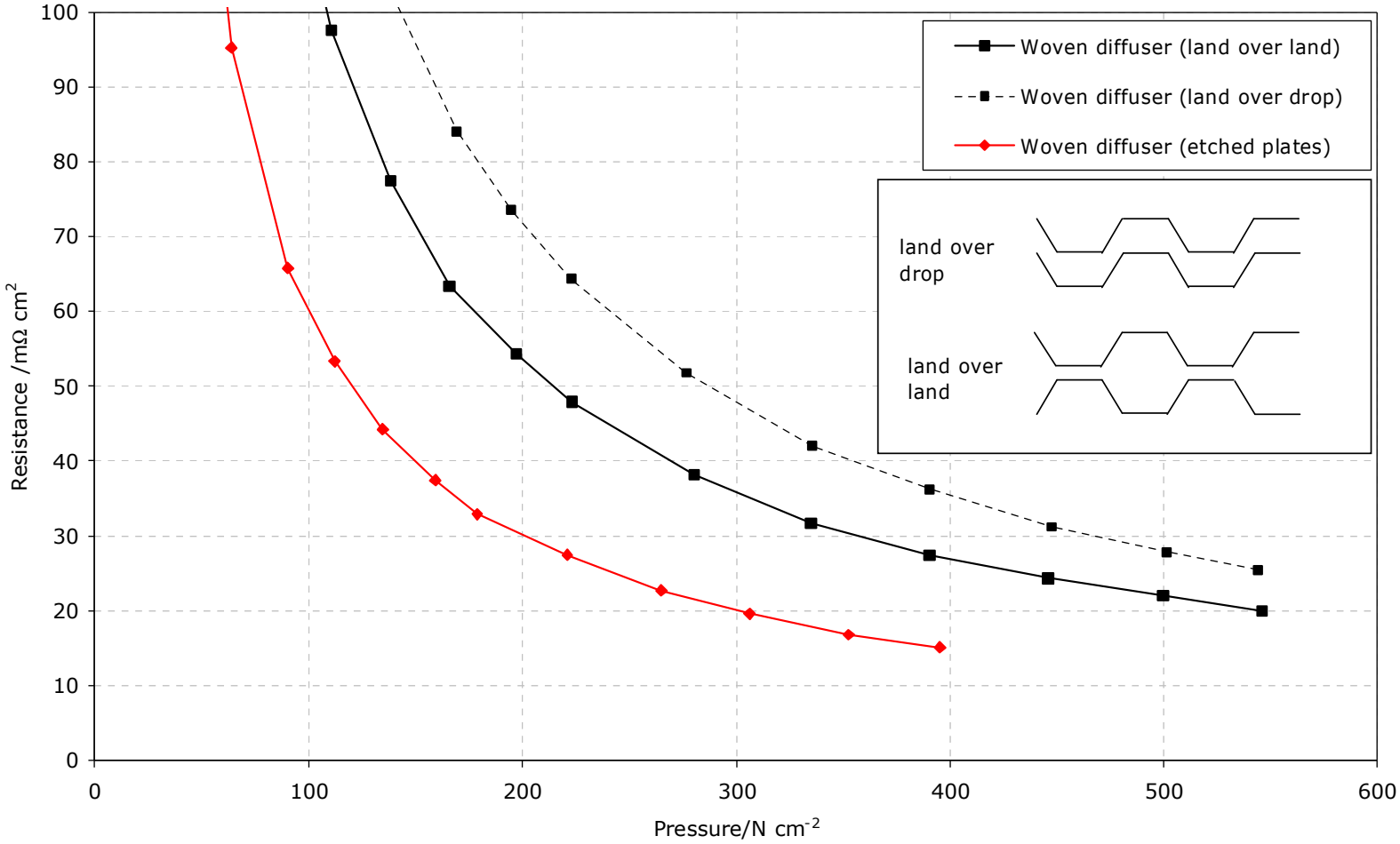

Figure 35. Force–resistance comparison.

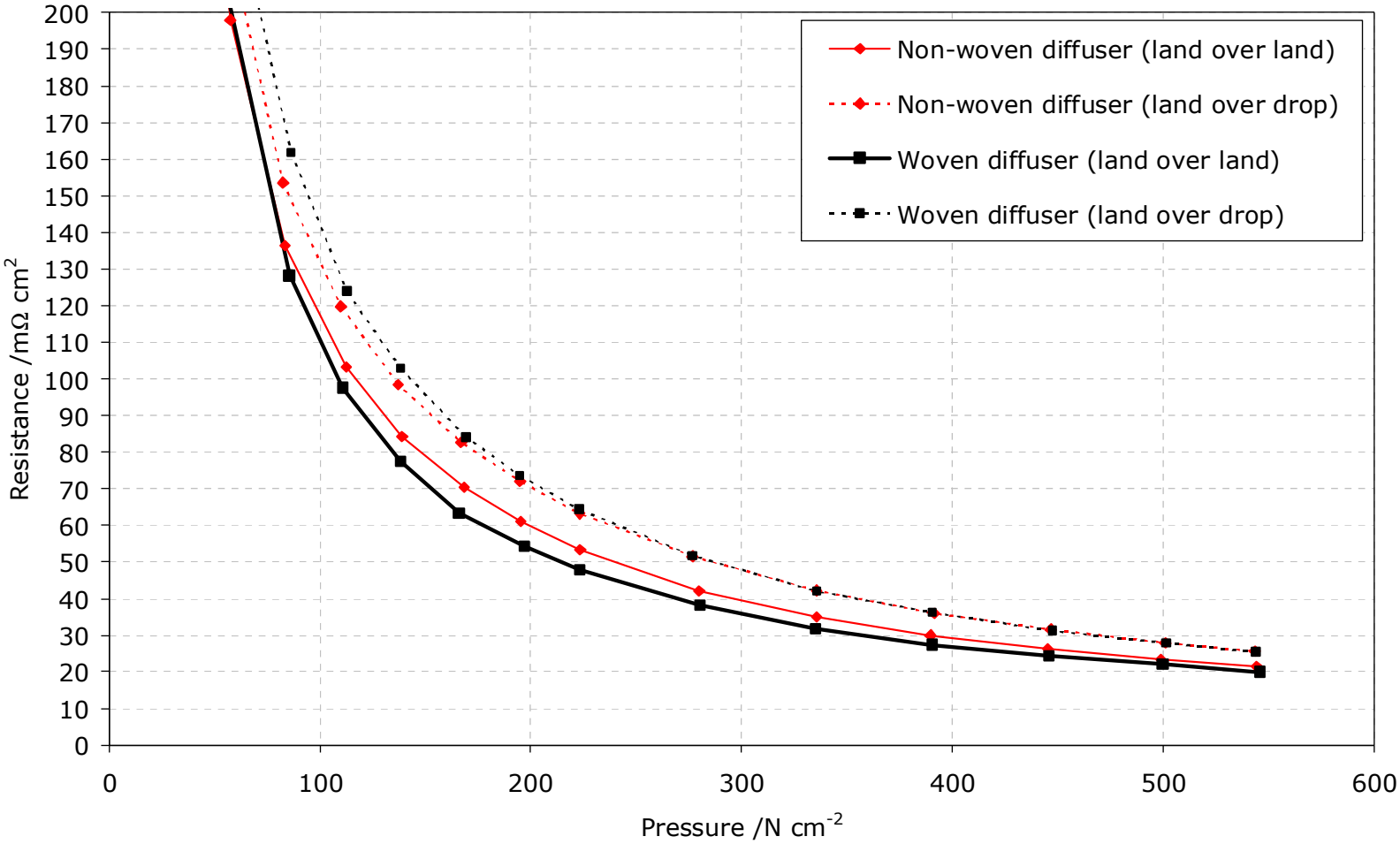

Figure 36. Force-resistance comparison for 2 different diffusers.

3.5 Single Width Stack Component Manufacture

3.5.1 Pressed Plate

The Mk 1 "formed metal" design incorporated track turns in the plate pressing, giving a channel pattern more like the etched plate, hence making them easier to compare. The pressing was designed to have a similar thickness to the etched plates (0.6mm), but this made track pitch an issue due to the draft angle required when pressing the tracks into the plate. A number of design iterations were drawn up while trying to maintain a similar electrode size and area compared to the etched plate stacks. Strain analyses were performed on these designs by the contractor chosen to form the plates (see figure 37 and figure 38), until a design was reached which they considered could be formed without the metal tearing. Plates were manufactured by both hydroforming and conventional pressing. At this stage, to retain design flexibility and keep tooling costs down, the ports were added to the plate periphery by laser cutting.

The Mk1 plate featured channels which were formed by pressing the plate above and below the plane of the unformed flat sheet. After single cell and short stack trials (see section 3.6) this design was found to have two major shortcomings (i), it meant that during cell assembly, the anode diffuser was difficult to locate in the anode gasket as the plate pressing raised the diffuser up out of the cavity normally formed by the gasket; (ii) it created a step at the edge of the MEA, generating unwelcome stress in this area, and a pinch point in the anode diffuser, restricting anode fluid flow. In addition, the track pitch used in the Mk1 plate design forced the pressed region to be wider than the active area of an etched plate. This meant that standard MEAs and diffusers could not be used in pressed plate stacks of this design.

These issues were addressed by redesigning the plate pressing to give the Mk2 plate. In this design the pressing was all toward the cathode face, allowing easier assembly of the cell and keeping the MEA relatively flat in operation. The anode face of the pressed area lies in the same plane as the flat perimeter of the plate, giving a level surface onto which the other cell components can be assembled. The pitch of the tracks was also reduced in the Mk2 design to allow the use of standard MEAs and diffusers in pressed plate stacks.

Mk2 plates were produced by conventional pressing only, as it was decided that hydroforming could not be used to produce plates at the right cost. Pressing is a quicker and cheaper method which lends itself better to mass production of bipolar plates, and allows the ports to be cut at the same time as the plate is formed. At this development stage however, the ports were laser cut as they were in the Mk1 plate, to retain design flexibility, although they would ultimately be cut as part of the plate pressing.

Before embarking on production of a press tool, further computer modelling of the plate forming process was performed to give a profile with the required track depth and pitch, which could be formed without the metal splitting (figure 39). However, as the plates were to be produced by conventional pressing rather than hydroforming, this was used as a starting point only for the form of the press tool. A number of small tools with part of the track pattern were produced by the press tool manufacturer. The tools were used to perform trial pressings to see if the profile

could be produced without tearing the metal. If the metal did tear the profile was altered, keeping the desired depth and pitch, and the test repeated, until a profile was made which could be formed. Having arrived at a satisfactory form, a full tool was produced which was used to manufacture plates for stack assembly and testing.

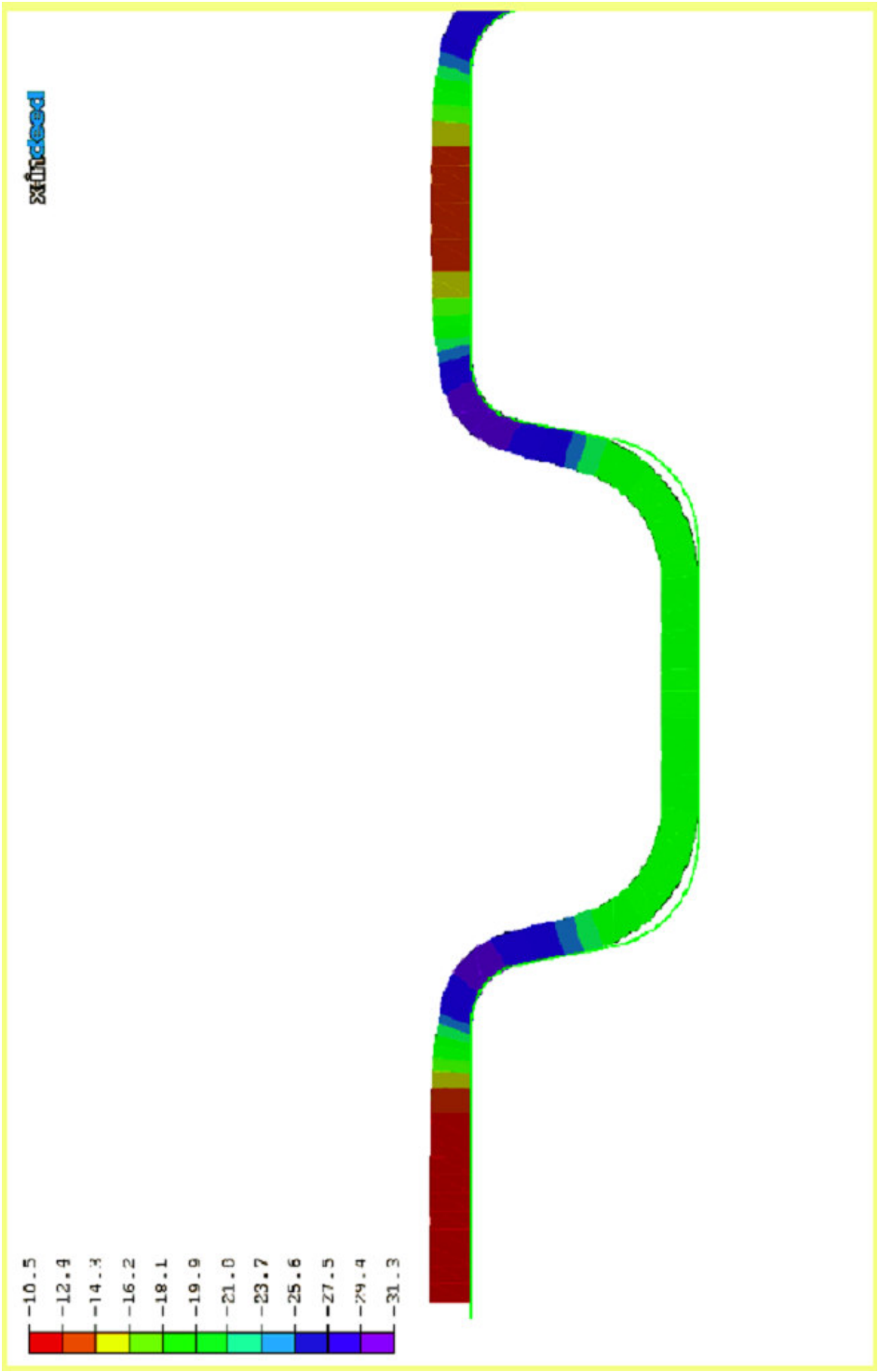

Figure 37. Material thinning analysis of initial pressed plate profile.

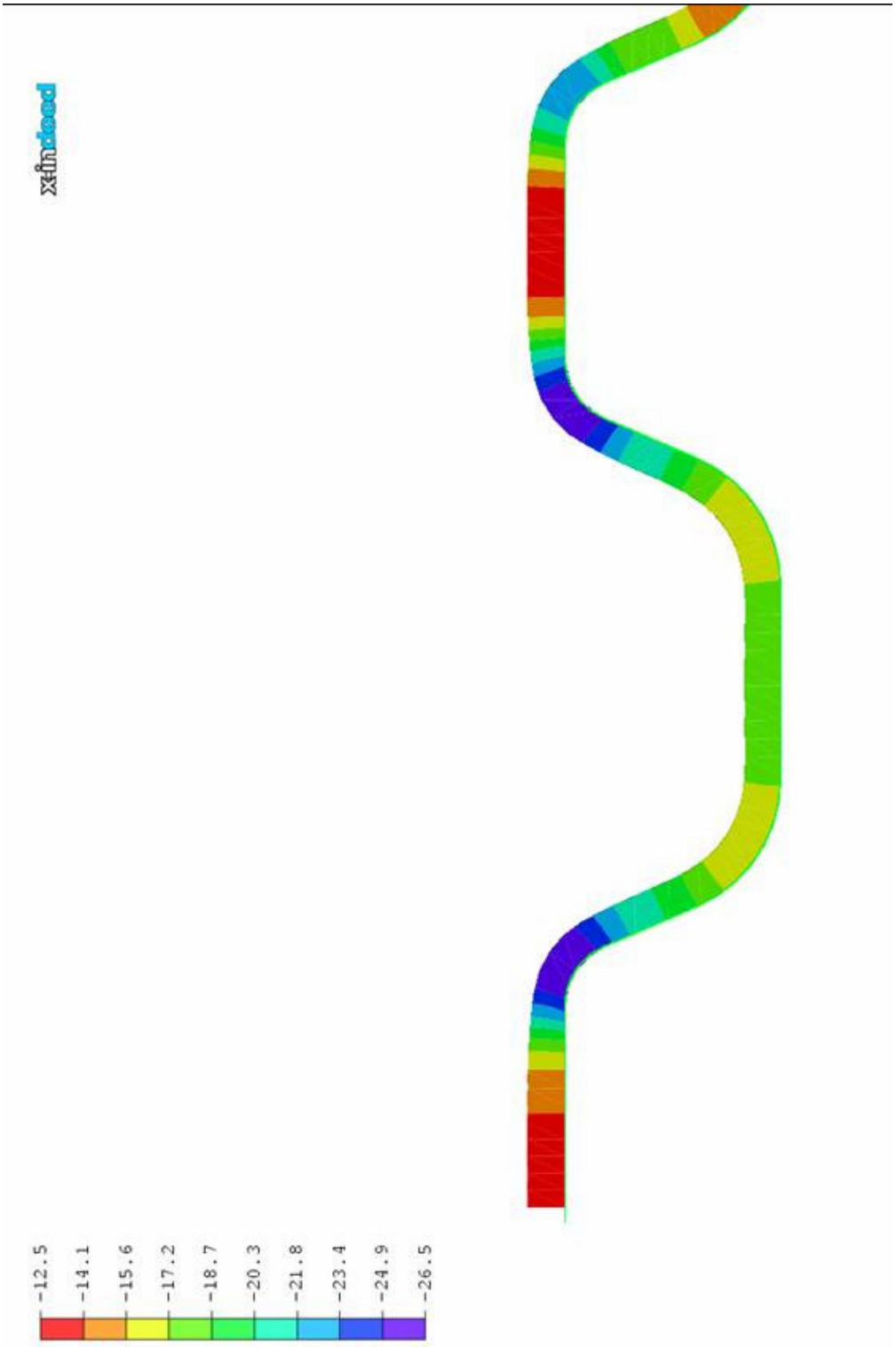

Figure 38. Strain analysis of revised profile proposed by the hydroforming company.

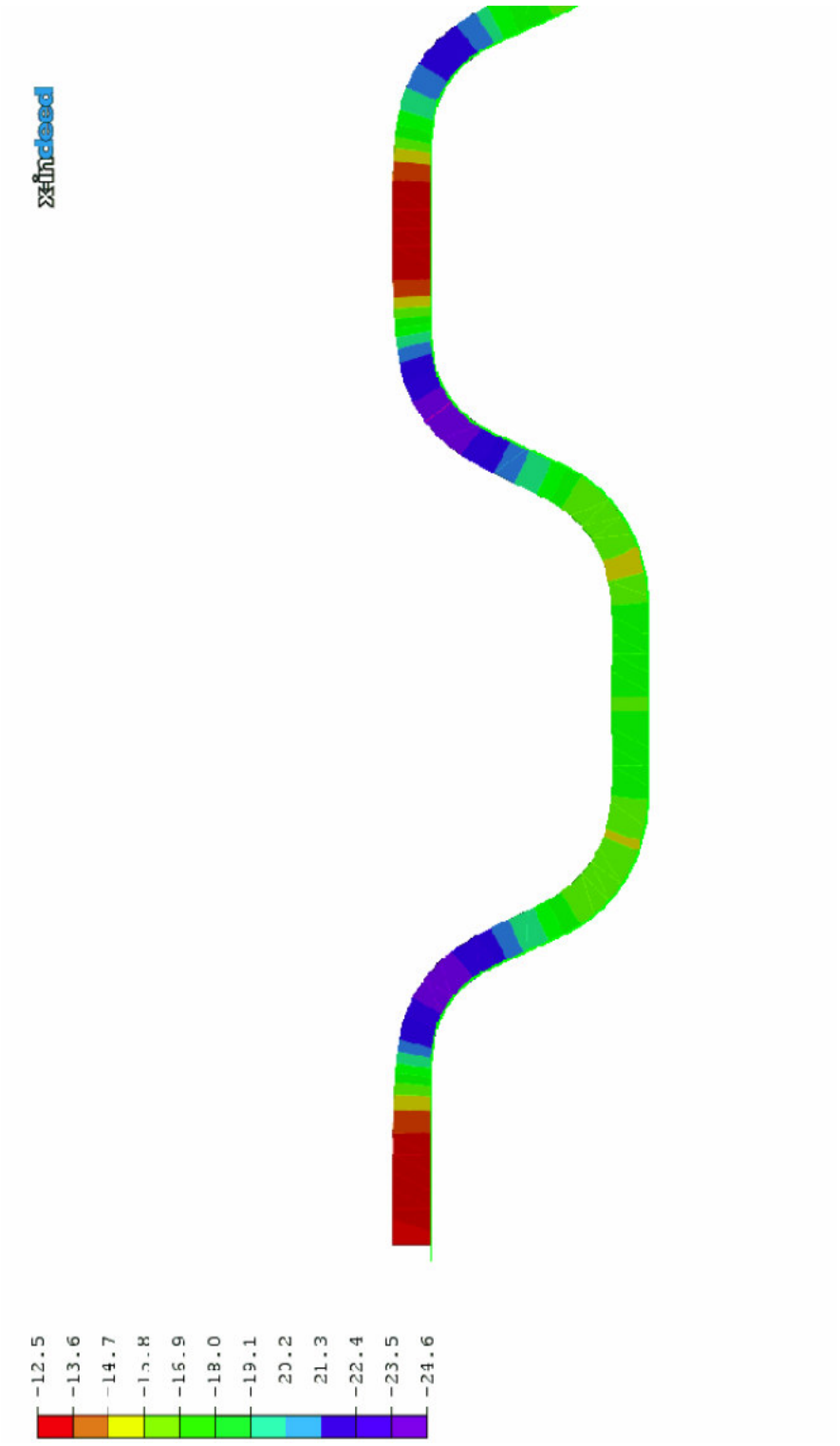

Figure 39. Final pressed plate profile proposed and adopted by Intelligent Energy.

A further complexity arose during plate manufacture, the stainless steel alloy used to manufacture IE's etched plates is a high specification, corrosion resistant material with low electrical contact resistance which has relatively limited availability; efforts to source this material in a 0.1mm thick, fully annealed (i.e. pressable) form were unsuccessful and as a result all plates were manufactured using 316L which is much more freely available but also has a higher electrical resistance. As a consequence, it was to be expected that given this and the previously highlighted resistance issues associated with the pressed form, achieving etched plate performance using the pressed plate technology was likely to be challenging.

3.5.2 Plastic Fluid Distribution Component

As described above, it was originally envisaged to use a plastic part on both sides of the plate periphery, giving a combination metal and plastic part which would be similar to the etched plate. Consultation with manufacturers indicated that the very thin mouldings – less than 0.3mm thick - needed for this would be very difficult to make, as the pressures required to fill such a thin mould cavity would be extremely high. It was decided that a single plastic part, incorporating both anode and cathode delivery channels, would be easier to mould.

Plastic parts for the Mk1 pressed plate stack were manufactured by injection moulding, demonstrating the possibility of making stack components via a well known mass production technique. This process highlighted a number of areas where care was required, particularly in the location of ejector pins and gates.

The Mk2 plastic fluid distribution component was similar to the Mk1 design, but with the ports rearranged to fit with the new plate active area and the thickness tailored to the depth of the new pressed plate. Mk2 parts were machined from acetal sheet on a CNC milling machine, as it was felt that the volumes required did not justify the cost of injection mould tooling. It was also possible that the lead-times associated with mould tool manufacture would have compromised the programme and it was felt that the Mk1 manufacturing programme had already shown that the technology was amenable to this type of production technique.

3.5.3 Cathode Seal

A seal is required between the plastic component and the face of the plate which it contacts. In early stack assemblies, a cut gasket was used, but plastic fluid distribution components have also been produced with a printed seal. The printed seal has two distinct benefits over a cut gasket. The total height of the peripheral components is critical to achieving good diffuser compression and to minimising the cell pitch and a printed seal adds less height to the plastic component than a gasket. Also, as the printed seal is bonded to the plastic component no further positioning is required, simplifying assembly. As a further development of this idea, small test parts were produced with an injection moulded silicone seal within an injection moulded plastic part, as shown in Figure 40. As the moulded seal would sit within its channel, it adds no height at all to the plastic part when compressed within a cell assembly. This technique would allow mass production of a finished part with a built in seal in a 2 stage moulding process with no need for further finishing or assembly operations.

Figure 40. Silicone seal moulded onto injection moulded plastic component.

3.5.4 Anode Gasket

A number of anode gasket materials have been used and the profile of these has been developed during this programme. As with etched plate stacks, grafoil was used initially as this was a material well known to us and it fulfilled the requirements of sealing and absorbing changes in component height such as that found at the edge of the MEA. Due to the plastic fluid distribution component having both anode and cathode delivery tracks on one side of the plate, as well as sealing around the ports and the periphery of the cell, the anode gasket was now required to perform the function of delivering gas to and from the anode active area. Throughout Mk1 stack testing, crossover was a significant problem and this was thought to be largely due to the interaction of the plate and the anode delivery feature in the gasket. In the Mk2 stack design, the profile of the gasket was modified to give better sealing while still performing the function of anode gas delivery.

A new moulded anode gasket has also been developed to replace the material historically used. This features a closed cell structure which allows deformation of the gasket after the initial sealing load has been applied, with much lower compressive loads than required to seal and deform the gasket material used to date. After initial testing in etched plate stacks, the concept was further developed for the pressed plate stack, by incorporating an anode fluid delivery region. This novel gasket is currently the subject of a patent application.

3.6 Mk1 Stack and Single Cell Testing

Initial Mk1a short stacks gave poor performance, as shown in Figure 41, for which a number of causes were identified. Gas crossover was a problem in all stacks, partly due to unsuitable positioning of ejector pins in the plastic part mould tool, although this was reduced to some degree with design revisions to the plastic part and the anode gasket. The most serious problem was dimension mismatching between parts, caused by a number of factors.

- Greater than expected spring-back of the steel resulted in the plate being thinner than originally designed.
- Ejector pin witnessing on the plastic component increased its effective thickness.

When combined, this led to a thickness increase around the periphery of the cell, with a decrease in thickness in the active area, leading to a lack of diffuser compression. Both issues could only be addressed by tooling modifications, the lead-times for which could not accommodated within the programme, hence, as it was likely that further tooling evolution would be required, testing continued with the components as received.

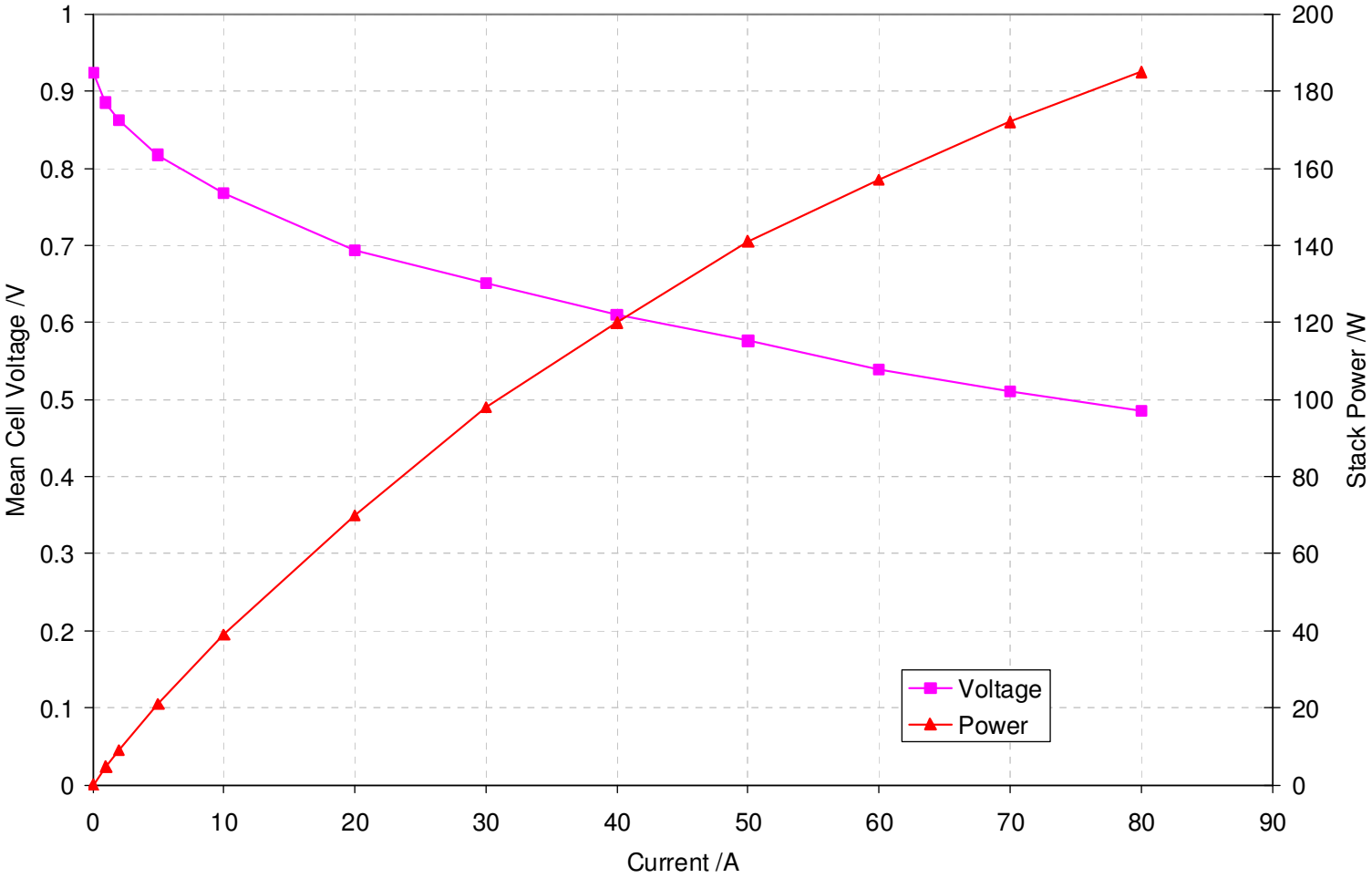

Figure 41. Initial polarisation curve of Mk1a 5 cell pressed plate stack at 6.75x air stoichiometry.

In order to understand better the issues affecting cell performance, a series of single cell tests was performed. In single cell testing cell balance is not an issue, so cell performance can be developed more easily. The single cell tests covered the original design (Mk1a), as well as updated designs to improve sealing and diffuser compression (Mk1b, Mk1c). The issues highlighted by these tests are summarised below:

- The ability of the cells to deliver high current was found to be limited severely by an anode delivery problem. A feature in the plate pressing incorporated on the advice of the plate manufacturer to avoid possible metal splitting issues, caused a pinch point in the anode diffuser limiting flow in the anode delivery and exhaust areas. To counter this, the anode diffuser was modified in the inlet and exhaust track areas, leading to much improved anode flow, which allowed the cell to be run up to much higher currents.
- A range of diffuser configurations were investigated, including extra diffusers in both anode and cathode to improve compression, and although performance was improved, air flow and cell resistance were still high. To overcome this, plastic fluid distribution components were manufactured by CNC machining, in a range of overall thicknesses, and tested in single cell assemblies to find the optimum. Using these, the correct amount of diffuser compression could be achieved, with the diffuser configuration as originally designed.

All of these modifications put together in a single cell (Mk1b) produced a much higher performance than previously achieved with pressed plate cells. Just as significantly the performance was now very stable and achieved at comparable air and water flow rates to those used in etched plate cells. Figure 42 shows the polarisation curves of Mk1a and Mk1b single cells. The performance of the Mk1b design increased dramatically to around 0.58V at 80A, only a few tens of millivolts below the performance of the etched plate technology, a difference which might be expected given the difference in resistance of the different metal alloys used. Figure 43 shows the air stoichiometry sensitivity for the Mk1b cell with different diffuser configurations. There is a clear benefit to matching the working dimensions of the different components – compensating for a mismatch by adding extra diffusers raises the operating voltage (at higher flow rates) but also compromises the air flow sensitivity of the cell.

The cell design was further refined (Mk1c) and the plastic part was redesigned to deliver air more evenly over the cell's active area. A cell was assembled with parts machined to the new design and although performance under standard test conditions was similar to the previous Mk1b design as shown in figure 44, the air stoichiometry sensitivity was also within normal etched plate bounds, see figure 45. This cell performed consistently for an extended period of testing and the voltage was seen to be stable during this period, figure 46 shows a summary of the entire test which included polarisation curves and fluid flow diagnostics.

With the correct diffuser compression, the single cell exhibited stable performance in excess of 90% of etched plate stack performance, at standard fliud flow rates. A Mk2 design was thus generated, using all that had been learned during the development of the Mk1c cell design.

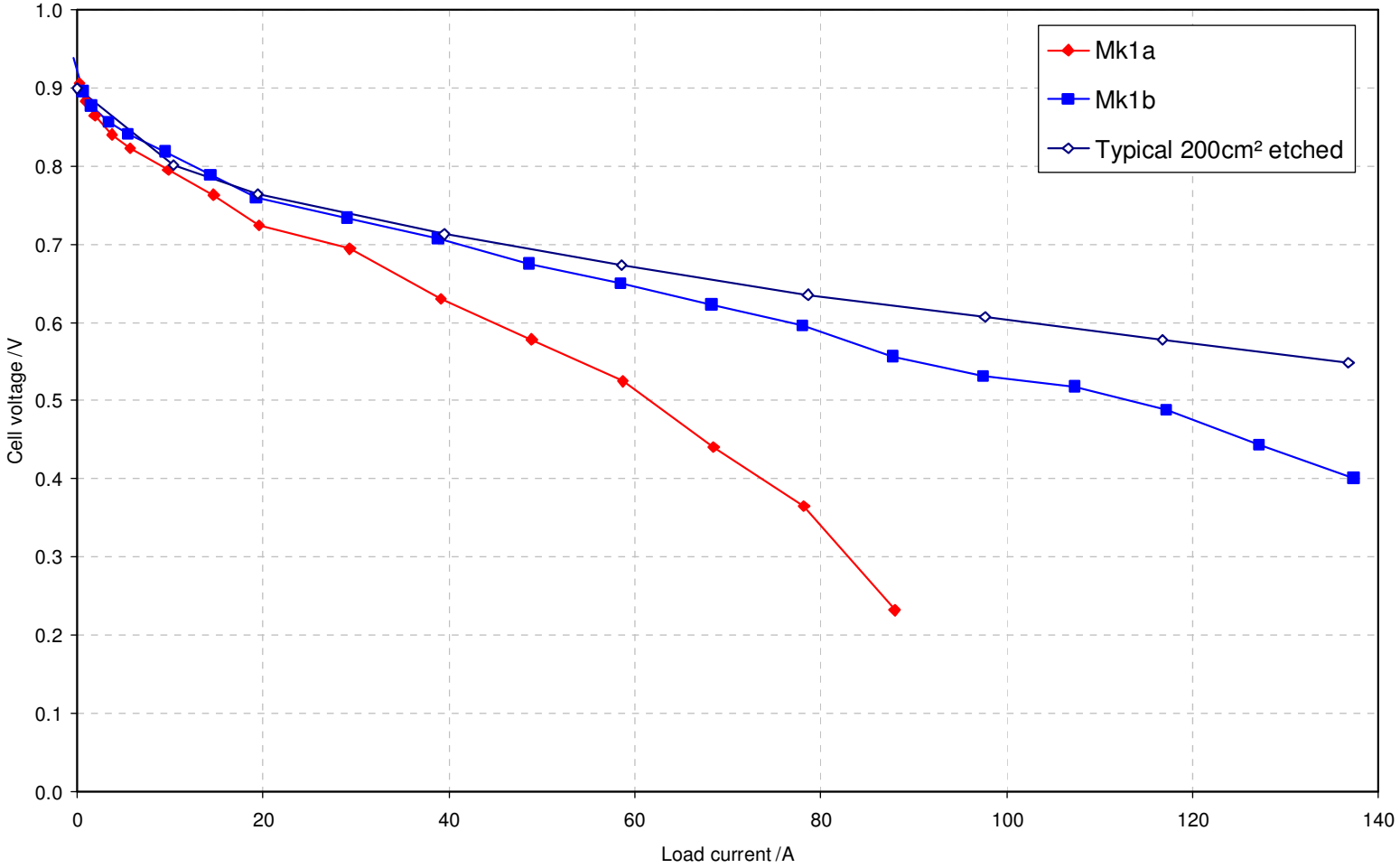

Figure 42. Polarisation curves for Mk1a and Mk1b single cells.

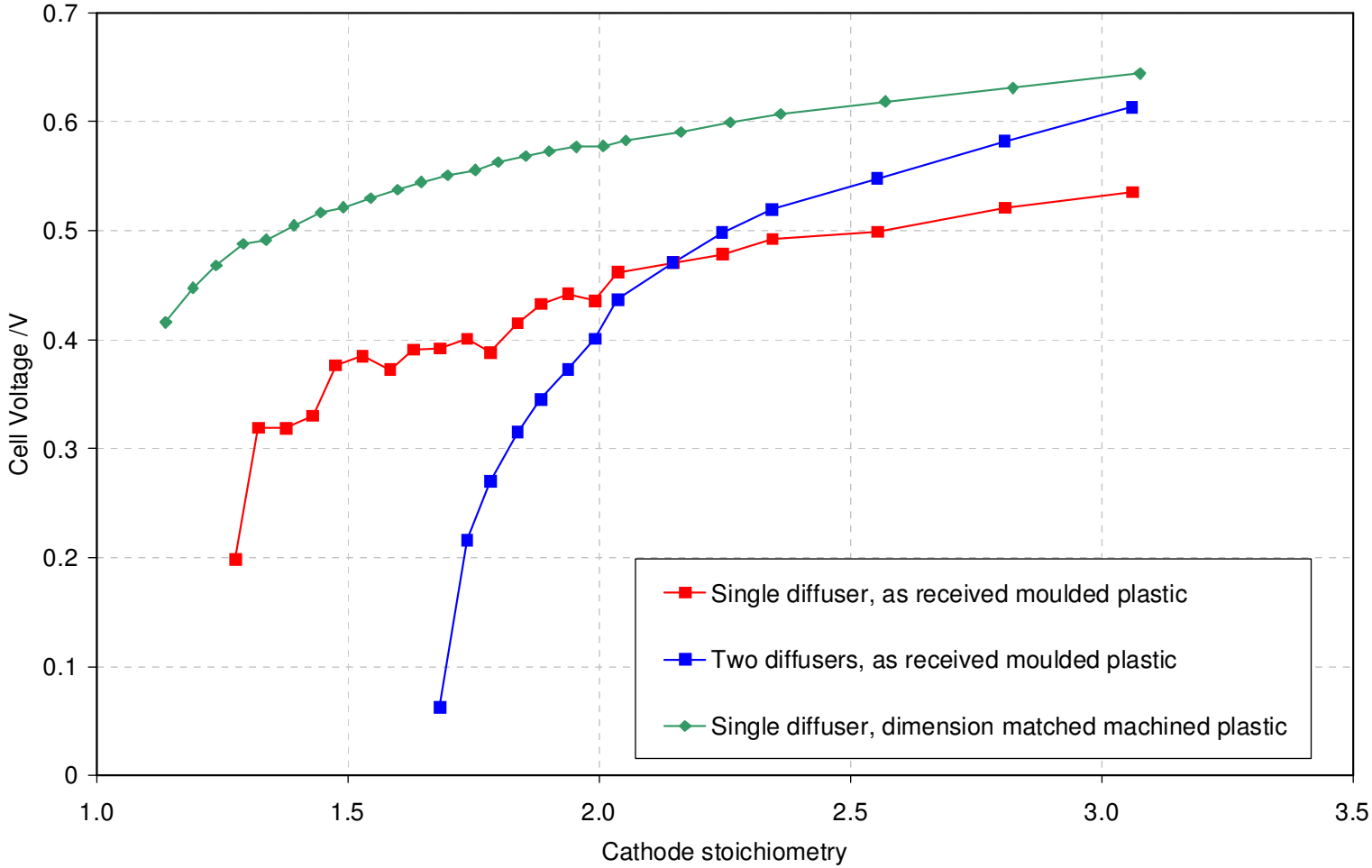

Figure 43. Air stoichiometry sensitivity at 80A for Mk1b single cells with different thickness plastic gaskets.

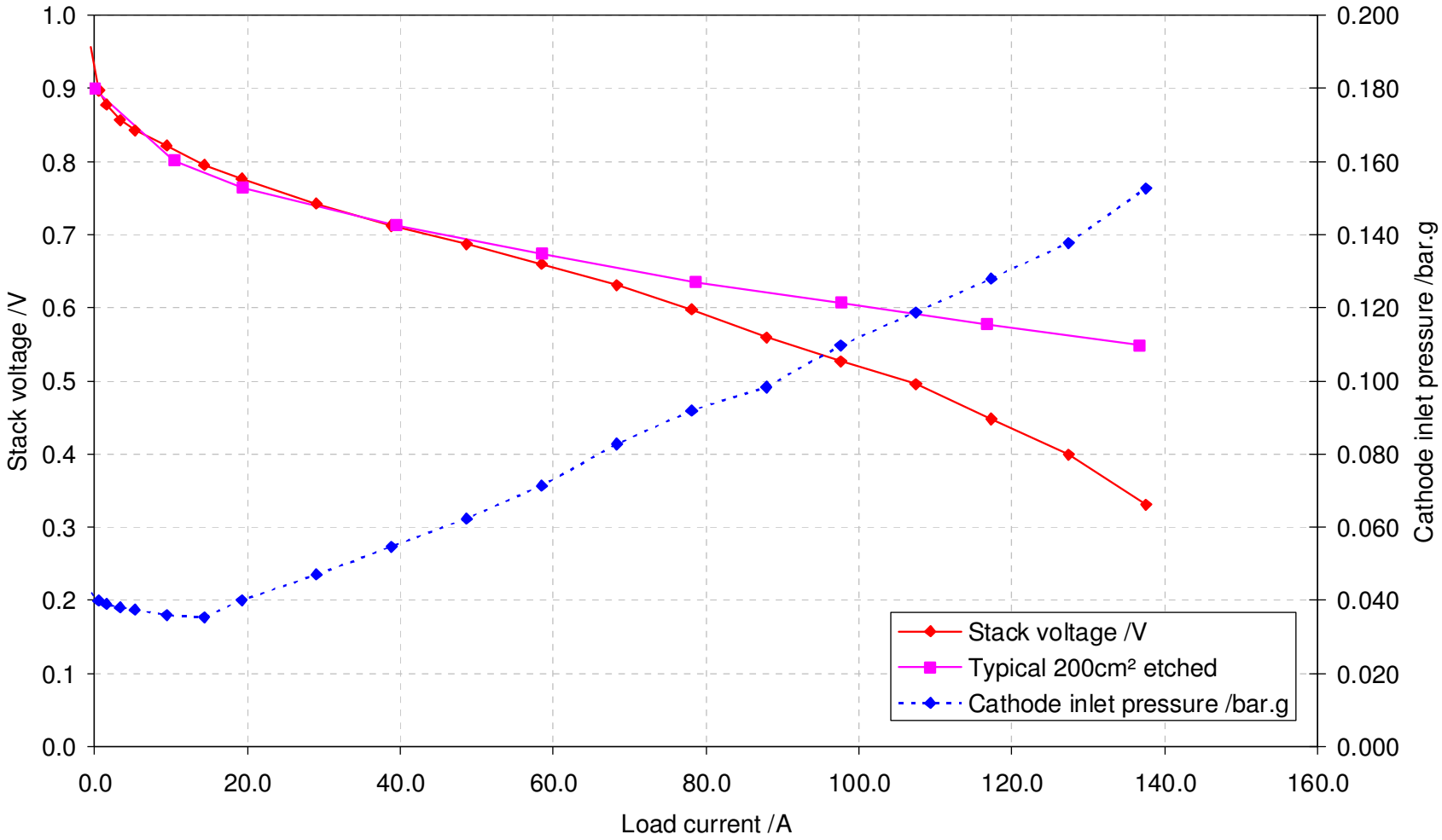

Figure 44. Polarisation curve for Mk1c single cell at 2x air stoichiometry.

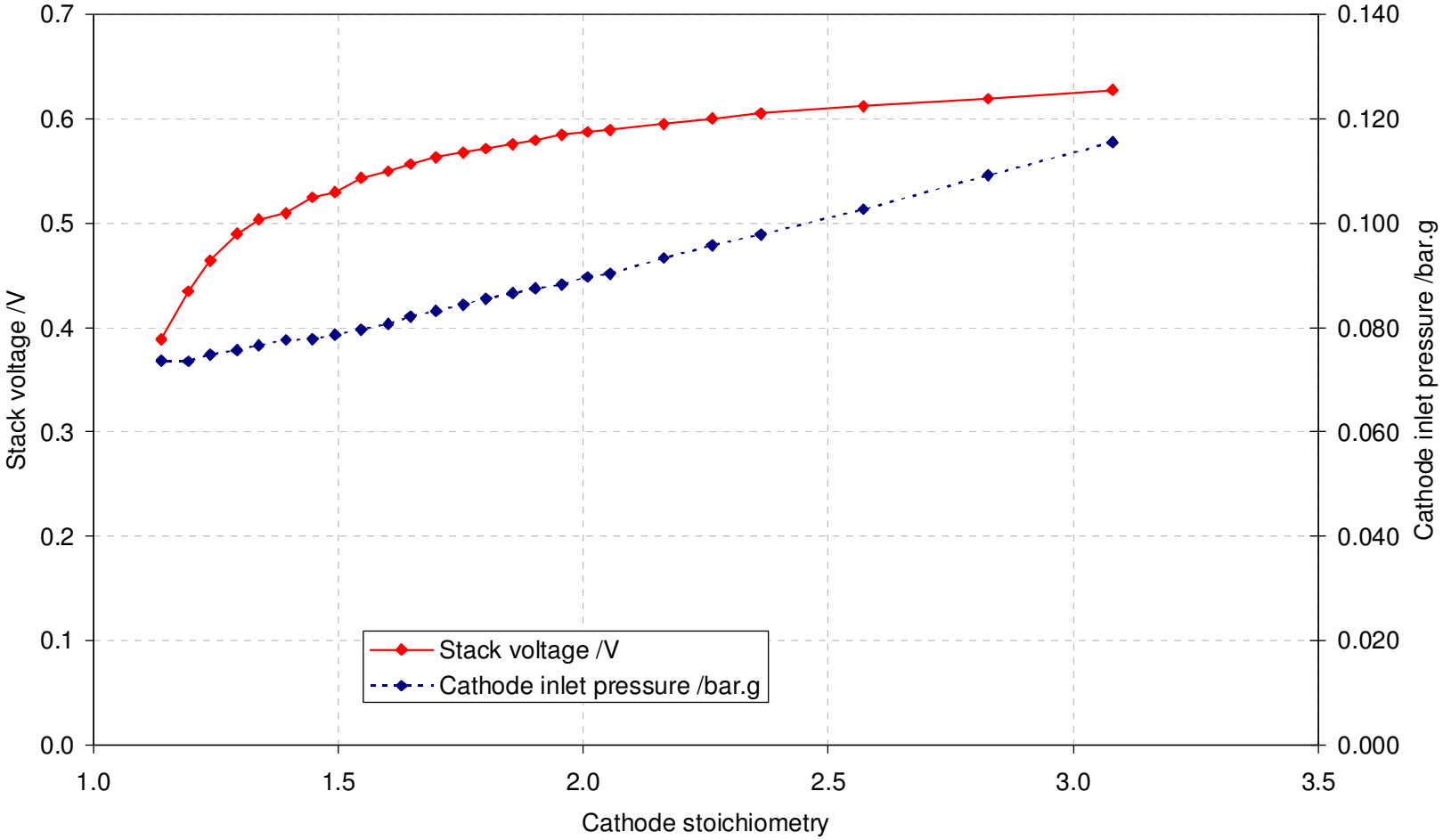

Figure 45. Air stoichiometry sensitivity test for Mk1c single cell at 80A.

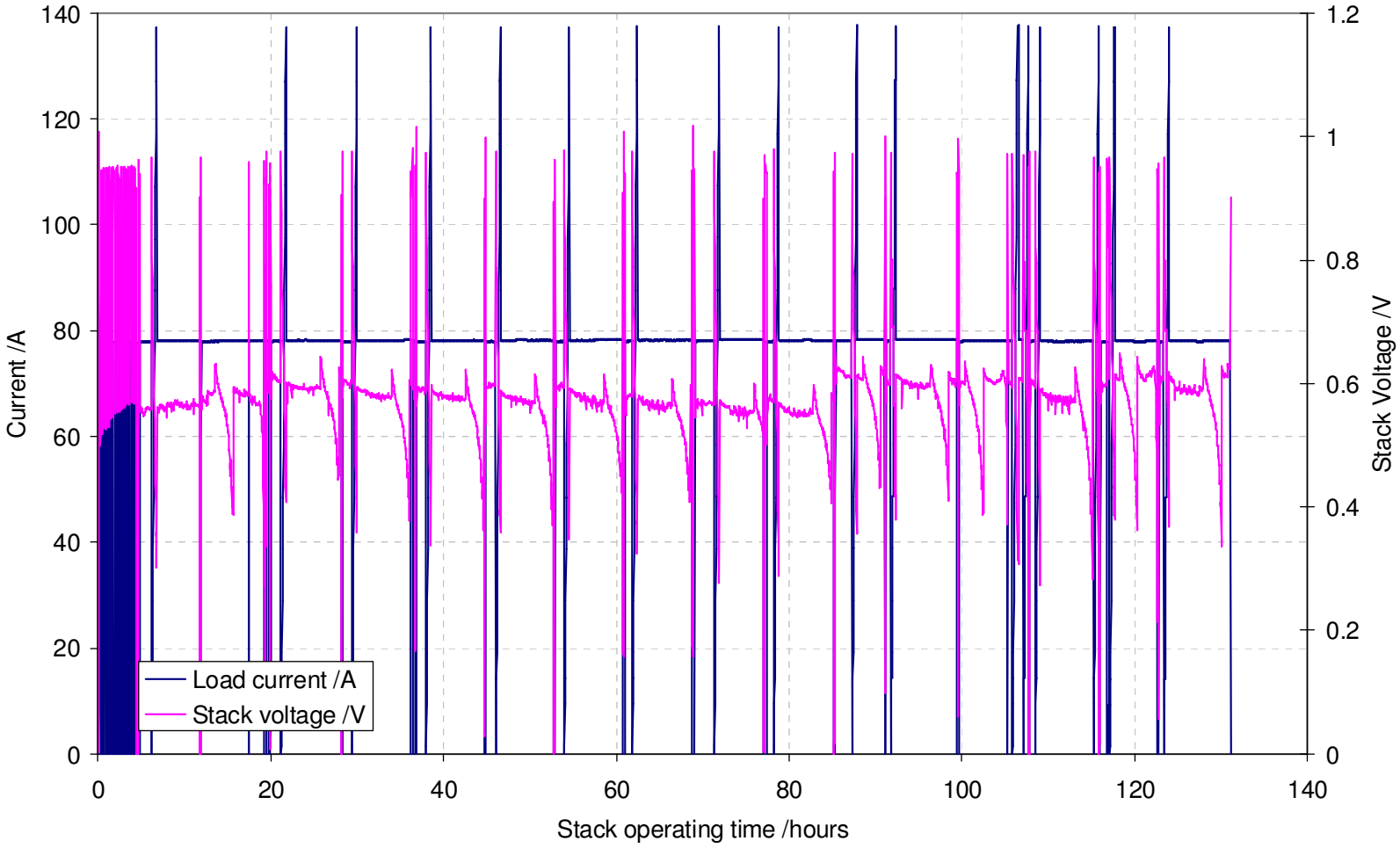

Figure 46. Durability data for Mk1c single cell.

3.7 Mk2 Short Stack Build and Test

A number of single width stacks were built and tested and details and results are reported in this section. Key issues in producing these stacks were the long lead times associated with the new design components. In particular, the press tools to produce the pressed plates were complex and there was a period of development associated with producing a profile which could be formed safely. A new anode gasket profile introduced for the Mk2 design improved sealing of short stacks dramatically, virtually eliminating crossover.

Figure 47 shows a polarisation curve for a 5 cell Mk2 pressed plate stack (figure 48). The stack exhibited almost no crossover and good anode flow, showing that the modification to the anode gasket profile had been effective. This stack was installed on a test station and was tested for approximately 200 hours. Mean cell voltage was 0.57V at 80A.

Figure 49 shows the effect of cathode stoichiometry on stack performance at 80A. Although stack performance still falls with decreasing air flow rate, it should be noted that this test ran down to a much lower flow rate than previously.

3.8 Long Stack Build and Test

Following the success of the 5 cell stacks both in terms of sealing and performance, a 48 cell pressed plate stack was assembled using the same fundamental design. This was intended to highlight any difficulties during assembly and also allow the characterisation of stacks with larger numbers of components manufactured using the high volume techniques being explored.

Figure 50 shows the 48 cell stack installed on the test stand. On initial assembly, the stack showed high crossover flow rates, the cause of which was not immediately apparent. Despite this, it delivered power at the 80A nominal test point at a voltage only slightly below that achieved by the 5-cell short stack. Figure 51 shows a polarisation curve. The low open circuit voltage of certain cells highlighted where the crossover was taking place and a takedown was carried out to enable ex-situ characterisation of the faults.

Figure 52 shows a further polarisation curve for the stack after removal of a number of cells exhibiting crossover and reassembly. Cell performance was improved significantly the mean cell voltage increasing from 0.51V to 0.56V at 80A. It is clear from the best cells, that the pressed plate technology is capable of performance close to that of the etched technology if the variability can be addressed.

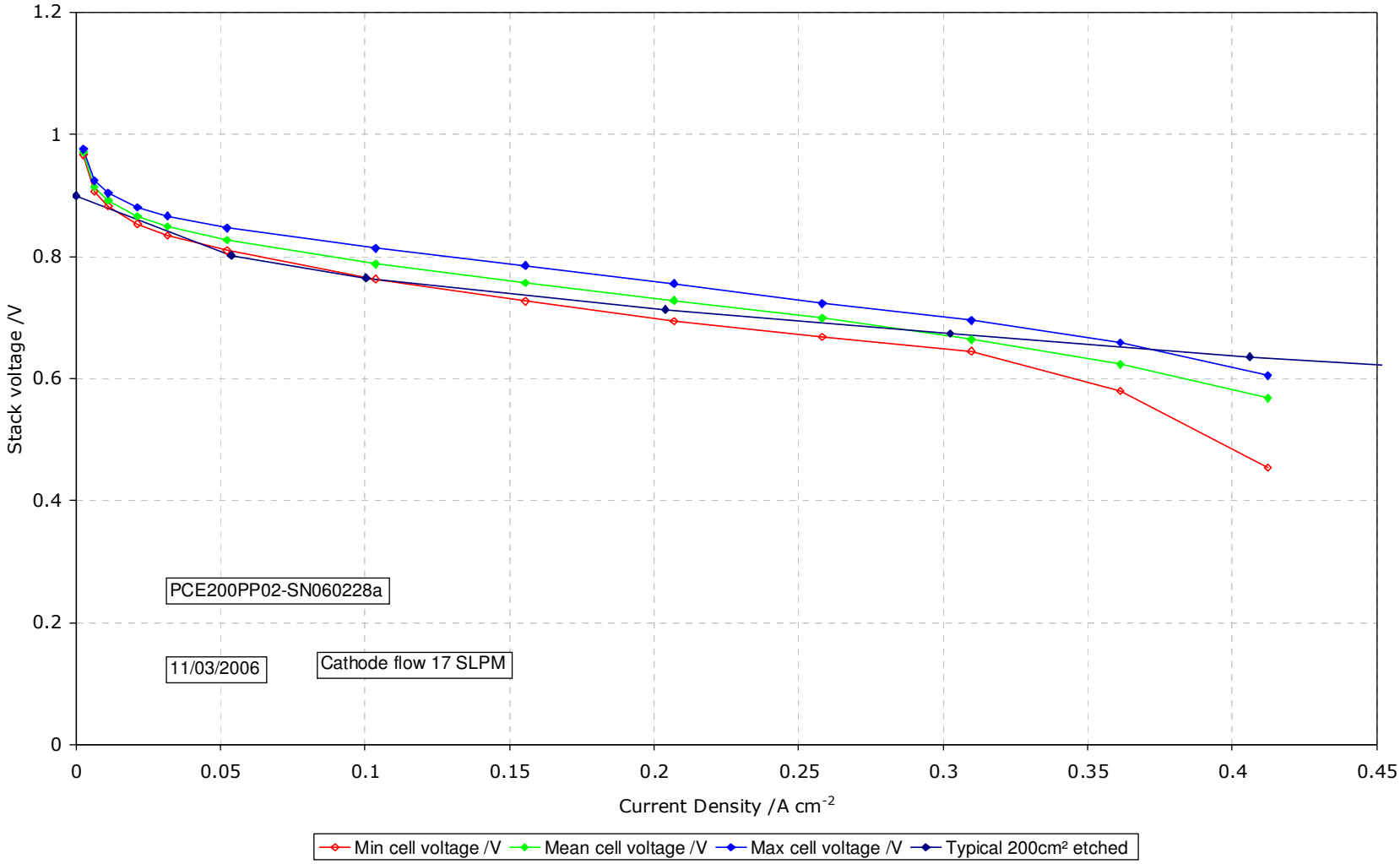

Figure 47. Fixed flow polarisation of 5 cell Mk2 pressed plate stack.

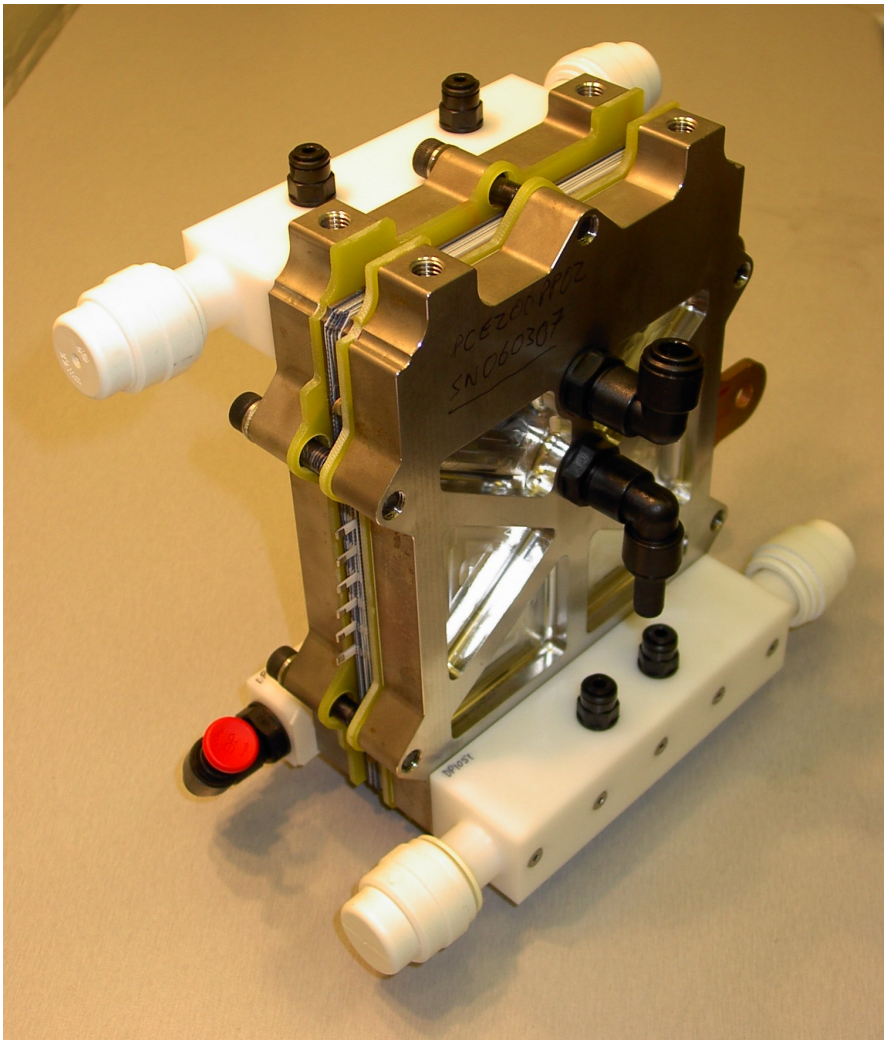

Figure 48. 5 cell Mk2 pressed plate stack.

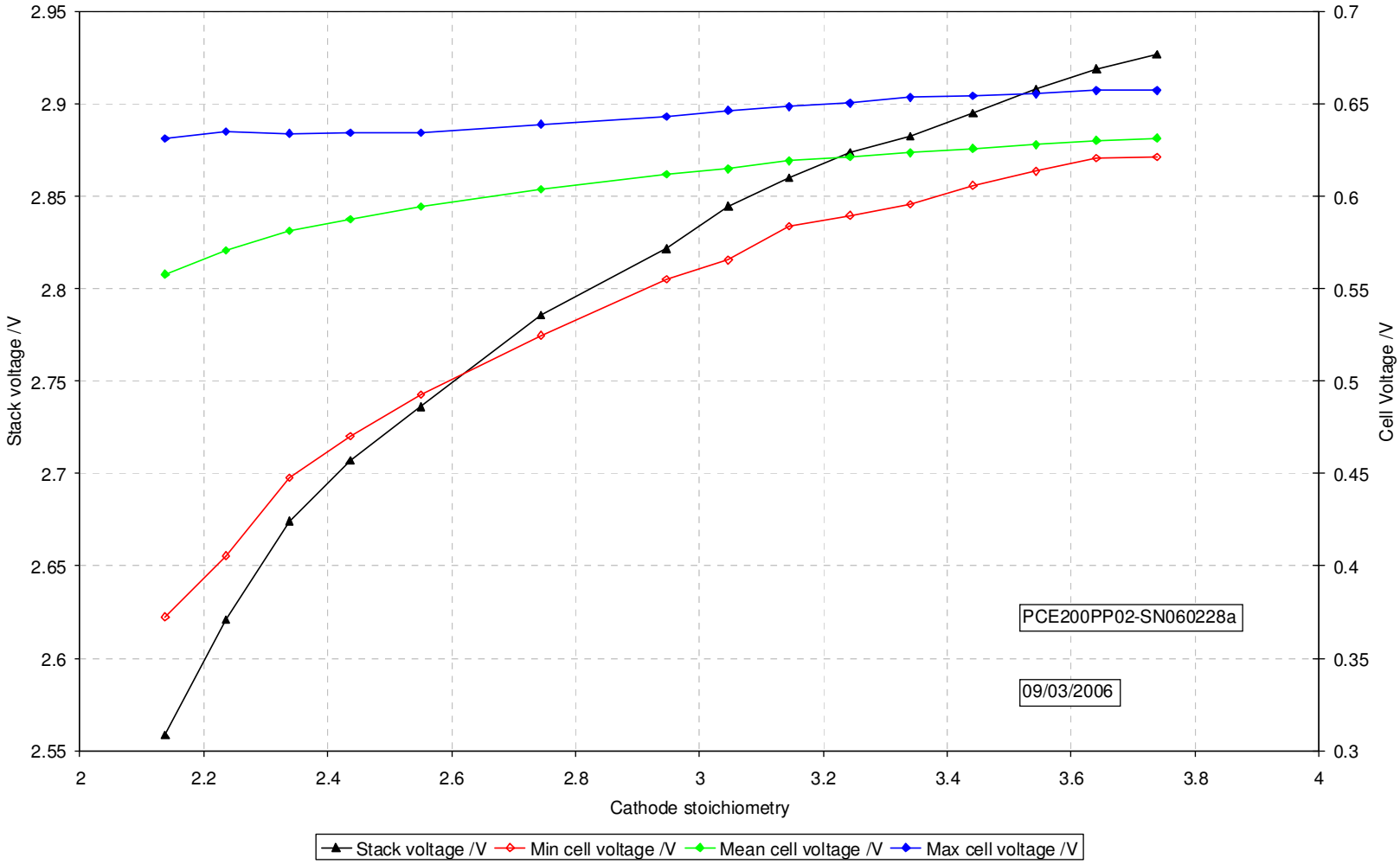

Figure 49. Air stoichiometry test.

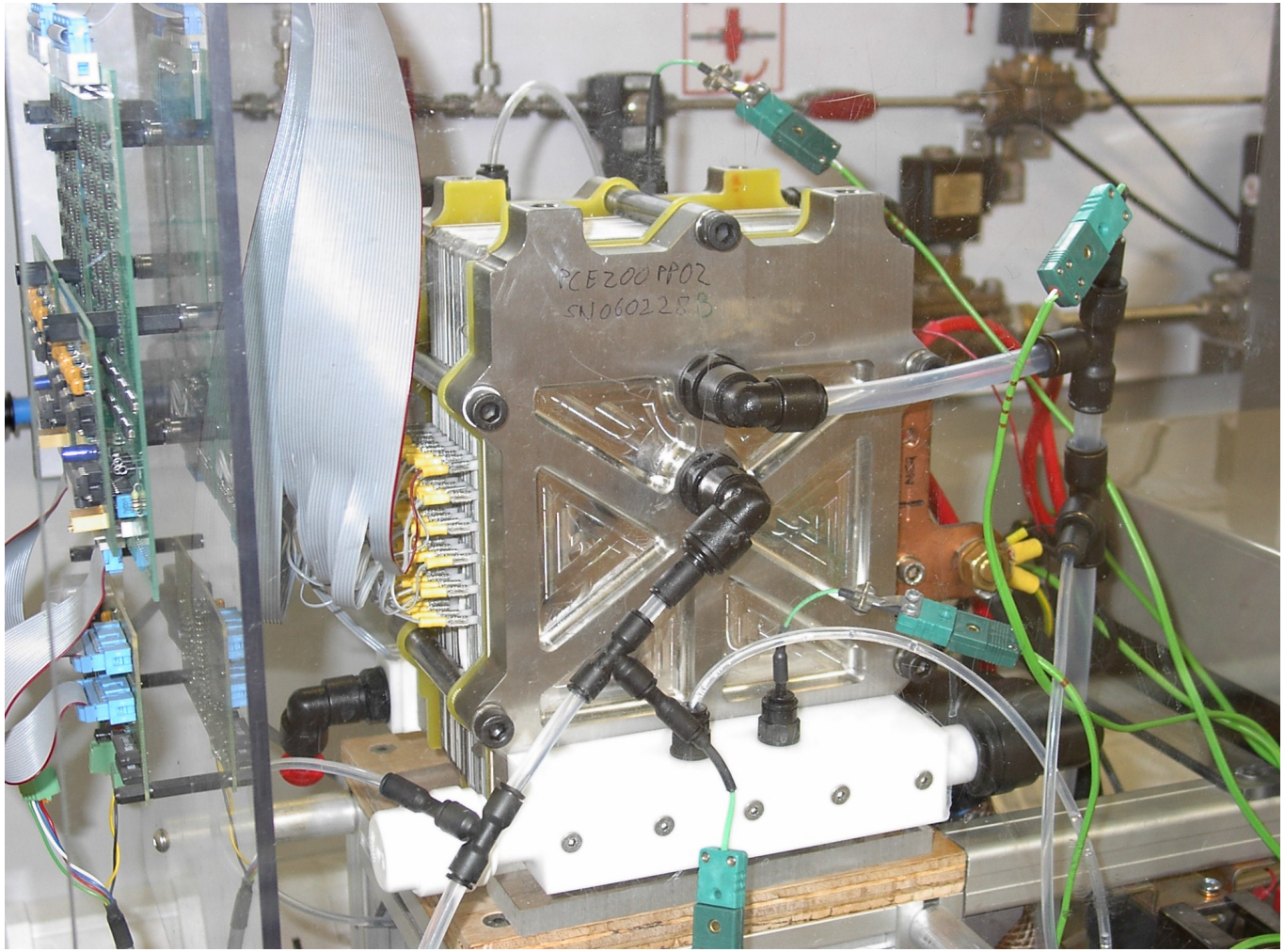

Figure 50. 48 cell Mk2 pressed plate stack installed on test stand.

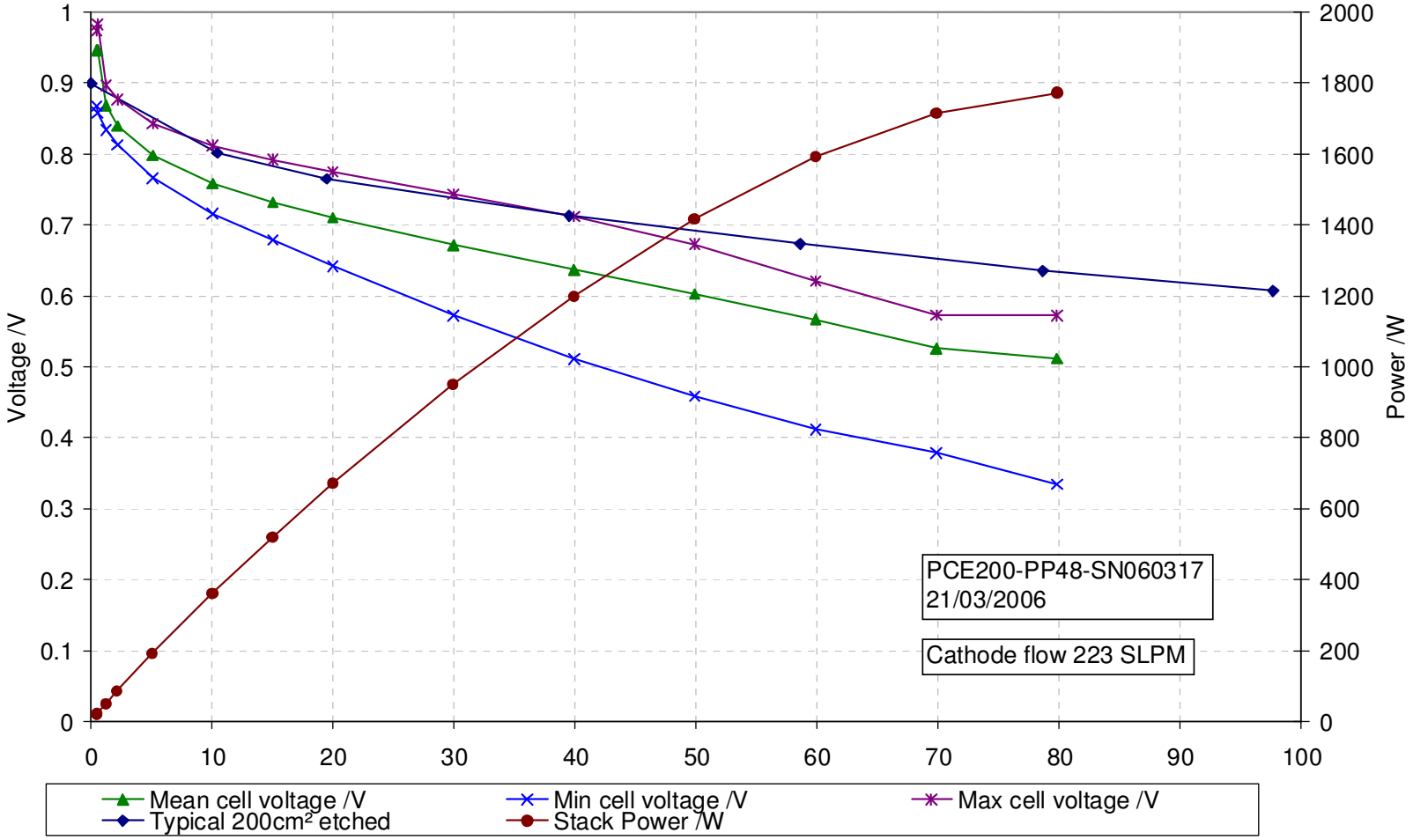

Figure 51. Polarisation curves for 48 cell Mk2 pressed plate stack.

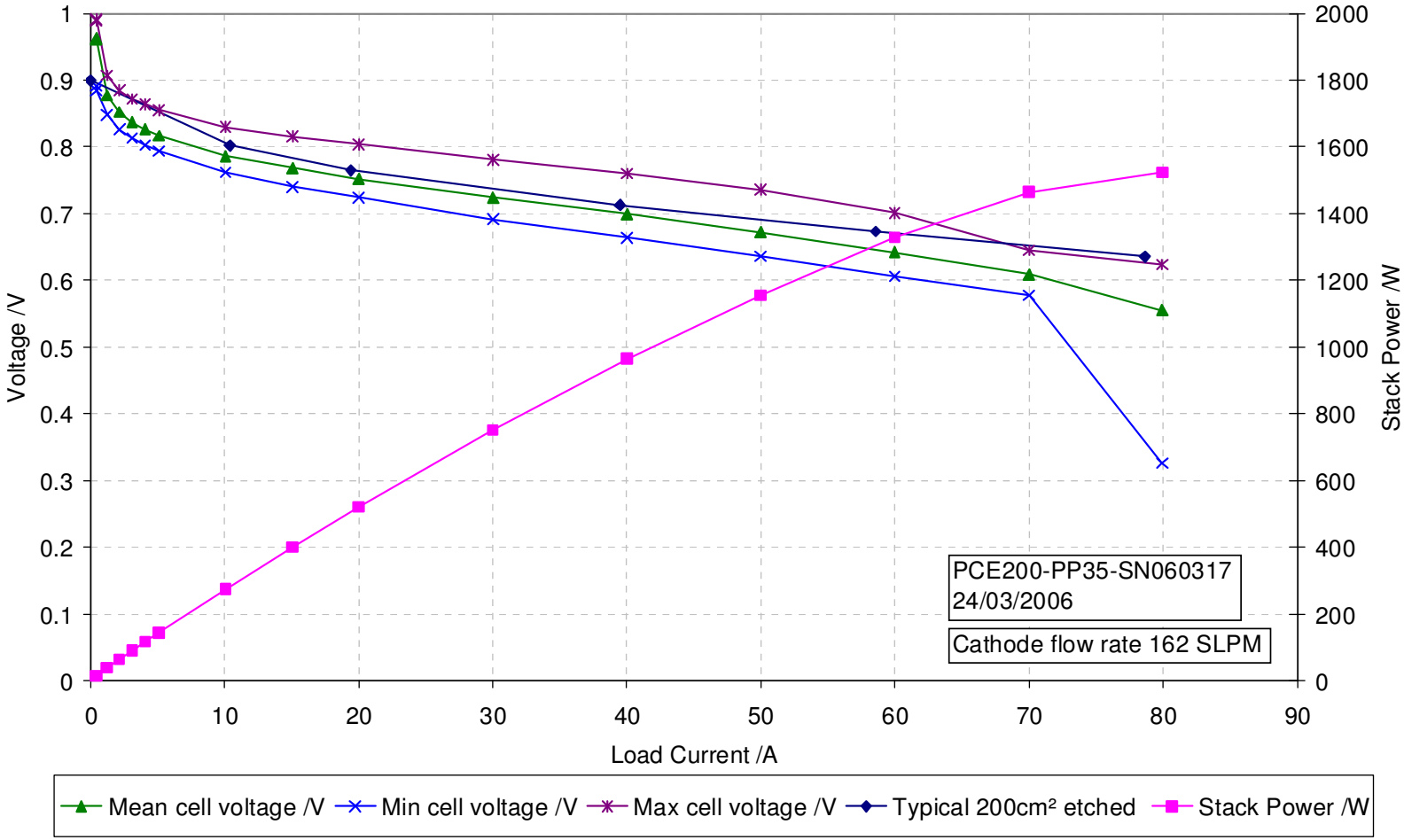

Figure 52. Polarisation curves for 35 cell Mk2 pressed plate stack.

3.9 Scale-Up To Triple Width

It was reported in section 2.2 that the active area chosen when scaling up the etched stack technology was determined chiefly by the MEA size available. In scaling up the pressed plate, the same active area was selected to allow direct comparison with etched plate triple width technology and to allow the use of common diffusers and MEAs. Many of the lessons learned in the scale up of etched plate designs had already been applied to the single width Mk2 pressed plate components.

It was envisaged that the triple width plate pressing would be one of the major technical obstacles, and the toolmaker initially had reservations about producing these parts. The channel profile of the pressed region remained the same as for the single width tool, while the clamping rib feature was extended to the full perimeter of the tool. In addition, the punches for cutting locating holes for laser cutting the ports were included in the press tool. These were not included in the single width tool and the holes were added in a separate operation, using the pressed region for location. This adds another stage to operations, as well as an opportunity for misalignment and subsequent scrapping of plates. Punching the holes at the same time as forming the pressed region ensures accuracy of alignment of the two features. It also suggests that punching the ports and profile and forming the pressed region should be possible in a single operation, reducing the cost of plate production. Long lead time was once again a major factor in meeting the project milestone, but technically, the plates were produced without any significant difficulty, and to the correct dimension.

The plastic fluid distribution component represented the greatest difficulty in component manufacture. Again, the design was achieved by multiplying the single width features across a larger component but due to the relatively small number of components required, and the cost and lead time of mould tooling, they were produced by CNC machining of sheet plastic, rather than being injection moulded. However, the flimsy nature of the finished component caused problems with mounting and machining hence, high scrap rates were encountered.

A number of assembly issues were encountered, principally related to the inherent flexibility of the components, this was less significant a problem under the etched plate programme because of the greater strength of the thicker etched plate, but is certainly a matter for further development attention. Figure 53 shows a 5 cell triple width pressed plate stack assembled and integrated into its test stand.

Polarisation curves for the 5 cell, 600cm^2 pressed plate stack are shown in Figure 54. The operating voltage was significantly reduced by a particularly weak cell, thus the mean cell voltage was only 0.49V at 80A. In contrast, the performance of the best cell (3) was as good as that of the best cell in the 48 cell single width pressed plate stack, delivering 80A at 0.57V.

Most of the performance deficit can be attributed to the plastic component. The machined components were substantially more difficult to produce and this resulted in thickness variations and the presence of burrs and plastic swarf. Manufacture of these components by the injection moulding route already demonstrated would have dramatically improved their quality and hence the overall stack performance, but on a lead-time basis that could not be accommodated within the programme.

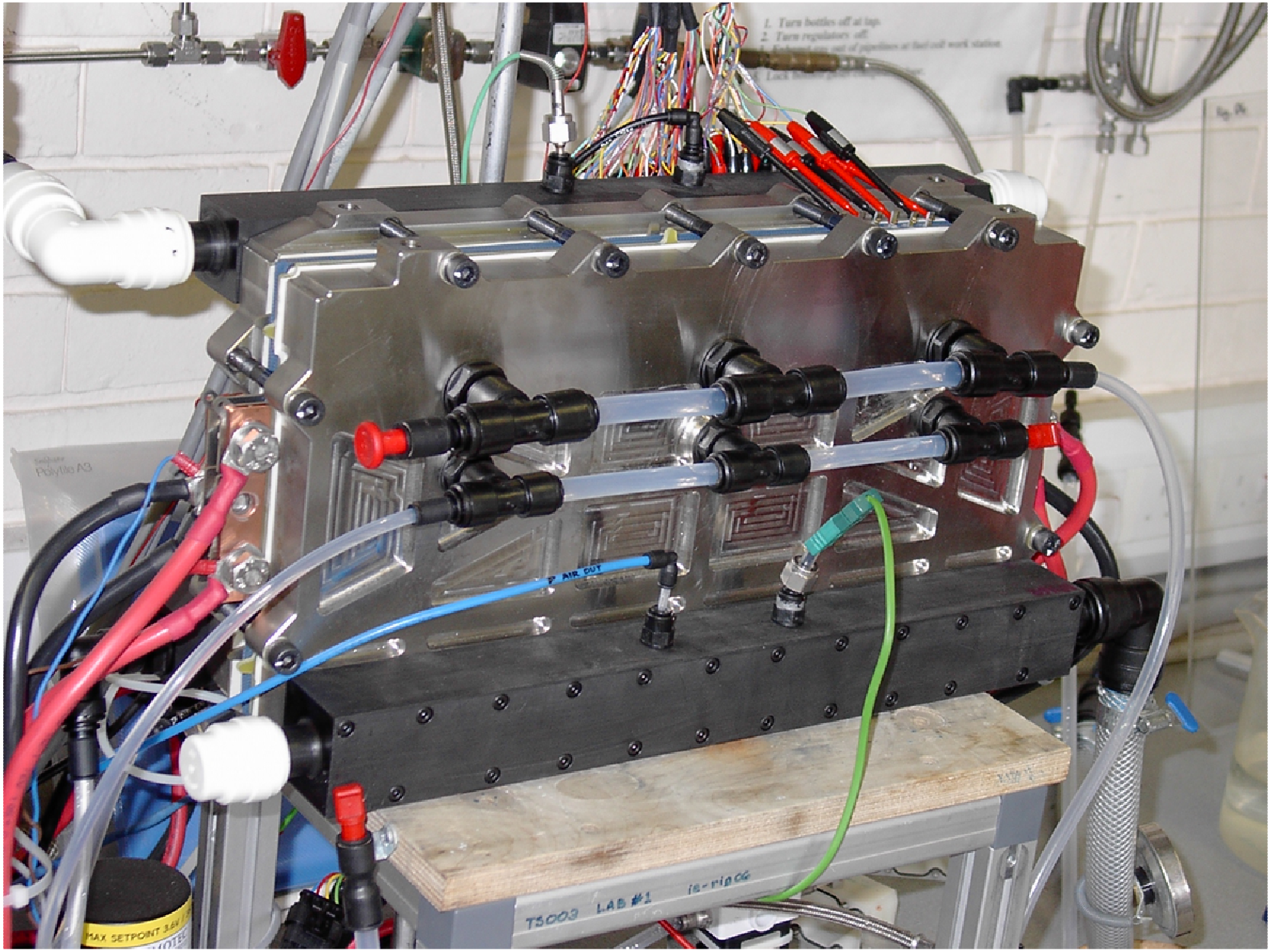

Figure 53 5 Cell triple width pressed plaee stack installed on test stand.

3.10 Performance Comparison with Etched Plate Technology

Figure 55 shows polarisation curves for a variety of stacks for the purposes of comparison. The performance of the Mk2 pressed plate stack in its five-cell manifestation is similar to that of the etched plate technology. However, the performance of the 48 cell unit was compromised by component inconsistencies. Taking the performance of the five cell unit, at present, despite using a more resistive alloy, the performance of the pressed plate technology is approximately 90% of the etched plate performance at 80A. Table 3 below gives details of plate and cell mass and volume and a comparison of power density on gravimetric and volumetric basis (quoted at a current delivery of 80A). The mass of the pressed plate is 27% of the etched plate mass and the total cell mass is 42% of the etched plate cell mass. This means that although in terms of power from MEA area the pressed technology is slightly behind the etched plate, on a gravimetric basis, it already offers double the power density. The cell pitch of the pressed plate stack is slightly reduced compared to the etched stacks, but not by enough to counter the power deficit per cell, so volumetric power density is slightly reduced.

Stack Type	*Plate weight /g*	*Cell Weight /g*	*Cell pitch /mm*	*Cell Power at 80A /W*	*Gravimetric Power Density /kW kg^{-1}*	*Volumetric Power density /kW L^{-1}*
Etched Plate	*90*	*110*	*1.2*	*52*	*0.47*	*1.44*
Pressed Plate	*24*	*46*	*1.15*	*46*	*1.00*	*1.33*

Table 3. Mid-stack power densities for etched and pressed plate technologies

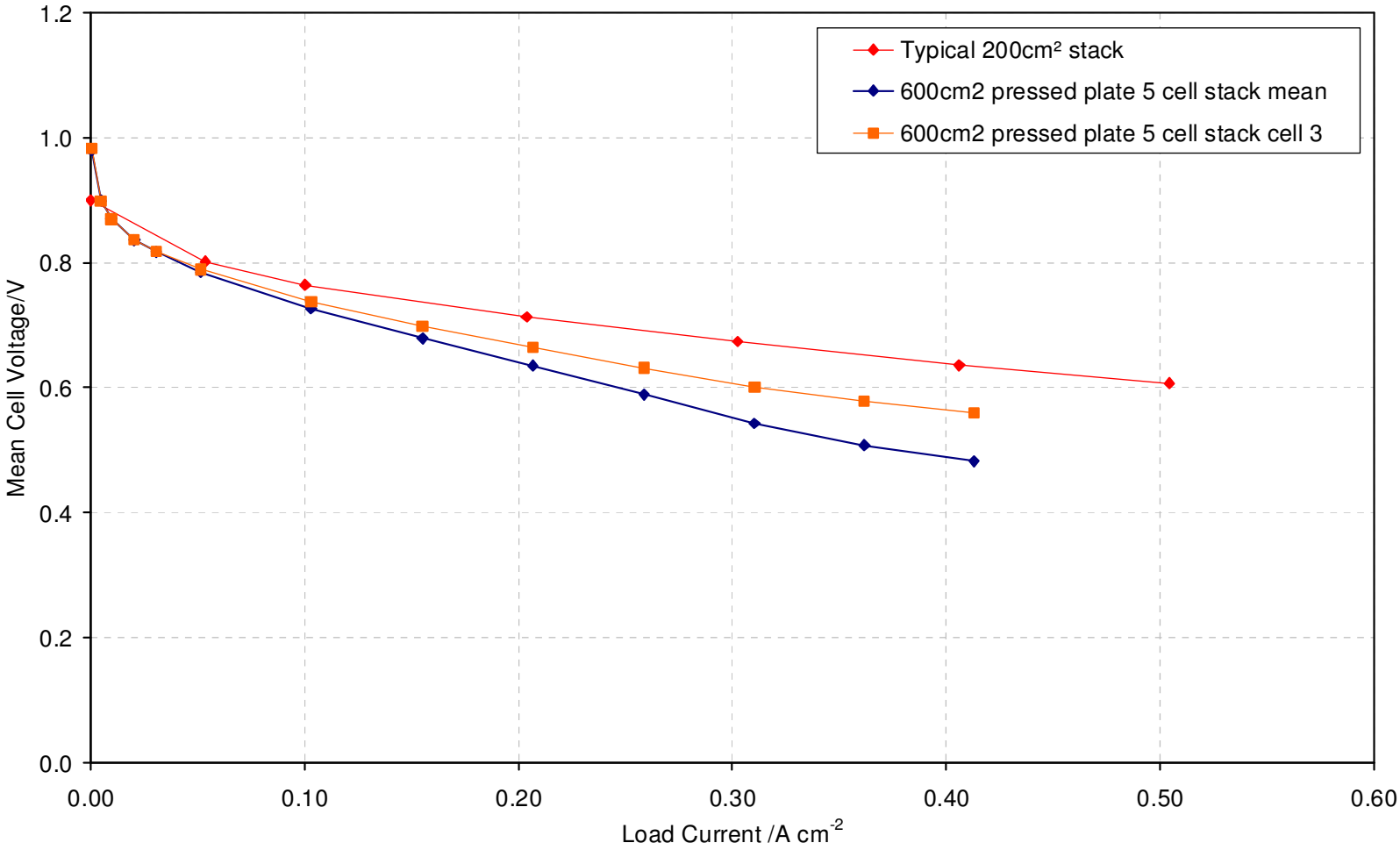

Figure 54. Polarisation curves for triple width pressed plate stack.

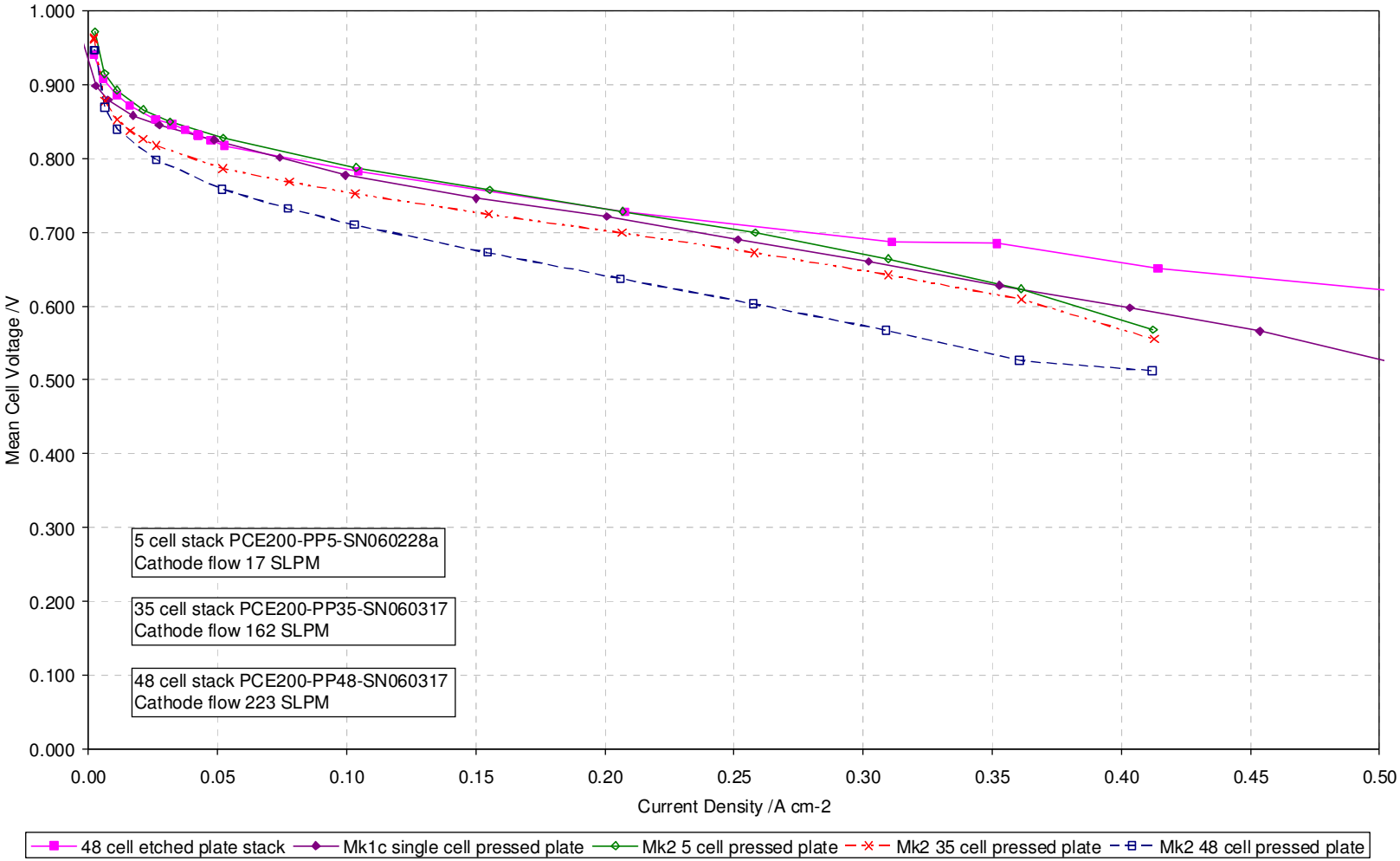

Figure 55. Performance comparison between single width etched and pressed plate technology.

4 JMFC MEA DEVELOPMENT

4.1 Introduction

This project comprised two phases with a number of milestones in each phase; the details of these milestones are shown in Appendix 1. In the first phase of JMFC work on MEA development for the Intelligent Energy hardware, sealed MEAs employing an early version of a developmental JM GDL material were developed that attained the first phase performance targets for hydrogen of 650mV at 400mA cm^{-2}, and 618mV at 400mA cm^{-2} for reformate, off gold tabs in an early version of IE single cell hardware based on the etched plate approach. Following a review of this work, both for hydrogen and reformate operation, it was decided to focus the remainder of the project on developments aimed at achieving more aggressive performance targets.

The target for Phase 2 was to demonstrate progress in the new IE single cell design towards enhanced and stable performance, with a goal of at least 0.65V at 500mA cm^{-2}, for hydrogen, measured directly off the stainless steel bipolar plates. The reformate target was set at 95% of the hydrogen target at the same current density (0.618V at 500mA cm^{-2}, 2% air bleed). In addition, a new etched plate Phase 2 single-cell design was provided by IE, to provide a test environment closer to that experienced by MEAs in stack hardware. Measurement directly off the SS plates of the single-cell was implemented, as this better replicates the situation in a practical stack. Testing had also shown that a commercial non-woven GDL material used by IE gave some benefits compared to a range of other materials; consequently this GDL was used for all testing in Phase 2 of the project.

4.2 Experimental

4.3 MEA Design

4.3.1 Hydrogen Operation

The particular operating conditions of the unique Intelligent Energy (IE) hardware design dictate that many of the key MEA design elements are related to water management in the GDL, membrane and catalyst layers. For Phase 1 of the project, work focused on developmental GDL materials (LCS – low cost substrate), while for Phase 2 work focused on using a commercial GDL material used by IE in their hardware and has been shown to function well in the IE cell set up with respect to mechanical and dimensional properties. For the membrane, a specific commercially available type was selected to facilitate good water diffusion between the cathode and anode.

With these two components of the MEA design fixed, the focus of the MEA design and development work for the hydrogen milestones was on development of catalyst layers that optimised performance and stability with the membrane/GDL combination and the particular IE operating conditions. Catalyst coated membrane (CCM) MEAs were used throughout, to avoid any influence of the substrate on the properties of

the catalyst layer, and to be consistent with the work in previous milestones.

The design intent as followed in this activity was firstly to maximise the performance (cell voltage), then to modify the catalyst layer structure to give longer-term voltage stability. To gain maximum voltage performance the catalyst layers were initially designed with a combination of materials known to provide enhanced performance but could also possibly result in poor long-term stability. Subsequent design iterations were then aimed at optimising the catalyst layer to enhance the multi-component transport properties of the catalyst layer, i.e. air (O_2) into the catalyst layer and product water out of the layer.

4.3.2 Reformate Operation

The major MEA components of membrane, substrate and cathode catalyst types employed in this task were based on those developed for the parallel studies on hydrogen operation, as reported above. The CCM MEA construction route was also used throughout, to ensure consistency with the work performed in earlier milestones.

The focus of the MEA design and development work for the reformate milestones was on the development of a suitable reformate-tolerant anode catalyst layer. A recently developed high-performance anode catalyst was employed, as it had shown excellent CO tolerance and performance stability in other hardware types. With the introduction of the new single-cell design and optimisation of the anode catalyst layer, it was anticipated that the water management issues would also be improved.

The initial development activity was to assess the performance of the new anode catalyst layer, followed by modifications to this anode catalyst layer structure to increase performance stability and to maximise air bleed response. The aim was to minimise water build up in the GDL and catalyst layer and prevent the occlusion of Pt catalyst sites, which was believed to have caused stability problems in the earlier design version of the IE hardware.

4.4 Operating Conditions

For both hydrogen and reformate operation the cell temperature was controlled at 75°C. In both cases the cathode pressure (outlet) was close to ambient, and the anode pressure (outlet) was 500mb for hydrogen operation (dead-ended, with intermittent purge) and close to ambient for reformate operation. The oxidant outlet humidification was quoted by IE as 100% RH. The fuel humidification level (inlet) was 0% RH for pure hydrogen feed, and 50% RH for reformate feed. For reformate operation, a simulated methanol reformate was used, containing 50ppm CO, and the air bleed level for the conditioning, diagnostics and durability testing was fixed at the target 2% level.

More detailed operating conditions and test and diagnostic protocols for hydrogen and reformate operation are not reported, as these are commercially proprietary to JMFC and IE.

4.5 Results And Discussion

4.5.1 Phase 1

Hydrogen BoL (Beginning of Life) Performance Objectives (Milestone B)

The objective of this work was to design an MEA that met the performance targets for pure hydrogen in the IE single cell, using the IE etched plates, using JM LCS GDL material developed with Technical Fibre Products:

- 610 mV @ 400mA cm^{-2} measured off gold tabs (conservative target)
- 650 mV @ 400mA cm^{-2} measured off gold tabs (aggressive target)

Hydrogen BoL Performance Results (Milestone B)

MEAs using four variants of LCS with different levels of hydrophobic agent were evaluated. In all cases, the MEAs reached their operating voltage within approximately four hours, Figure 56. Two of the MEA variants (04-1699-12, 04-1699-13) were clearly superior and exceeded the aggressive target of 650mV at 400mA cm^{-2} when the voltage is measured from gold tabs between the GDL and the etched bipolar flow field plates. The two best MEAs also exceeded the conservative target when the voltage was measured directly from the metal flow field plates (FFPs), figure 57.

The reasons for the differences in the MEAs were deduced from 3-way oxidant polarisation curves and current interrupt (CI) resistance measurements. The worst performing MEA was poorer due to a high CI resistance, which accounted for most of the voltage difference, but also had higher mass transport losses at high current density compared to the other MEAs. The GDL for this MEA was probably too hydrophilic: liquid water being held within the GDL, impeding mass transport of the oxidants and preventing water from reaching the membrane to hydrate it. The differences between the other MEAs were less significant, but the MEA performing best at high current density had more hydrophobic agent.

Thus, the main determinant of performance for these LCS materials was the level of hydrophobic agent. Other differences between the GDLs do exist in the way they were prepared, but did not appear to be the dominant factors and are beyond the scope of this report.

Hydrogen Durability Objectives (Milestone D)

The objective was to show that the MEAs developed above were capable of stable operation without failure for over 500 hours under constant current conditions.

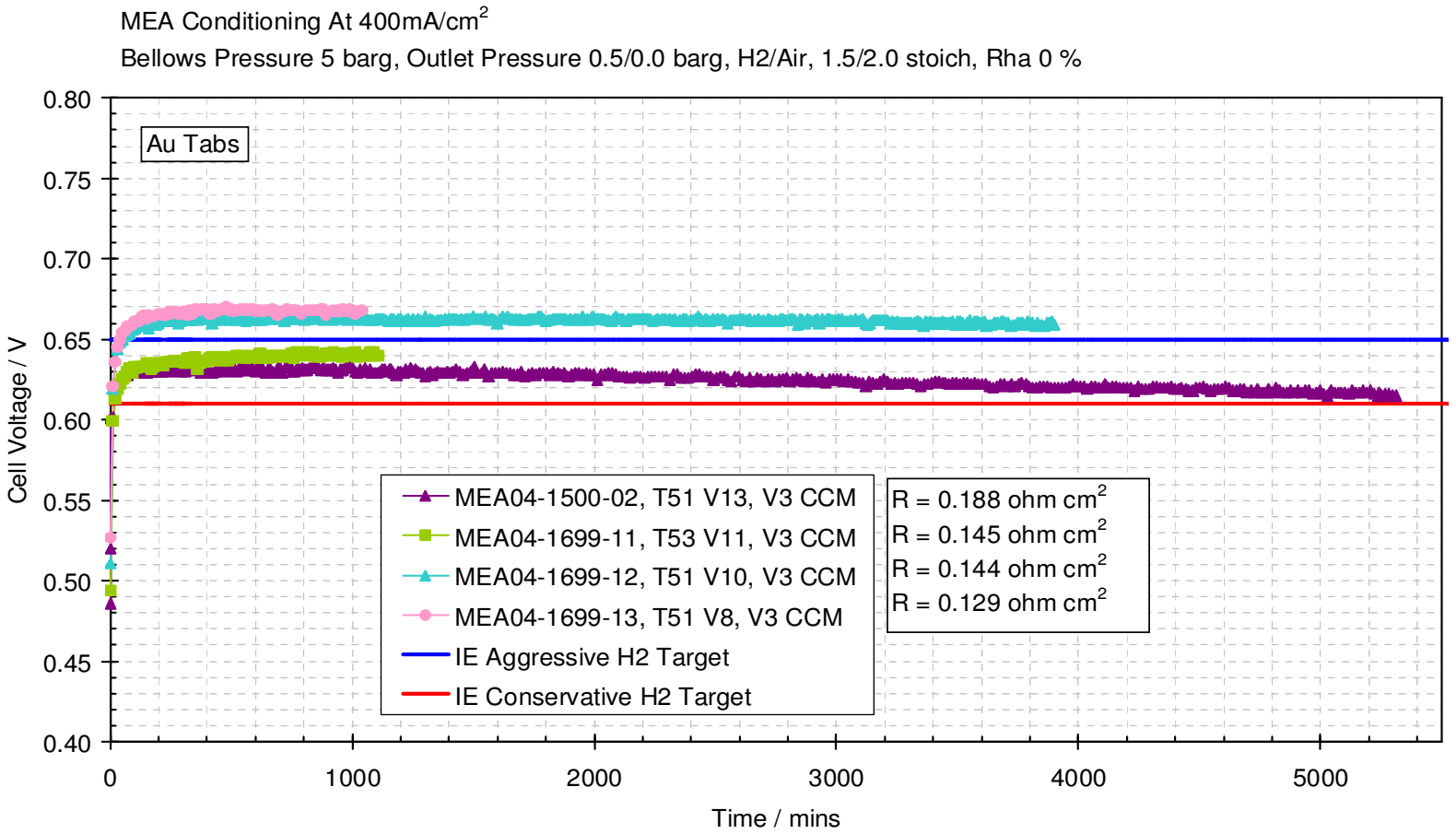

Figure 56: Voltages recorded in the V4 (Phase 1) IE cell from the gold tabs during conditioning of MEAs made with different LCS types

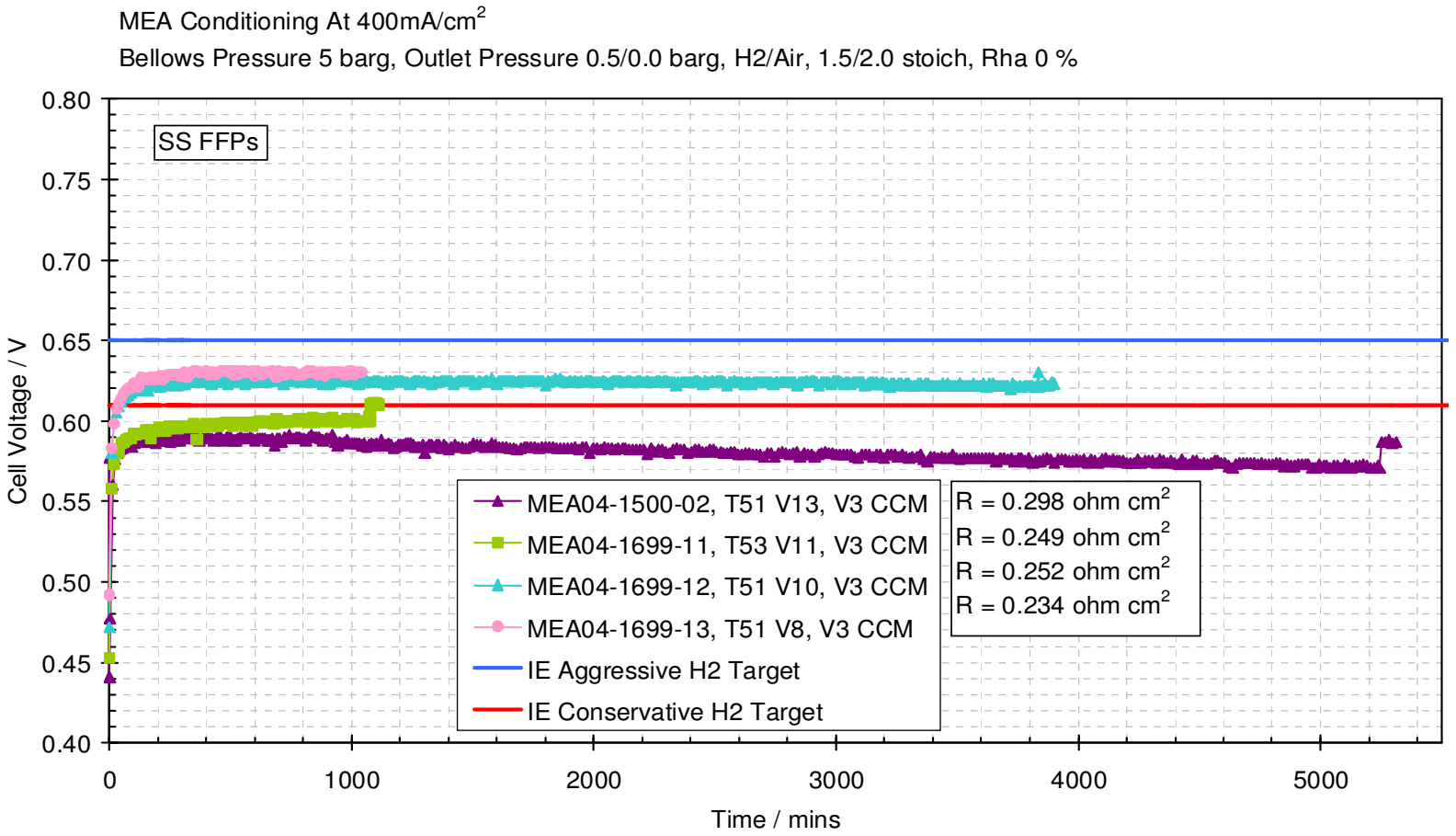

Figure 57: Voltages recorded in the V4 (Phase 1) IE cell from the stainless steel FFPs during conditioning of MEAs made with different LCS types.

Hydrogen Durability Results (Milestone D)

First Durability Test:

The first durability test showed that after a small initial decline in voltage over the first 100 hours, performance was very stable showing no further decline, figure 58. At about 370hours the test stand tripped and on re-starting the performance initially increased by about 50mV. This feature has been seen quite often in the IE cell and is thought to be caused by clearing of water from the cathode electrode. Support for this theory is given following the 3-way oxidant diagnostics: a similar increase in performance is observed following these high flow rate conditions. In other words, it appears that water is more effectively cleared from the cathode side of the cell by running at higher current densities than the standard 400mA cm^{-2}, which happens during the 3-way oxidant tests. This points to water removal by entrainment being important at the higher gas flow rates, as is commonly seen in other hardware types. The test was stopped after 540hours (clearly meeting the 500hour durability target) to allow the next sample to be tested.

Another possible explanation for the increase in performance after the trip is the reduction in current interrupt (CI) resistance. This drops from about 0.12 cm^2 to about 0.1 cm^2. At 400mA cm^{-2} this would only account for a voltage increase of 8mV however. It is not clear whether the trip caused the reduction in CI, or whether this reduction was already in progress.

After running for 540 hours on the durability test, the MEA was characterised with a 3-way oxidant set of polarisation curves. Performance increased substantially (60mV at 400mA cm^{-2}) upon switching to helox, suggesting that there was significant gas-phase mass transport restriction within the cathode, probably within the GDL. Further significant gains were also seen with pure oxygen indicating that the cathode catalyst layer had also been occluded by liquid water. This data supports the theory that water clearing is responsible for the increase in performance discussed above and that performance in this hardware is limited by the water management system. There is more liquid water present than in more conventional fuel cell hardware and this liquid water restricts the access of oxidant to the cathode catalyst. Another consideration in this respect is the difference between single cell and stack operation. Within the stack a more uniform temperature gradient is expected and higher average temperatures due to the insulating effects of adjacent cells. This probably accounts for the better performance in the stack due to less liquid water being present.

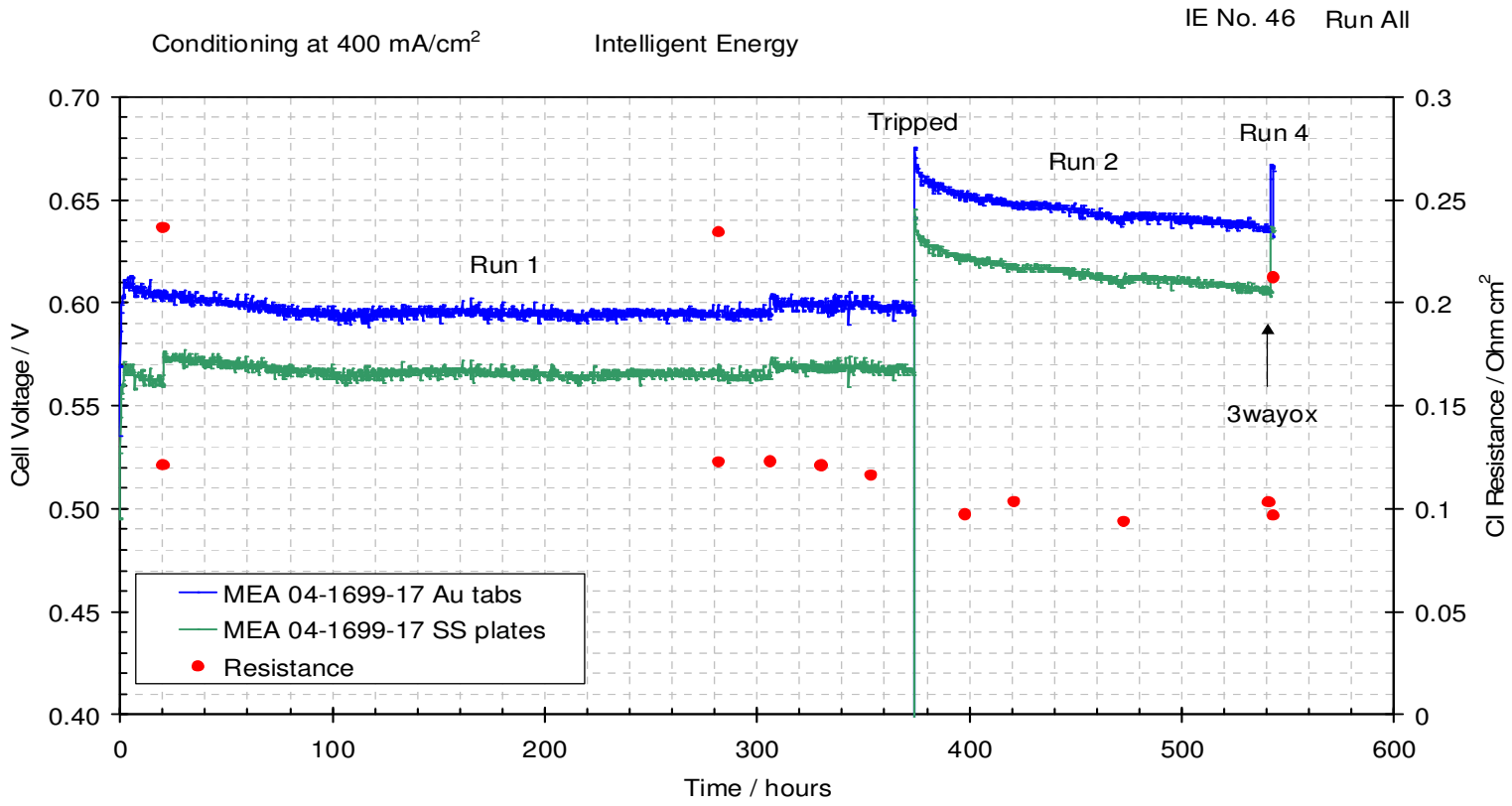

Figure 58: Constant current hold for MEA 04-1699-17 at 400mA cm^{-2} on H_2/air showing stable performance until about 370 hours when the stand tripped and performance increased. Cl resistance values at about 0.2–0.25 cm^2 are measured from the stainless steel plates.

Second Durability Test:

Similar behaviour to that described above was seen for another sample run on the durability test. This sample used a developmental GDL that gave slightly lower performance than GDL used in the hydrogen BoL performance testing described above, but had a higher level of hydrophobic agent and the effect of this on stability was of interest. Again no difficulty was seen in the MEA exceeding the durability target of 500hours. The initial performance of this sample was ~ 50mV higher, but with a slightly higher decay rate. The MEA was initially run at 800mA cm^{-2} for 20hours, as this had been found to increase subsequent performance at 400mA cm^{-2}, in some cases. After 480hours the air supply in the laboratory had to be turned off for maintenance for 2.5hours. Upon restarting the cell the performance had dropped significantly, presumably due to water condensing in the GDL, but this was recovered following a 3-way oxidant test. The voltage rose further after the stand tripped a few minutes later. Following these events, the voltage stability was poorer, both in terms of short-term fluctuations (noise) and in terms of progressive decay.

It was not apparent why this change in behaviour should have occurred after the starting and stopping of the cell. Comparison of the 3-way oxidant tests at 20 and 490hours shows some changes in the water handling of the system. This was most probably caused by gradual build up of excess water in the GDL, despite the higher level of hydrophobic agent. The data indicated that losses due to flooding of the GDL/baselayer had increased over the 500hours, whilst very little change in the catalyst layer losses has occurred. Pressures of the water and gas inlets were all monitored during testing and again no significant changes were detected. The higher CI resistance for this MEA (0.1 versus 0.13 cm^2) probably reflects the higher level of hydrophobic agent, which is known to reduce GDL conductivity slightly and which may also prevent water from reaching the membrane, however this would not fully account for the instability observed.

Reformate BoL Performance Objective (Milestone E)

The objective of the reformate performance work was to meet the target of 95% of the pure H_2 voltage under simulated steam-reformate conditions (measured off gold tabs). A conservative target of 610mV and an aggressive target of 650mV had been set for hydrogen operation, so the target for the reformate performance was a voltage in the range 580 to 618mV with 50ppm CO and an appropriate level of air bleed.

Reformate BoL Performance Results (Milestone E)

Initial testing at constant current (400mA cm^{-2}) showed a steady voltage level was achieved within 5hours, much of this period being used to adjust cell operation conditions and set points, figure 59. The performance was good at about 630mV on dry hydrogen and improved

to about 660 to 670mV on wet hydrogen (100% RH). This improvement was often seen when switching to humidified anode gas and is attributable in part (typically 10 to 20mV) to a drop in CI resistance because of better humidification in the membrane. The rest of the benefit may have been due to better utilisation in the anode when it is more fully hydrated.

The 3-way oxidant test at about 18hours gave a helox gain of 54mV, indicative of slightly more water holding within the cathode GDL than seen on dry hydrogen operation (30 to 40mV). This helox gain had not changed after 180hours of operation however, despite the use of humidified anode gases, indicating that the cathode design was giving stable water management, presumably helped by the lower water uptake of the developmental GDL variant.

Having established that the cathode was operating effectively on both dry and wet hydrogen, reformate testing was started. The sample had been run with wet hydrogen and had reached a voltage of 670mV as the CI resistance fell. Introduction of 25% CO_2 lowered the performance to about 650mV, due to dilution and introduction of 10ppm CO reduced the cell voltage further, as expected, to around 600mV but also introduced very large voltage fluctuations up to 90mV in amplitude, figure 60. The period of these fluctuations appears to be 50 to 60minutes. Such fluctuations can be caused by the fact that oxidation of CO to CO_2 on Pt is affected by the potential of the Pt, since oxidation can occur via an electrochemical reaction ($CO + H_2O = CO_2 + 2H^+ + 2e^-$) as well as a chemical one ($Pt\text{-}CO + Pt\text{-}O = 2Pt + CO_2$). Thus the anode over-potential can rise on poisoning with CO to such a point that the CO is then electrochemically oxidised, with a resultant decrease in over-potential for hydrogen oxidation and a cell performance gain. Such large fluctuations are not often seen in other types of hardware, but further discussion is beyond the scope of this report.

On switching to the simulated steam-reformate (50ppm CO, 25% CO_2, 75% H_2), the performance fell to about 480mV. An air bleed sensitivity test was then carried out with successive increases in the amount of air introduced into the anode gas stream, figure 60. The voltage fluctuations obscured some detail of the test, but the clear trend of increasing voltage with increasing air bleed is seen, with a level of 7.5% being required to bring the performance back up to 650mV. To check that this was the level at which the MEA would operate without any CO poisoning, the CO and air bleed were removed from the anode gas mix leaving wet H_2 and CO_2. The voltage was level at 650mV indicating that 7.5% air bleed had completely recovered the diluted hydrogen MEA performance level. This MEA had successively met the aggressive performance target of 618mV at an air bleed of 5% and exceeded the target with an air bleed of 7.5%.

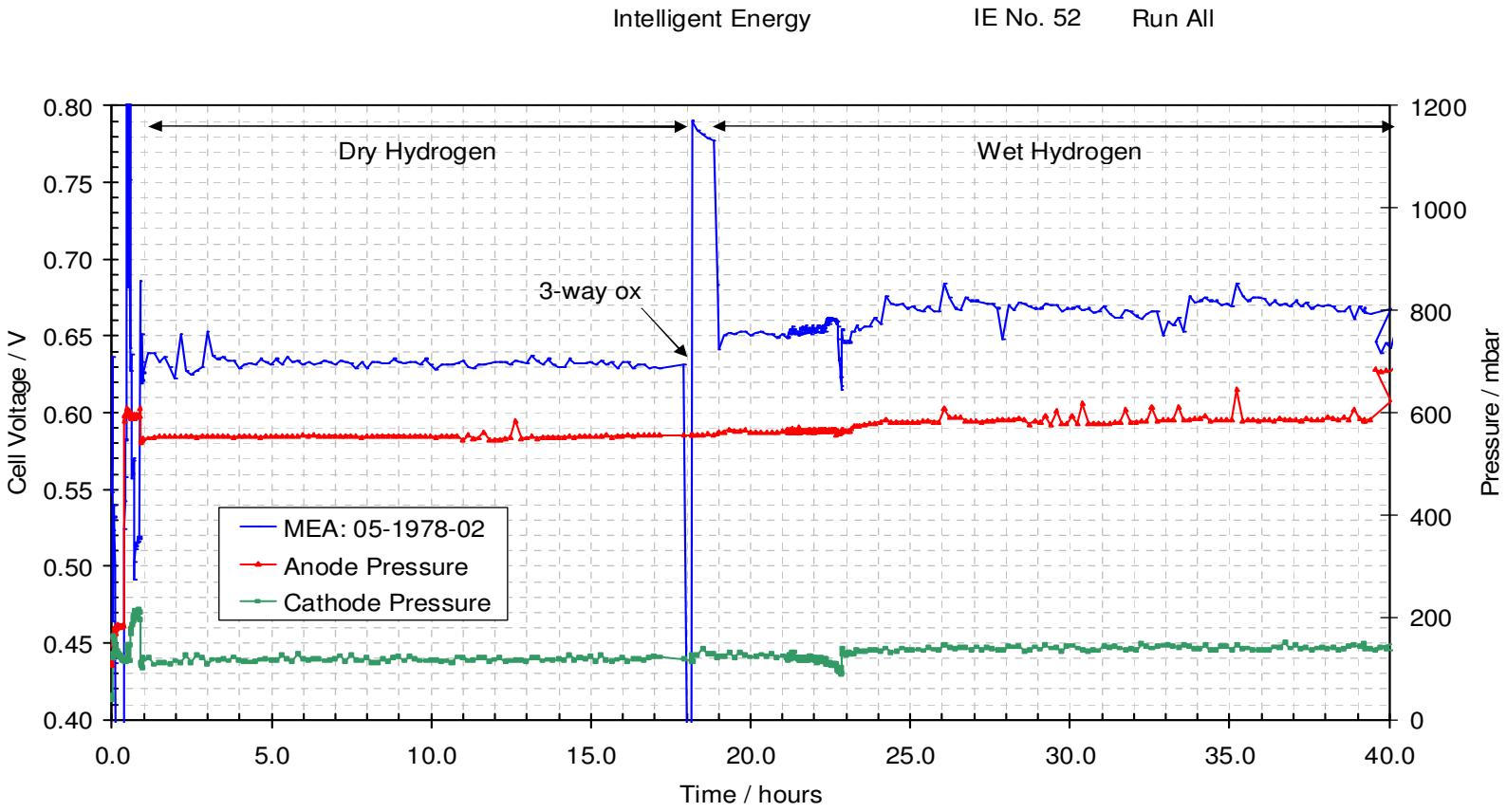

Figure 59: Constant current hold for MEA 05-1978-02 at 400mA cm^{-2} on H_2/air showing an increase in performance when the hydrogen was humidified.

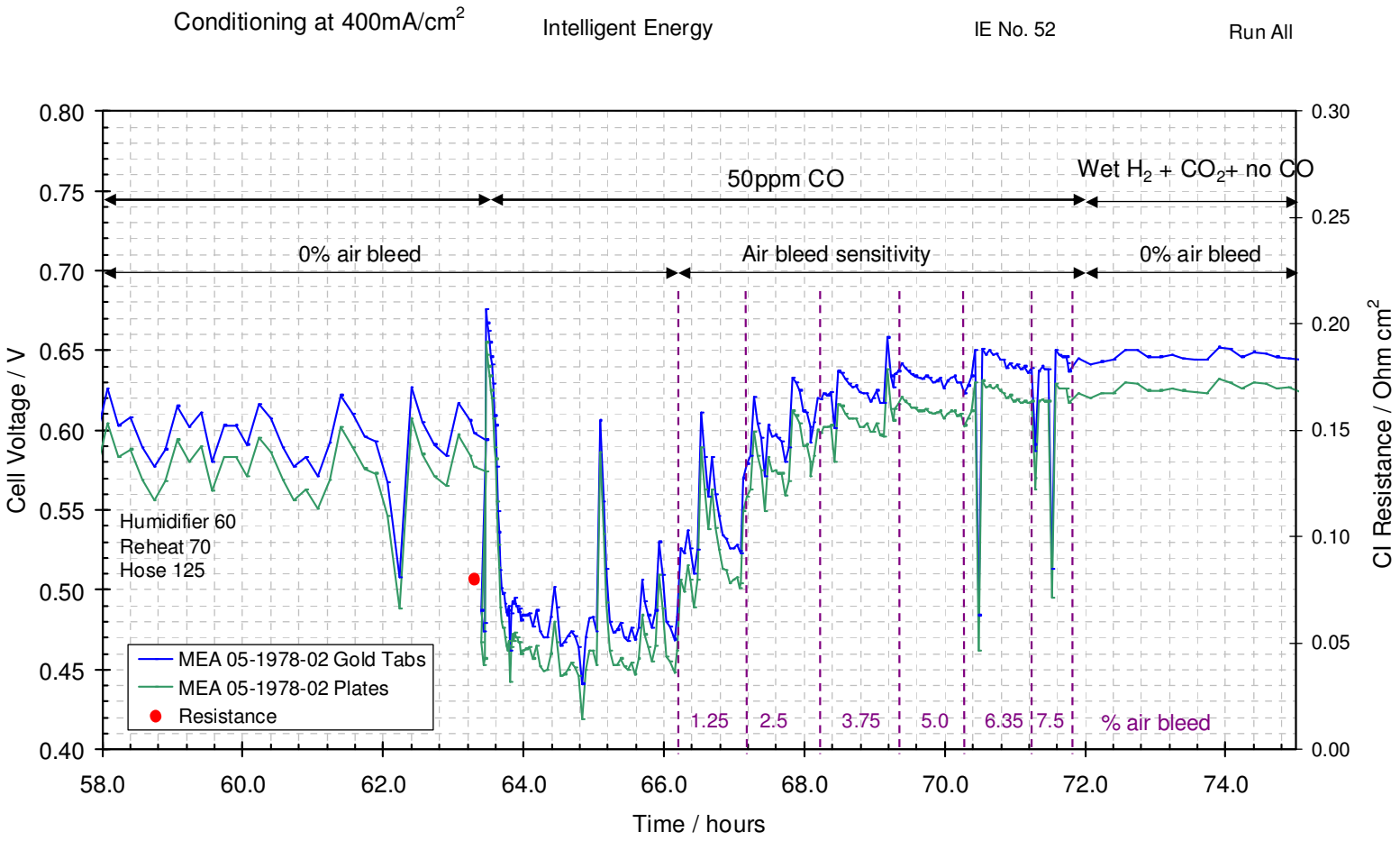

Figure 60: Effect of different CO and air bleed levels on the voltage of MEA 05-1978-02 showing good performance on simulated steam-reformate.

In summary, the MEA design implemented was clearly capable of meeting the reformate performance target, albeit with a higher than usual air bleed. It would normally be expected that a reasonable performance can be recovered, with 50ppm CO containing reformate, with a 2-3% air bleed level. We believe that this requirement for high air bleed is connected with the water management in the Phase 1 cell design used for testing. The most likely explanation comes back to the different behaviour of the single cell hardware compared to the stack, particularly with regard to its different temperature distribution from the stack. Typical inlet and outlet temperatures for the stack and single cell were measured, showing that the single cell runs about 15 to 20°C cooler on the anode side than the stack. It is known that reformate tolerance is highly dependent on anode operating temperature, for example Tada shows that a rise in temperature from 70 to 80°C gives a performance improvement of 20mV using 100ppm CO reformate with 25% CO_2, 75% H_2 (T. Tada, p.481, Handbook of Fuel Cells, Volume 3, Eds Vielstich, Lamm and Gasteiger, John Wiley & Sons, 2003).

It is not just the air bleed required to achieve desired performance that was of concern here however, the instability remains the most unusual aspect of the anode behaviour on reformate. Temperature may also explain this stability difference between single cell and stack. A change in behaviour when switching from dry to wet hydrogen was observed; the stability is much worse on wet hydrogen, which may be attributed to water accumulation in the anode flow-field plate.

If this instability happens on pure hydrogen, it will be far worse on reformate where there is a dilution effect and a poisoning effect, such that only a small percentage of the Pt sites are active at any moment (usually estimated to be about 1%). Raising the temperature would be expected to have a significant effect on the water removal by evaporation from the anode electrode, increasing stability and performance. However, with the Phase 1 single-cell design, it was difficult to raise the cell temperature, especially on the fuel side. An attempt was made to do this, by raising the gas preheat temperature above the humidifier and raising the temperature of the heated-hose that carries the gas to the anode inlet.

Reformate Durability Objective (Milestone F)

Here the objective was to show 500 hours durability on the type of MEA that had met the performance target of Milestone E, under the steam-reformate and air bleed conditions used.

Reformate Durability Results (Milestone F)

Several different MEAs with different GDL types, but the same anode and cathode design, were run on reformate durability testing. All showed a similar pattern of good initial performance followed by steady decay. This is in marked contrast to the hydrogen-only performance reported above, where good long-term stability was observed. Typically,

diagnostics such as air bleed sensitivity and 2- or 3-way oxidant tests were run on the MEAs to assess BoL performance and then the MEA was run under the target reformate conditions with intermittent diagnostics.

In a typical MEA run the first 80hours of testing can be ignored for the purposes of durability, as this period was used to establish BoL performance as described above, figure 61. From 80 to 160hours the MEA was run on simulated reformate with no CO and showed relatively stable performance in comparison to the subsequent behaviour with CO present. Reformate durability testing started after 160hours with 50ppm CO, 25% CO_2, 75% H_2 and a 7.5% air bleed. A 2-way oxidant test at 180hours showed modest helox gains (53mV) suggesting that the subsequent decay was not due to cathode flooding. This was confirmed after about 230hours when a cathode purge was performed, resulting in no significant improvement in performance. It was concluded that the decay was being caused by loss of anode performance, either by progressive CO poisoning or by water accumulation causing anode flooding.

At 290hours the anode humidifier dew point was reduced from 60 to 55°C (100% to 79% RH) and further reduced to 50°C (62% RH) at 320hours. No significant effect on performance was noticed. After 370hours the stand tripped and upon re-starting a large improvement in voltage was seen bringing the performance back above the aggressive target of 618mV. When the stand trips the gas flows are stopped, but the anode outlet valve that regulates the back-pressure opens to vent the gases. This will effectively purge the anode and remove water by the short period of high gas flow and by evaporation as the pressure falls. This observation appears to confirm that anode flooding was responsible for the performance decay in this experiment.

A similar improvement followed another stand trip at about 460hours. Following this trip the anode pressure was briefly set to ambient and performance improved further, indicating that a cross-over leak had developed. This leak grew and the test was stopped after 540hours due to a very large cross over measurement (120 ml/minute). Such large cross-over is indicative of membrane failure and it may be that the defect was initiated during the first trip (370hours) as the CI dropped at this point to an uncharacteristically low value (0.06 cm^2) indicating a short in the MEA.

Post-mortem inspection of the MEA showed that the membrane had holes in it that aligned exactly with the anode inlet channels. This is where the membrane would experience most heat due to CO oxidation by the air bleed. Clearly the highest concentration of CO and oxygen occurs at the anode inlet and SEM examination showed evidence of membrane softening due to high temperatures. A second, similar MEA, which ran for about 400 hours under the same conditions, also failed in the same way.

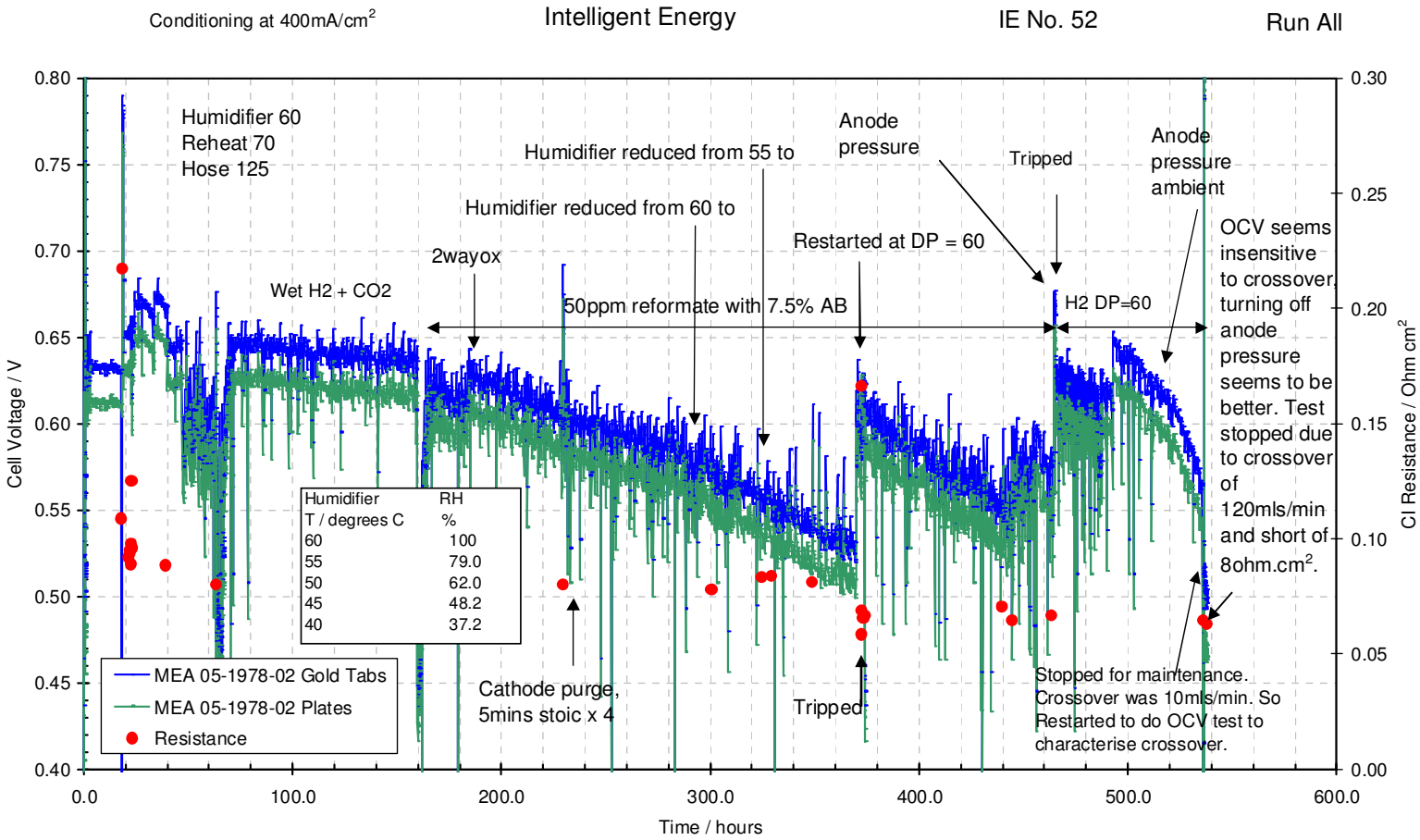

Figure 61: Durability run for MEA 05-1978-02 showing significant events during testing. 50ppm reformate testing started after about 160hours.

In an attempt to alter the water handling of the anode electrode, an MEA was run with a commercial GDL that IE had found to work very well in their stacks, figure 62. The BoL diagnostic tests showed that this MEA had good performance on dry hydrogen (up to 685mV) and achieved over 650mV with a 5% air bleed. Even though better performance was achieved with higher air bleeds (670mV with 7.5%), it was decided to run this MEA with a 5% air bleed in an attempt to prolong the durability. This was in part successful: the 50ppm reformate operation was started at 65hours and the sample ran for just over 500 hours, before being stopped at 570hours, again due to a high cross-over leak. The performance was not sustained however, and progressive voltage decay occurred.

At 260hours, routine inspection revealed that the air bleed had changed from 5% to 1.7%. This was rectified and the performance recovered by about 50 mV. From the shape of the curve it appears that the air bleed had fallen off after about 215hours, but re-setting the correct air bleed did not stop the voltage decay. Further increases in air bleed may have recovered more performance but would have compromised durability. Despite the use of a GDL known to work in the stack, the anode performance in the single cell could not be improved.

In summary, it can be concluded that the combination of low single cell temperature and unsuitable Phase 1 anode flow field design, which cause CO poisoning and flooding respectively, prevented effective long term anode operation in the single cell even at high air bleeds, and that the high air bleed leads to premature failure of MEAs by over-heating of the membrane at the anode gas inlets.

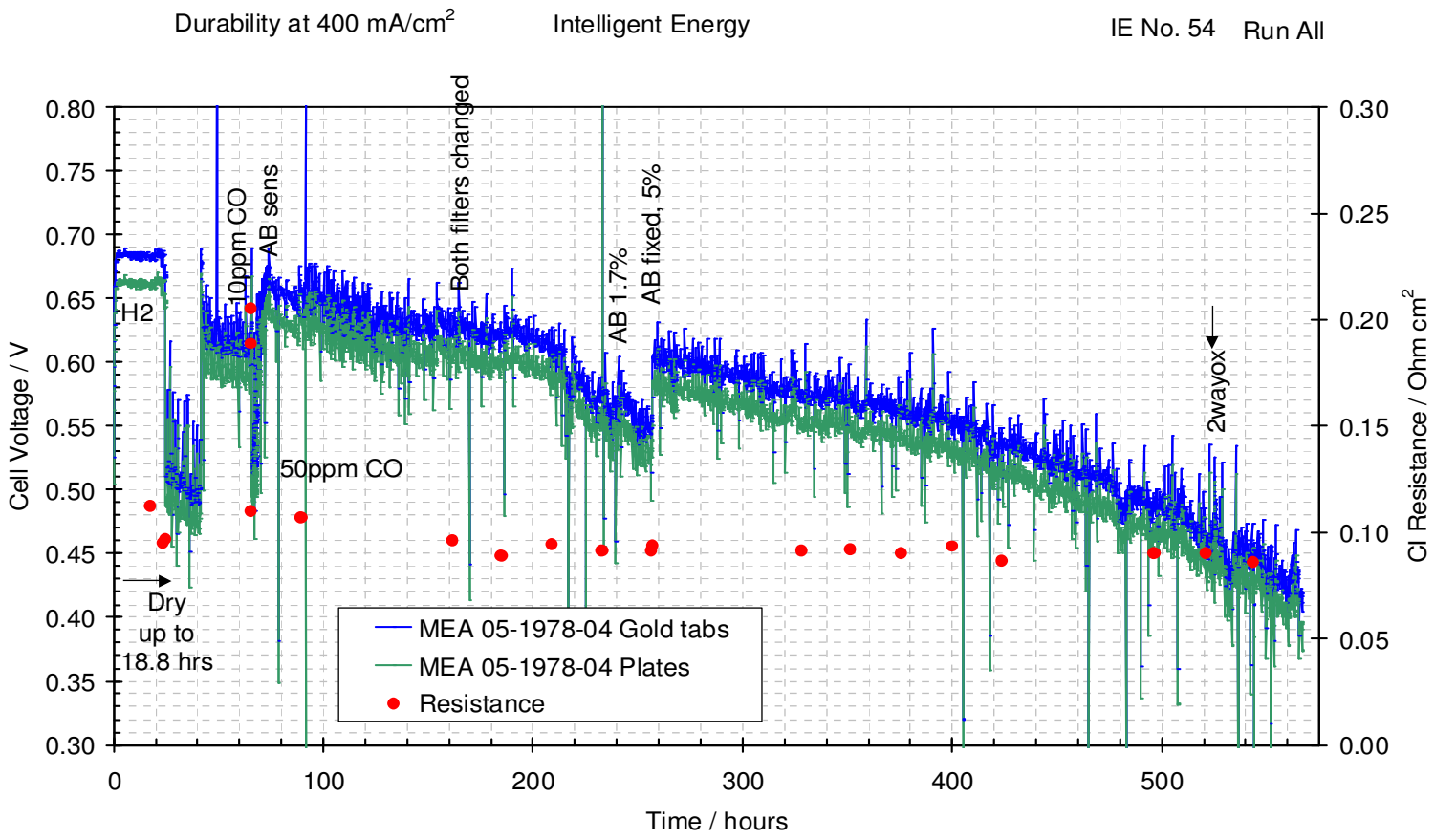

Figure 62. Durability run for MEA 05-1978-04 showing significant events during testing. 50ppm reformate testing started after 65 hours.

4.5.2 Phase 2

Hydrogen Operation (Milestone G)

A series of MEAs were tested in this work in the new Phase 2 single-cell hardware using detailed protocols and diagnostics, and a more detailed discussion is summarised below for the better performing MEA variants (V3, V14 and V12), which were designed, fabricated and tested in line with the design intent described in section 4.1. These results are summarised below and in figure 63 and figure 64.

V3 CCM, commercial membrane, commercial GDL on anode and cathode:

- 0.5A/cm^2, H_2/Air, 1.43/2.0 stoich, 50kPa/ambient, 75°C, dead-end
- 661mV performance at 200hrs, measured at plates.
- 50 V/hr degradation rate at 200hrs, 100 V/hr degradation rate average.

V14 CCM, commercial membrane, commercial GDL on anode and cathode:

- 0.5A/cm^2, H_2/Air, 1.18/2.0 stoich, 50kPa/ambient, 75°C, dead-end
- 653mV performance at 150hrs, measured at plates.
- 80 V/hr degradation rate at 150hrs.

V12 CCM, commercial membrane, commercial GDL on anode and cathode:

- 0.5A/cm^2, H_2/Air, 1.18/2.0 stoich, 50kPa/ambient, 75°C, dead-end
- 668mV performance at 110hrs, measured at plates.
- 33 V/hr degradation rate at 110hrs.

V3 showed initial good performance, in excess of the 650mV target, but with a high initial degradation rate due to build up of water in the cathode catalyst layer, as shown in figure 63. To further boost the voltage performance, changes were made to the proton conducting material in the catalyst layer, and in addition a different catalyst was used, to give the V14 CCM design. As shown in figure 63, this gave even better initial performance, but with no improvement in the stability/degradation rate.

The V12 design was based on further optimising the proton conducting network, and using a different cathode catalyst that influenced the cathode catalyst layer pore structure. This resulted in a catalyst layer with a more appropriate structure, to enhance the multi-component transport properties of the catalyst layer (giving good stability, as shown in figure 56), while at the same time maintaining good voltage performance, figure 64. The net result being a CCM cathode catalyst layer structure with an excellent combination of performance and stability, well in excess of the target, thus meeting the design intent outlined in section 4.1.

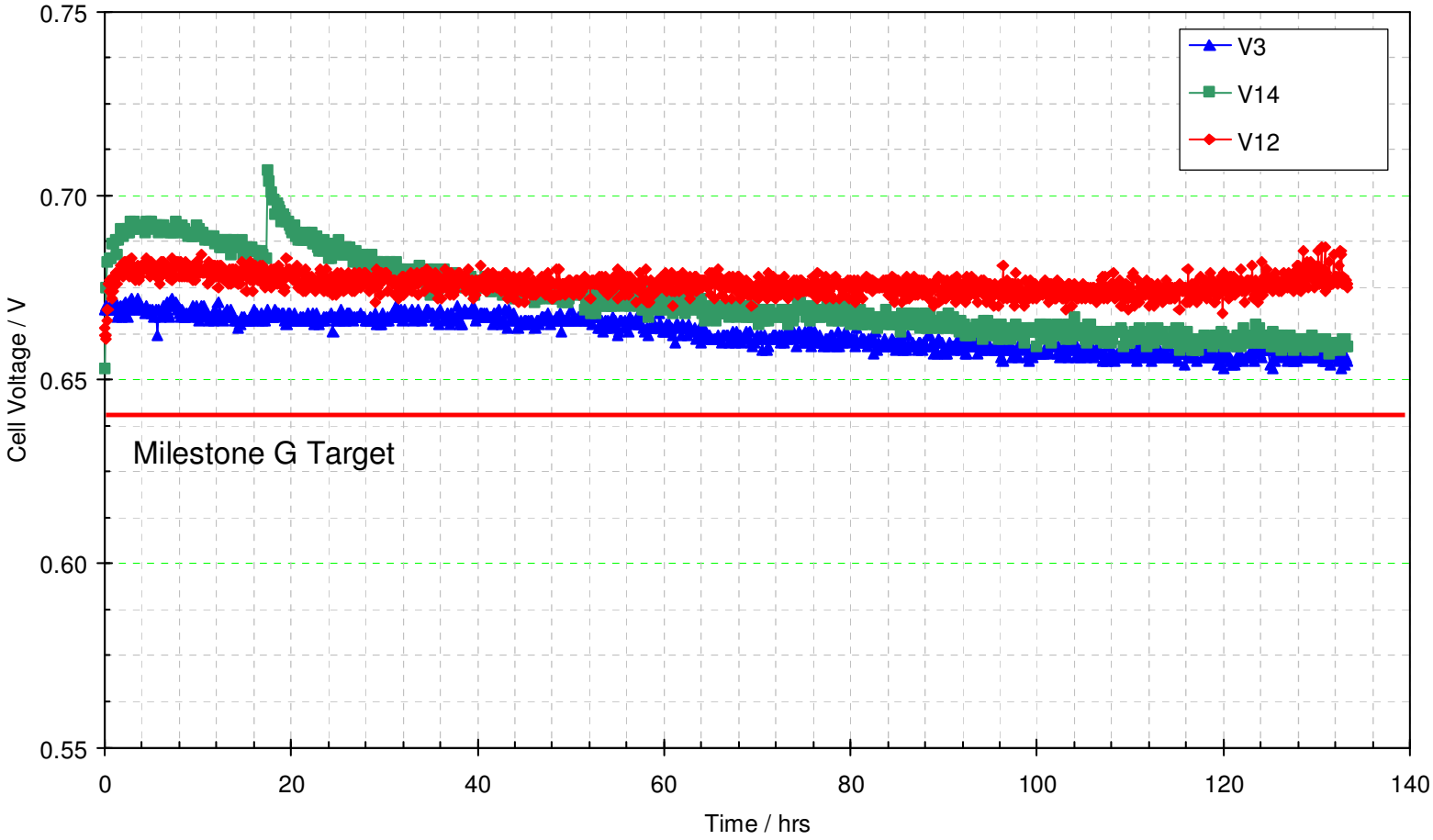

Figure 63. MEA stability at 500mA/cm^2. Cell at 75°C, Pressure: Deadend H2/Air.

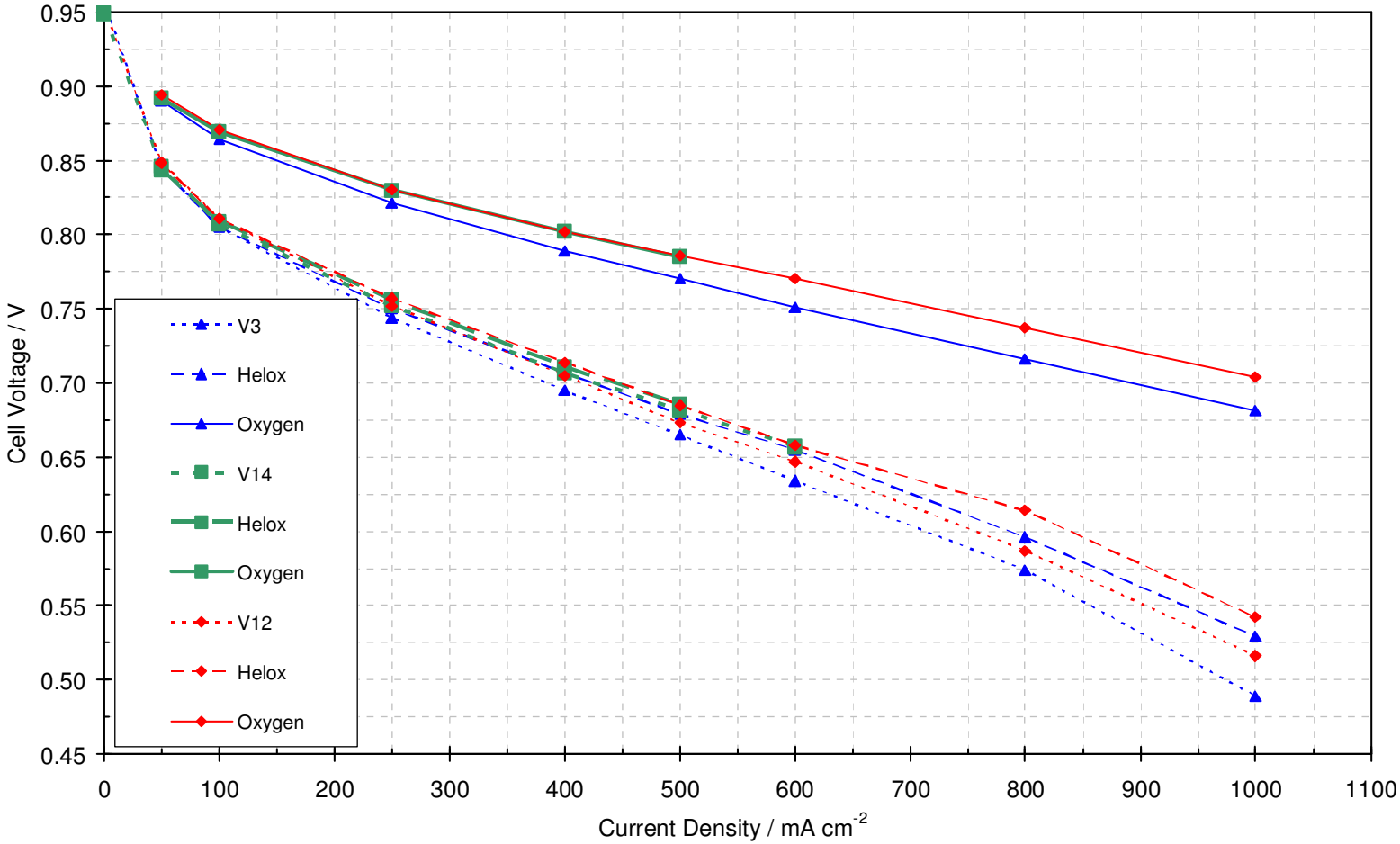

Figure 64. 3-Way-ox polarisation plots. Cell at 75°C, Pressure: Deadend H_2/Air.

Reformate Operation (Milestone H)

A series of MEAs were tested in this work using detailed protocols and diagnostics, and a more detailed discussion is summarised below for the better performing MEA variants (V10 and V12), which were designed, fabricated and tested in line with the design intent described in section 4.1. These results are summarised below and in figure 65 and figure 66.

Testing consisted of the initial evaluation of the standard CO tolerant anode CCM (V10) and the subsequent evaluation of the optimised CO tolerant anode CCM (V12). Initial testing with hydrogen showed that the performance and stability were identical to that shown for the hydrogen milestone above, which was expected as both utilised the same cathode design and membrane.

On reformate, the best CCM types developed exceeded the performance target of 618mV @ 500mA cm^{-2} at BoL and consistently achieved ca. 650mV. This was a significant improvement on the initial Phase 1 work, as these latest results were achieved with a reduced air bleed of 2%. The MEAs were run for longer than 500 hours at the 2% air bleed level without any dramatic MEA performance failure due to significant reactant gas crossover arising from membrane weakening and pin holing. There was however, a decrease in performance over the 500 hours of testing, of ca.150mV, figure 65.

Air bleed sensitivity tests (0-3%) were performed at BoL and End of Life (EoL), figure 66. These showed a similar level of performance decline as seen with the 2% air bleed (approx. ~150mV @ EoL vs. BoL). The voltage fluctuations at EoL obscure the details of the test, and as such the change in response to successive increases in air bleed is more difficult to interpret, although there does appear to be a small performance gain on increasing the air bleed from 2% to 3%. This suggests that the 2% air bleed is probably not totally sufficient to remove all the impurities and return the performance to hydrogen dilution (H_2 + CO_2) levels. Thus the stability trend could be partly explained by slow CO-poisoning of the anode catalyst.

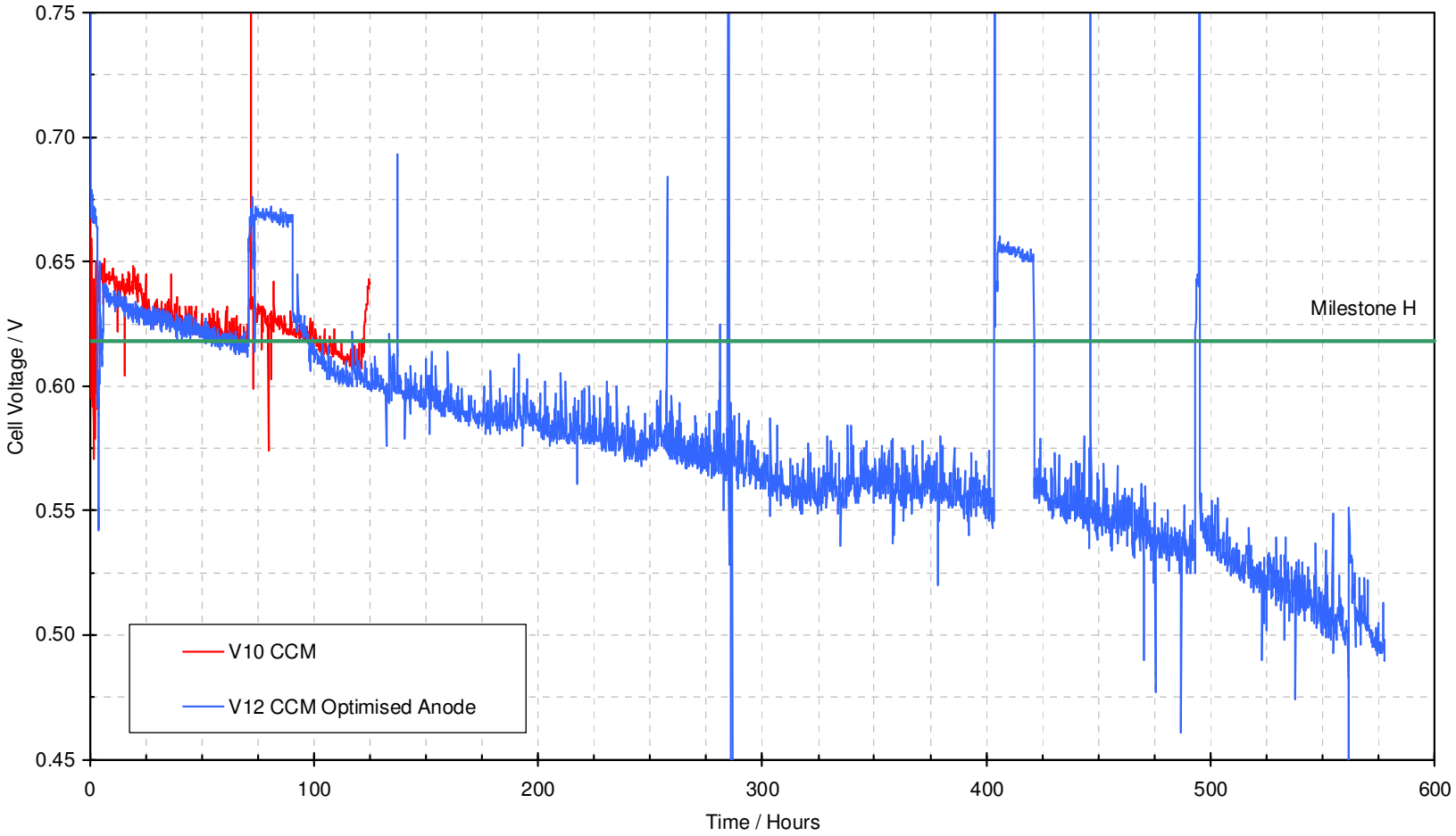

Figure 65. MEA reformate testing at 500mA/cm^2.

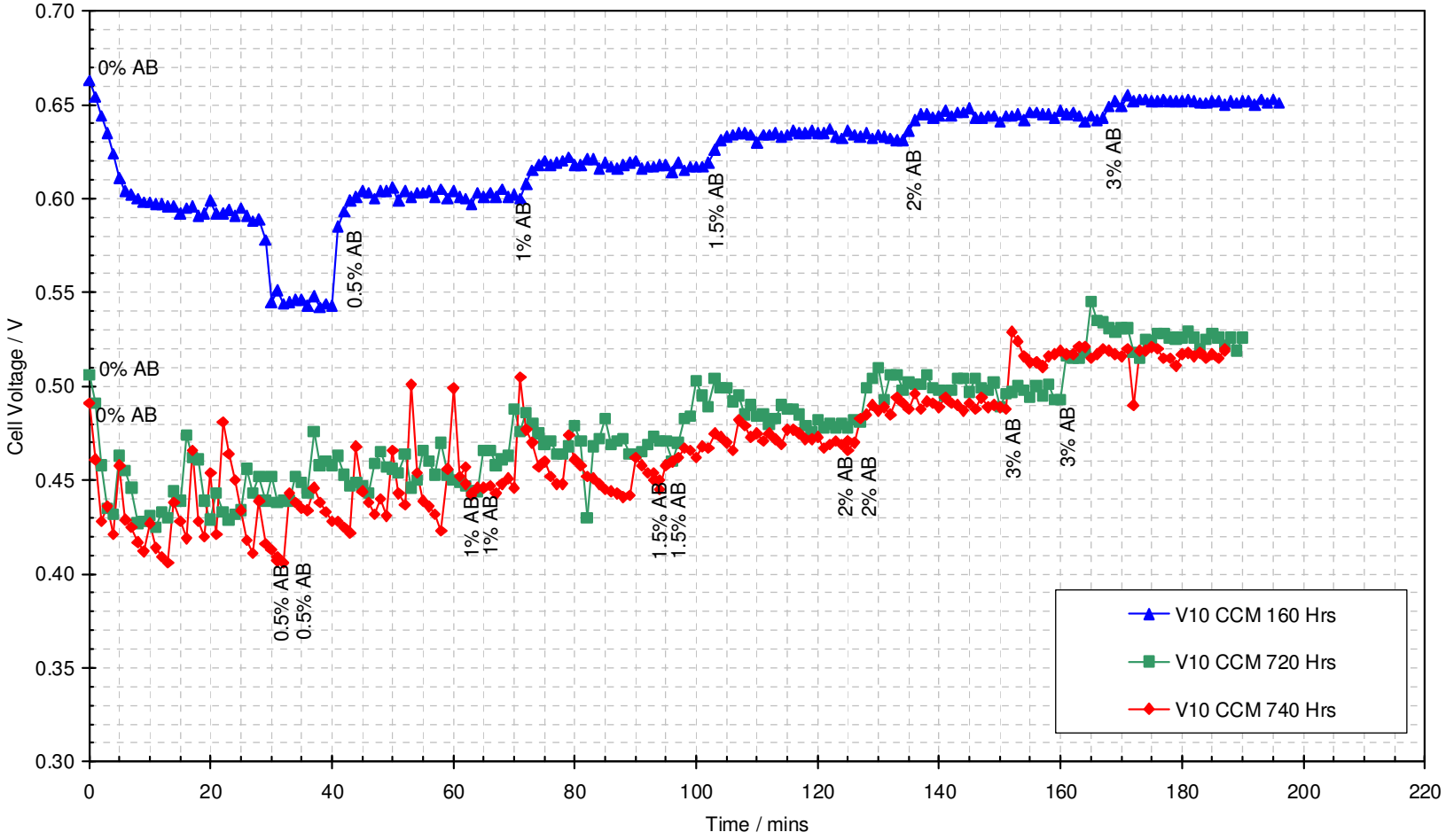

Figure 66. Air bleed sensitivity at 500mA/cm^2, 50ppm CO.

Further diagnostic evaluations were performed to determine the origin of the performance loss during durability testing:

- 3-wayox polarisation curves on both hydrogen and reformate were run to determine the proportion of this performance loss due to the cathode. Polarisation experiments (specifically oxygen) are not normally performed on reformate because even a small amount of crossover can act as an enhanced air-bleed, reduce anode CO poisoning and provide misleading results. In this case the tests on reformate were necessary to understand the water management under reformate conditions as the hydrogen mode of operation is significantly different from the reformate mode of operation.
- Reformate 3 way-ox data showed an increase in helox and oxygen gains with time and was consistent with a build up of water in the cathode GDL and catalyst layers. Because of the flow-through mode of operation and humidified reformate gas stream it was assumed that the anode was running much wetter than under hydrogen operation. The build up of excess water on the cathode was therefore probably due to the increased amount of water on the anode side of the MEA affecting the rate of back diffusion of water from the cathode to the anode.
- Hydrogen 3 way-ox data showed a surprisingly significant drop in cathode resistance-corrected oxygen performance over time. Superficially this would usually indicate a large loss in cathode kinetic catalyst activity. However, EoL cyclic voltammetry did not pick up any evidence of loss in cathode catalyst surface area or catalyst poisoning that was large enough to explain such a large loss of cathode activity.
- MEA resistances remained unchanged throughout testing and therefore did not contribute to the performance loss.

Considering these losses it would appear that the cathode accounts for close to 50% of the performance degradation over the MEA lifetime. This is surprising as it is normally the anode that is expected to be responsible for the majority of performance losses in reformate systems. The apparent observed loss in cathode catalyst activity is difficult to explain and requires further investigation, but may have been an artefact of the diagnostic testing on reformate.

Concerning the losses at the anode, EoL anode cyclic voltammetry did not show any loss in anode catalyst surface area due to catalyst sintering, and in fact an EoL utilisation of 84% was observed which demonstrated the stability of the anode catalyst over 580+ hours of reformate operation (740+hours total load time). Thus an intrinsic catalyst activity decrease from loss of metal surface area was not the cause of the anode performance degradation. It was seen in the earlier air bleed sensitivity that the 2% air bleed level was insufficient to fully

oxidise the CO in the reformate gas stream and this could have led to a slow poisoning of the anode catalyst layer during operation.

It is also possible that the increased amount of water in the system could have resulted in a steady accumulation of water, which could have occluded some Pt catalyst sites. This was observed previously with the earlier single cell design, and although the introduction of a new cell design and optimisation of the anode catalyst layer has had a significant positive impact in reducing the required air bleed level, it may well be that the issue with anode layer flooding might remain to some degree. It was also observed that the only way the voltage degradation could be arrested was by raising the cell temperature from about 75°C to 85°C (anode and cathode outlets). While this observation is not diagnostic (since higher temperatures can also partially mitigate CO poisoning and encourage water removal), it does suggest that performance stability in a stack should be better, as the temperature distribution is more uniform.

5 COST ANALYSIS AND DISCUSSION

5.1 Cost Analysis

Analysis of the potential cost of etched stack components when manufactured in a volume of 3 million per annum, shows that mid stack component costs could be reduced to around 50% of their current cost. The projected cost of pressed bipolar plates produced in the same high volumes is around 8% of the long term cost of etched bipolar plates; however, the cost of the other cell components of the pressed plate technology demonstrated here is such that cell cost could only be expected to fall to around 74% of the best etched cell cost (the slight performance penalty, -10%, of the pressed technology has been ignored on the basis that this minor loss could be won back through further development).

Table 4 shows a more detailed breakdown of the relative costs of the stack components; the first column shows the cost breakdown of high volume etched plate technology, and the second column shows the breakdown of the 74% mentioned above. Clearly, the pressed plate itself offers a dramatic cost benefit, it being more than an order of magnitude cheaper than the etched bipolar plate; the dominant cost is the MEA & diffuser combination, but a significant contribution is due to the fluid distribution and water delivery components developed under this programme. These items have not been optimised for volume manufacture; instead the focus has been on design and functionality, further development of these components is discussed in section 6.2.

	Etched plate High volume costs Percentage of cell cost	Pressed plate Percentage of etched technology cell cost
MEA & Diffusers	43%	43%
Bipolar Plate	26%	2%
Water delivery components	29%	12%
Gaskets	2%	2%
Fluid distribution component	n/a	15%
TOTAL	100%	74%

Table 4 Cost comparison for etched and pressed plate cell components.

5.2 Discussion

Under this programme IE has demonstrated significant developments of the etched plate technology and shown the capabilities and cost saving potential of a pressed plate version of its evaporatively-cooled technology; JMFC have successfully modified their MEA technology to address water management issues presented by the evaporative architecture, achieved the performance levels possible using IE's existing MEA supply and developed the technology such that greater efficiency levels are achieved.

Etched plate technology scale-up raised a number of issues which were successfully addressed; manifold and fluid distribution problems required the development of experimental hardware and procedures to enable the design process, whilst guaranteeing the enlarged technology was not hampered by poor cell balance required an in depth analysis of component quality and the design and proving of quality control equipment and procedures. These developments have all fed back into the whole stack manufacturing process ensuring that single width technology benefits from the improved quality control and design improvements. For these reasons, the 336-cell, 600cm^2 unit ultimately demonstrated better performance than the single width technology was capable of at the programme outset, and eventually delivered 70kW.

The pressed plate development programme demonstrated successful manufacture of pressed metal, moulded plastic and rubber over-moulded plastic components in single and triple width formats. The performance of stacks built approached that of the etched technology, but highlighted component inconsistencies where the high volume manufacturing routes had not been used because of unacceptably long lead times.

The pressed plate stack has evolved through two plate iterations and a number of cell component designs. Initial Mk1 pressed plate short stacks showed high levels of crossover and poor performance with little stability. Subsequent single cell testing allowed the development of the cell and components to the point where the cell exhibited 90% of the etched plate stack performance and this was stable at standard fluid flow rates.

The lessons learned from the Mk1 single cell development and seal testing were applied to a Mk2 pressed plate stack design, based around a second plate design iteration. Short stack testing of Mk2 stacks has shown similar performance to the best Mk1 single cell, and long stacks have been assembled and tested, with performance only slightly reduced.

Although the cell performance of pressed plate stacks is slightly below that of the etched technology, the reduced mass of the new stack gives double the gravimetric power density and comparable volumetric power density.

A series of new MEA structures and formulations, based on the catalyst coated membrane (CCM) construction route were developed by JMFC and were tested in a new Intelligent Energy etched plate single cell hardware with commercial GDL material under hydrogen and reformate operation. The design intent in developing these CCMs was to optimise the cathode catalyst layer structure for optimum water handling under the unique humidification method used in IE hardware. In addition, the focus of the MEA design and development work for the reformate milestone was on the development of a suitable reformate-tolerant anode catalyst layer.

The MEA design intent for hydrogen operation was achieved through several iterations of developmental variants, resulting in a final variant cathode catalyst layer with an improved structure, which enhanced the multi-component transport properties of the catalyst layer, whilst simultaneously maintaining high effective catalyst activity. This optimum variant provided an excellent combination of stability and performance characteristics (669mV @ 0.5A/cm^2, measured at the SS plates), well in excess of the hydrogen milestone target set for this project (650mV).

Under reformate operation, the use of an improved single cell design together with CCM designs with new anode catalyst layer structure and catalysts enabled the initial BOL performance target of 618mV at 500mA cm^{-2} (50ppm CO) to be readily achieved with 2% air bleed. The MEAs could be run for longer than 500 hours at the 2% air bleed level without any MEA failures due to significant reactant gas crossover arising from membrane weakening and pinholing.

There was still a marked decrease in performance over the 500 hours of testing, which would need to be resolved for practical long-term use in reformate applications. Diagnostics indicated that the loss was due equally to losses at the anode and the cathode. The anode losses could be due partly to anode flooding still not being fully resolved, but mainly due to the low level of air bleed being not quite sufficient to avoid a slow build up of CO, which poisons the anode during long term testing. Cathode losses were consistent with a build up of water in the cathode catalyst layers, but there was also evidence that a decrease in oxygen reduction activity could have contributed to the losses.

6 CONCLUSIONS AND FURTHER WORK

6.1 Conclusions

Development of the etched plate stack technology progressed well and according to plan. The technical challenges involving design and sizing of fluid flow manifolds and the production challenges of component manufacturing efficiency, component quality control and stack assembly were all successfully addressed, culminating in the assembly and demonstration of a 50kW unit which actually achieved 70kW. The demonstration stack also achieved its target performance at a greater efficiency than the incumbent single width technology demonstrated by Intelligent Energy prior to the inception of this programme.

A pressed plate manifestation of Intelligent Energy's evaporatively cooled architecture has been demonstrated in single width and triple width form. During the course of the development of this technology the suitability of the designs for manufacture by high volume techniques such as conventional metal pressing, plastic injection moulding and plastic-to-rubber over-moulding has also been demonstrated. This technology has shown the capability to achieve the high volumetric power density of the etched plate technology whilst also offering a gravimetric power density of over 1kW/kg and the potential for a dramatic cost reduction with further development of certain components.

The MEA design iterations focused on the cathode catalyst layer structure resulted in significant advances in performance and stability, in combination with improved single cell hardware. On the anode side, improved CO tolerance was achieved with a new catalyst and an improved catalyst layer structure.

A series of new MEA structures and formulations, based on the catalyst coated membrane (CCM) construction route were developed by JMFC and were tested in a new Intelligent Energy etched plate single cell hardware with commercial GDL material under hydrogen and reformate operation. The design intent in developing these CCMs was to optimise the cathode catalyst layer structure for optimum water handling under the unique humidification method used in IE hardware. In addition, the focus of the MEA design and development work for the reformate milestone was on the development of a suitable reformate-tolerant anode catalyst layer.

The MEA design intent for hydrogen operation was achieved through several iterations of developmental variants, resulting in a final variant cathode catalyst layer with an improved structure, which enhanced the multi-component transport properties of the catalyst layer, whilst simultaneously maintaining high effective catalyst activity. This optimum variant provided an excellent combination of stability and performance characteristics (669mV @ 0.5A/cm2, measured at the SS

plates), well in excess of the hydrogen milestone target set for this project (650mV).

Under reformate operation, the use of an improved single cell design together with CCM designs with new anode catalyst layer structure and catalysts enabled the initial BOL performance target of 618mV at 500mAcm^{-2} (50ppm CO) to be readily achieved with 2% air bleed. The MEAs could be run for longer than 500 hours at the 2% air bleed level without any MEA failures due to significant reactant gas crossover arising from membrane weakening and pin holing.

There was still a marked decrease in performance over the 500 hours of testing, which would need to be resolved for practical long-term use in reformate applications. Diagnostics indicated that the loss was due equally to losses at the anode and the cathode. The anode losses could be due partly to anode flooding still not being fully resolved, but mainly due to the low level of air bleed being not quite sufficient to avoid a slow build up of CO, which poisons the anode during long term testing. Cathode losses were consistent with a build up of water in the cathode catalyst layers, but there was also evidence that a decrease in oxygen reduction activity could have contributed to the losses.

In conclusion, the MEA design iterations focused on the cathode catalyst layer structure resulted in significant advances in performance and stability, in combination with improved single cell hardware. On the anode side, improved CO tolerance was achieved with a new catalyst and an improved catalyst layer structure.

6.2 Further Work

In this programme, pressed plate components have been produced using techniques suitable for mass production, and these have been assembled into stacks which have shown good cell performance. Future work must address three areas: performance improvement, further cost reduction, and design for assembly.

Although some cells have shown performance comparable with that of etched plate stacks, cell balance has been an issue throughout stack testing. It has not been possible within this program to investigate the causes of this and further work is needed to determine whether poor cell balance is due to component variation or assembly issues. A range of quality control tests would allow the effects of component variability to be determined, and attention to some design aspects would eliminate some potential component mismatch issues. The pressed plate stacks tested to date have used the same diffuser used in the current etched plate stacks. So far it has not been determined whether the best diffuser for the etched plate stacks is also best for the pressed plate technology. Further work is clearly needed in this area to optimise the diffuser configuration to give maximum performance in pressed plate stacks.

Reducing the cost of pressed plate stacks may be achieved in a number of ways. As shown in the cost analysis previously, although pressed

plates can be produced at very low cost, the water and fluid delivery components now form the bulk of the non-MEA cell cost. Further cost reduction may therefore be achieved if the cost of the fluid delivery components is reduced by using lower cost material or by rationalising the components altogether, combining their functionality into a single component. This would also remove the opportunity for misalignment of this component during assembly, improving stack reliability. Reducing the cost of the plastic component by 50% would bring the pressed plate cell cost down to 20% of the potential etched plate cell cost. In the long term all fluid delivery functions could be handled by the moulded gasket in addition to sealing and the cost of this component would be similar to the plate cost.

Development of stack components will also focus on assembly issues. Using moulded plastic components and pressed plates allows features which project from the plane of the component, unlike etched plates and cut gaskets. This would permit the use of alignment features in the plate and peripheral components which would ensure correct positioning during assembly and operation. Combining multiple components into fewer parts would also make assembly easier.

Future new work beyond the scope of this project on further MEA developments could continue to be performed in single cell hardware, but as the single cell (even in the newer improved form) cannot exactly simulate the conditions in a full stack, it is recommended that future MEA designs are evaluated in a stack configuration to rule out the effect of heat distribution and flow field effects on performance and stability.

APPENDIX 1 – PROGRAMME MILESTONES

Intelligent Energy Milestones

1 Review of end-plate finite element stress analysis: the stress analysis is a key factor in determining the most appropriate scale for larger stacks so the findings and recommendations will relate to the format for the scaled up stack.

2 Initial results from the design and test manufacture of the large format cell to be documented.

3 Pressing and frame design concepts to be documented.

4 Complete single cell design.

5 Install and commission single cell at Intelligent Energy.

6 Install and commission single cell at Johnson Matthey.

7 Preliminary results from diffuser materials testing, initial pressing tests and assessment of alternative manufacturing options associated with pressing of bipolar plates.

8 Component trials and tooling outcome to be documented. Preliminary results from plastic/metal bonding development work.

9 Test results from large format cells to be documented, inclusive of relative progress, successes and any specific 'failures' in the early development process.

10 Interim results on sealing and assembly processes to be documented - inclusive of evaluation of design refinement requirements needed to accommodate increased tolerances for the enlarged format.

11 Results from plate pressing and insertion moulding processes to be documented, inclusive of design drawings, photographic media, etc.

12 Design, develop and install 50kWe test stand.

13 Interim report on test cell results for the larger format plate.

14 Test results from large format short stacks to be documented, inclusive of relative progress, successes and any specific 'failures' at this stage of the development process.

15 Plate evaluation report inclusive of manufacturing process, quality, cost and other critical criteria for alternative suppliers.

16 Results and conclusions from short stack gasket trials.

17 Gasket design confirmation and results from standard format long stacks.

18 Test results from reformate short stacks to be documented.

19 Initial test results from 50kW etched plate stack, plus results from pressed plate short stacks to be documented.

20 Detailed report (in conjunction with JM activities re MS C) detailing the operation of single cells and short stacks on hydrogen with the developed MEAs. Final test results from the 50kW stack to be documented.

21 Interim results on large scale pressed plate cell development and performance.

22 Design issue report relating to the scale up process, inclusive of relative successes and any specific 'failures'.

23 Results from single width pressed plate short stacks.

24 Test results from reformate short stacks incorporating JM or/and alternative MEAs.

25 Build process report documenting build process experience and QA procedures and issues.

26 Pressed plate design variant analysis. Test results from single width long stacks.

27 Demonstration of enlarged format short stack. Cost/performance analysis -comparison with enlarged format etched plate technology.

Johnson Matthey Fuel Cells Milestones

Phase 1

A Cell Installation & Commissioning.

B Development of a MEA to meet the performance targets for pure hydrogen in the IE single cell, using the IE etched plates, using JM LCS (Low Cost Substrate) GDL material developed with Technical Fibre Products:

610 mV @ 400mA/cm^2 measured off gold tabs (conservative target)

650 mV @ 400mA/cm^2 measured off gold tabs (aggressive target)

C Development of Sealed MEAs Suitable for Use in Intelligent Energy Stacks.

D Demonstrate that the MEAs developed in MS B were capable of stable operation without failure for over 500hours under constant current conditions.

E The objective of the reformate performance work was to meet the target of 95% of the pure H_2 voltage (MS B) under simulated steam-reformate conditions (measured off gold tabs). A conservative target of 610 mV and an aggressive target of 650 mV had been set for hydrogen operation, so the target for the reformate performance was a voltage in the range 580 to 618 mV with 50ppm CO and an appropriate level of air bleed.

F Demonstrate 500 hours durability on the type of MEA that had met the performance target of MS E, under the steam-reformate and air bleed conditions used.

Phase 2

G MS G: Develop a MEA for Operation on Hydrogen, Demonstrating Progress Toward Target of Stable Performance of at Least 0.65V at 500mA/cm^2 off SS Plates.

H MS H: Develop a MEA for Operation on Simulated Steam Reformate, Demonstrating Progress Toward Target of Stable Performance of 95% of Hydrogen Performance at Max. 2.0% Air Bleed off SS Plates.